Eindhoven University of Technology

Eindhoven University of Technology

MASTER

CO2 removal by amine absorption and condensed rotational separation
energy consumption & equipment sizing

de Rijke, S.J.M.

Award date:
2012

Link to publication

CO2 removal by Amine Absorption and Condensed Rotational Separation: Energy Consumption & Equipment Sizing

by

STEVEN JAN MARTIN DE RIJKE
BSc in Mechanical Engineering

THESIS

submitted in partial fulfillment of the requirements for the degree

MASTER OF SCIENCE: MECHANICAL ENGINEERING

Department of Mechanical Engineering
Technical University Eindhoven
Document Number: WPT201214

November 30, 2012

Approved by:
prof. dr ir J.J.H. Brouwers
dr. ir H.P. van Kemenade
prof.dr. M. Golombok
dr.ir. J. van der Schaaf

Acknowledgment

The author wishes to thank

SUMMARY/ABSTRACT

The Rotational Particle Separator (RPS) is a compact device capable of separating micron-sized droplets from gases by centrifugation. Combined with expansion cooling in a turbine at semi-cryogenic temperatures, it provides the opportunity to remove contaminants like CO2 and H2S from natural gas. Potential advantages of this technique are lower energy consumption and compactness. To demonstrate its potential, the technology is compared on the basis of installed volume and energy consumption with conventional amine technology for a range of CO_2 concentrations. The comparison is made using a model of both processes and their components separating a range of CO_2 contents from a 125 MMscf/day gas stream. The results show that for CO_2 concentrations greater than 15% the CRS technology offers significant advantages in both installed volume and energy requirement, unlocking natural gas fields with sour gas concentrations that cannot be treated with conventional technology up until well in the 70% CO_2 content.

Table of Contents

2

Figures and Tables

Tables in Main Text

Tables in Appendices

Introduction

Global gas reserves and new resource opportunities are becoming increasingly challenging, with as much as 1/3 of global reserves having significant amounts of CO_2 and H_2S. Fields with >30% CO_2 and >10% H_2S are not uncommon, and in the extreme, methane can be less than 50% of the total gas stream. This makes the economic viability very challenging when smaller amounts of methane and other light hydrocarbons in the full well stream must bear the added cost of producing, removing and disposing of the larger amounts of contaminants, mainly CO2 and H2S. There is a clear need for more economical processing of resources with decreasing hydrocarbon content. Furthermore, the focus on CO2 levels in the atmosphere has made release of CO2 to the environment less desirable, leaving geosequestration as the most promising alternative where there is no market for CO2. Similarly, sulfur production from H2S has saturated many markets and prompted the need for an alternate way to dispose of H2S.

Enter Condensed Rotational Separation, a novel method for separating sour gases from natural gas. A promising technology, relying on fast expansion cooling to establish phase change of the sour gases and subsequent phase separation using a patented new technology, the Rotational Particle Separator. The main advantages of this process are the low energy requirements, no matter the solute concentration and its small equipment size, especially in comparison with distillation processes. Furthermore, in many situations the sour gases come out of the CRS process as a pressurized liquid, ready for further processing or geosequestration.

Prototypes have been built and tested at Eindhoven University of Technology, which have shown the proof of principle and have successfully modeled equivalent sour gas streams from large gas fields. The technology has matured over the past years and is ready to be implemented on a large scale. This report is made to assess the viability of the process on such a large scale, by comparing it to the conventional technology for sour gas treating, Amine Gas Sweetening. Both processes are discussed in detail and both processes are modeled both in energy cost and required installed volume. The model is able to size the 2 processes for any mass flow and any composition of CH_4-CO_2. There are possibilities to expand the model to include H_2S and other fractions, as well as different types of amines. The report shows the results of the model, the model itself is explained in the appendices.

In short, this report will show why and how the CRS process has the potential to unlock gas fields that were previously not economically viable, up to large concentrations of CO_2 and H_2S.

1 Comparison of Condensed Rotational Separation with Amine Gas Sweetening

This report is a comparison in energy consumption and installed volume between Amine Gas Sweetening and Condensed Rotational Separation. Both processes had all their important components included in a model, built in Microsoft Excel, where all the stream properties were correctly linked with each other. A simple example is the mass balance over the absorber tower which returns a required amount of amine circulation for a certain amount of CO_2 separation.

The report is structured as follows. The main text specifies the main assumptions that have been made, so that one can at a glance see the involved flows, pressures and compositions considered. Then in chapter 3 and 4 the most important choices and conclusions for each technology are presented, both for volume and for energy considerations. In chapter 5 the results of the model are shown and chapter 6 lists the conclusions and recommendations. The appendices provide background information on each of the components and processes and specify in detail the used formulas and assumptions. Where possible a reference for an assumption is cited. In order to keep the main text readable not every opportunity was seized to refer to the appendices, but an effort was made to keep both the main text and the appendices readable as stand-alone texts.

2 Assumed Process Properties

The following assumptions are made to compare Condensed Rotational Separation to Amine Gas Sweetening.

The considered flow rate is 125 MMscf/day, which compares to 38,76 nm^3/sec and 6225 kmol/hr. This value is roughly equivalent to the flow rate used at the recently discovered Arabiyah and Hasbah gas fields in Saudi Arabia (Alami, 2010). The assumed conversion factor was $3,733 \cdot 10^{-5} \, MMscf/nm^3$.

The gas is assumed to be a binary CH_4-CO_2 mixture and the composition is varied to assess the effect of increasing CO_2 content. The mass flow that corresponds to the volume flow depends heavily on the composition of the gas stream. For a 15% CO_2 stream the mass flow equals 34,5 kg/s and for a 70% CO_2 stream the mass flow equals 60,8 kg/s

Amine Gas Sweetening can be considered at any CO_2 content of the feed gas stream using the model presented here. CRS however is dependent on vapor-liquid equilibria, therefore the main pressures and temperatures of the equipment have been calculated using a different program. CRS is considered for 15, 30, 50 and 70% CO_2 content, all of which end up as 13,6% CO_2 content after the CRS separation process. The parameters that were specified by the other model are shown in Figure A.5. Amine Gas Sweetening is used to bring the flow from 13,6% CO_2 to pipeline specification.

The goal of separation is a CO_2 content of 0,7%, which is equal to the pipeline specification for natural gas in the US, (NAESB, 2010), as shown in Table A.1.

The CRS process is considered at a feed gas pressure of 70 bar and a temperature of 293K. The amine process is considered at a feed gas pressure of 40 bar and a temperature of 293 K (equal to the outlet pressure and temperature of CRS). Choosing the operating pressure of the amine absorber is a trade-off between volume of the absorber and energy cost of pumping the lean amine from the stripper towards the absorber. Therefore the operating pressure of the amine absorber is chosen to be 40 bar, regardless of the presence of CRS equipment. This ensures that the energy cost of amine, up to the outlet concentration following the CRS process (up to 13,60% in this case), is equal, and a good comparison can be made. Keep in mind that the lean amine pump energy cost is in the order of 3% of the total energy cost, so the choice of operating pressure doesn't severely affect the total energy cost.

Table 2.1 Important Used Values in the calculations

Values for Amine Process	Value	Unit
Amine Used	MEA	
Solution concentration	15%	wt% MEA in water
Lean Amine Loading	0,10	mol CO_2/mol MEA
Rich Amine Loading	0,40	mol CO_2/mol MEA
Reflux Ratio	2:1	mol steam/mol CO_2
Absorber Pressure	40	bar
Absorber Temperature	20	°C
Stripper Pressure	1,5	bar
Reboiler Temperature	126	°C
Boiler Efficiency	80%	[-]
Combustion Efficiency	99%	[-]
Pump Efficiency	85%	[-]

Values for CRS Process	Value	Unit
Compressor Efficiency	85%	[-]

Values valid for both processes	Value	Unit
Unit Conversion for Volume	3,733	$\cdot 10^{-5}\ MMscf/nm^3$
Gross Heating Value Natural Gas	37800	kJ/nm3
Heat Rate N.G. Fired Power Plant	8350,45	kJ/kWh
Electromotor Efficiency	96%	[-]

3 Amine Gas Sweetening

The amine gas sweetening process contacts the sour gas in counter flow with an amine solution in an absorption tower. CO_2 dissolves in the solution and the amines in the solution react with the CO_2, creating a CO_2 rich solution. The rich solution from the absorber flows into a three phase flash tank that is operated at lower pressure permitting the venting of any entrained light hydrocarbons from the solution. The rich solution is pumped through a product-feed exchanger and then heated in a stripper tower by a reboiler at the bottom of the stripper tower, until the bond between amine and CO_2 breaks. The CO_2 flows out the top of the stripper while the CO_2 lean amine solution is pumped to the absorption tower. As some impurities in the gas stream tend to react with the amine as well, to form heat stable salts, a reclaimer is necessary to remove these salts. An extensive overview of the process is shown in Figure A.1 and the process is discussed in detail in Appendix B .`

3.1   Energy

The main energy users for the amine process are the steam furnaces providing steam to the reboiler and reclaimer. Other, much smaller, energy consumers are the pumps involved in the process, which are assumed to use an electromotor. This required electrical energy is converted into equivalent gross heating value of natural gas using a value for the heat rate of natural gas fired power plants, see section C.10. All relevant efficiencies and other energy calculations are listed per unit in the respective sections of Appendix C .

All energy consumption scales linearly with the CO_2 content of the feed gas stream. Therefore the energy cost distribution listed in Table 3.1 is valid for all CO_2 concentrations in the feed gas stream.

Table 3.1 Energy Cost distribution for a 125 MMscf/day gas stream

Amine Energy Cost Distribution	*% of total Energy Cost*
Heating Rich Amine	37,49%
Heating Reflux drum water	17,60%
Breaking CO2-amine bond	16,58%
Vaporizing water in reboiler	2,74%
Steam Piping Heat Loss	2,20%
Steam Furnace inefficiency	20,12%
Steam Production Total Heat Required	96,72%
Rich Amine Pump	Not Used
Lean Amine Pump	3,26%
Steam Condensate pumps	0,01%
Reflux Pump from condenser	0,001%
Reclaimer Feed Pump	0,004%
Electricity Consumption Total Heat Required	3,28%
Total Heat Required	100,00%

As the reclaimer is fed directly from the reboiler and the vapor coming from the reclaimer eventually returns to the reboiler again, the heat duty of the reclaimer is subtracted from the heat duty of the reboiler, see section C.3. Therefore there's no mention of the reclaimer duty in Table 3.1, as both the reclaimer and the reboiler contribute to the heat duty posed by the first 4 parameters in the table. More information on this subject can be found in sections C.3&C.4.

The total energy use of the amine process for a 125 MMscf/day flow is listed in section 5, "Comparison Results".

3.2 Volume

The main components that contribute to the installed volume are:
Absorber, Stripper, Inlet Knockout Drum, Three Phase Flash Tank, Reboiler, Reclaimer and the Reflux Drum. An extensive explanation of the volume calculations per component is given in Appendix C .

An important aspect to recognize is that *the flow of amine solution scales linearly with the molar flow of CO_2 in the feed gas stream*.
In turn the Stripper, Three Phase Flash Tank, Reboiler, Reclaimer and the Reflux Drum *all scale linearly with the flow of amine solution*, either through fixed residence times or through heat duty per kg of flow, which, in combination with fixed temperature differences, result in larger vessels.

Absorber
The absorber volume is subject to a number of parameters, which are explained below. The diameter either scales with the superficial gas velocity (which in turn depends on the gas density, according to the Souders-Brown Equation, (Souders and Brown, 1934)), or the diameter is calculated from a flooding constraint, which scales with the liquid flow rate, (Cussler, 1997).

The height scales with the absorption rate and with the flow of inerts, which are all components that are not absorbed by the amine solution. One might suspect that the height of packing strongly increases with increasing CO_2 concentration, however there are 2 effects counteracting this assumption.

The first effect is that the bulk of the CO_2 removal contributes to only a relatively small portion of the total height of packing. Typically the last few % of CO_2 concentration that has to be removed from the flow contributes the most to the total height of packing required. The reason for this is that the absorption rate is strongly linked to the concentration difference between the gas and the liquid. In the example calculation by (Vaidya and Mahajani, 2006), where an absorber was sized based on an inflow composition 25% CO_2, it turned out that 73% of the height of packing could be attributed to the last 12,5% of the total amount of moles of CO_2 that had to be absorbed.

The second effect is that the height of packing scales linearly with the molar gas flow of inerts. This can be explained by taking 2 extreme cases, 5 and 95% CO_2 concentration inflow. Assuming the same molar flow rate from the gas field and a constant column diameter, pressure and temperature, the velocity of the gas through the column is directly proportional to the molar flow. When considering the removal process down from 5% CO_2 concentration to pipeline specification, in other words, the part that contributes most to the height, the gas velocity through the column is considerably higher in the 5% case than in the 95% case, as a large amount of CO_2 has already been absorbed. This is shown in Table 3.2

Table 3.2 Comparison of molar flow rates for different CO_2 concentrations.

	mol%		mol/second		
	CO₂	CH₄	CO₂	CH₄	Total
5% inflow case	5%	95%	50	950	1000
95% inflow case	95%	5%	950	50	1000
Last 5% from 95% inflow	5%	95%	3	50	53

Therefore, even though the absorption rate at 5% CO_2 concentration is practically equal for both cases, the total height is lower in the 95% inflow case due to the lower gas velocity in the column. There are also other factors contributing to the rate of absorption, a detailed explanation of this is given in section C.1.3. The different aspects mentioned in this paragraph are listed in Table 3.3

Table 3.3 Dimensions of the absorber column

CO2 Content	5%	13,6%	15%	30%	50%	70%	mol%
Gas density	28,9	32,9	33,6	40,6	49,9	59,2	kg/m3
Superficial Gas Vel.	0,4	0,3	0,3	0,3	0,3	0,3	m/s
Absorber Diameter	1,9	1,9	2,0	2,1	2,2	2,6	m
Absorber Height	21,9	20,1	19,9	16,1	15,0	11,1	m
Absorber Volume	61	60	60	53	55	57	m3

Stripper
The stripper can be seen as a heat exchanger, exchanging heat between the upwards flowing Steam and CO_2 and the downward flowing Rich Amine. The diameter of the vessel is calculated in the same way as in the absorber tower.
As a result of this calculation, an increase in flow of amine results in a direct increase of diameter, not in height. Therefore one can assume that the height of the tower only scales with the temperature difference between rich amine inlet and reboiler inlet. Strippers in practice do not vary a lot in height, as temperature differences between stripper towers also vary only slightly. Most strippers have between 16 and 26 trays or an equivalent height of packing (Kohl and Nielsen, 1997)
As this work keeps both inlet and outlet temperature values constant, the height is also assumed constant. Therefore this height is assumed to be 19,3 meters, based on operating data found in (Kohl and Nielsen, 1997).

The stripper size increases fairly quickly as the rich amine stream, the CO_2 gas stream, the steam generated in the reboiler and the reflux from the reflux drum all scale linearly with the CO_2 content of the feed gas stream.

Inlet Knockout Drum
Like the absorber and stripper, the inlet knockout drum volume scales with diameter, which depends on the droplet settling velocity in the Souders-Brown equation. The height of the drum is fixed by the slug catcher, liquid collection height and mist eliminator height.

Three Phase Flash Tank
Light hydrocarbons flash due to the pressure drop and are easily separated. The heavier hydrocarbons remain as a separate liquid layer, on top of the amine solution, because of their lower density. In order to obtain 2 well separated liquid layers, a minimum residence time for a three phase flash tank of 20 minutes is recommended, based on the flash tank operating a liquid capacity equal to a half full tank. (Sheilan et al., 2009) Amine systems treating very dry natural gas (<2% C_2^+) or syngas streams with very little hydrocarbon content can utilize a lower flash tank residence time of 5 minutes if a flash tank is incorporated into the amine unit design.
The high residence time in combination with the large rich amine streams for higher CO_2 contents results in a large vessel. Because this work utilizes a binary gas mixture, the tank is assumed to treat dry natural gas. A comparison is given in Table 3.4 between the 5 (dry) and 20 minute (wet) residence time.

Table 3.4 Three Phase Flash Tank size per CO_2 content of feed gas stream

CO_2 Content	5%	13,6%	15%	30%	50%	70%	mol%
Three Phase Flash (Dry)	61	184	204	419	704	990	m3
Three Phase Flash (Wet)	246	737	817	1674	2817	3960	m3

Reclaimer
The reclaimer vessel normally has a liquid capacity in volume of approximately 100 times the feed rate of the reclaimer in the same volume per minute. (Sheilan et al., 2009). This feed rate is approximately 3% of the total amine circulation. One can assume that the liquid capacity is 2/3^{rds} of the total volume of the reclaimer.

Reboiler
The reboiler is taken to be approximately the same size as the reclaimer, as both have the same operating principle. The reboiler handles a bigger volume flow, but isn't a batch process. As the sizing wasn't found in literature, and the vessel isn't the largest contributor to the total volume, this assumption was deemed appropriate.

Reflux Drum
The size of the reflux drum can be assessed by a 20 minute liquid hold up inside the drum. This capacity is necessary to enable a steady flow of reflux water during the first

20 minutes of start-up of the stripper column, after a turn-around or shut-down. One can assume the liquid capacity is 50% of the total installed volume of the reflux drum.

Results

The results of the model for the volume of the different system components in the Amine Process are listed in Table 3.5 and shown in Figure 3.1.

Table 3.5 Volume of the Amine Process for different CO_2 content of the feed gas stream

CO₂ Content	5%	13,6%	15%	30%	50%	70%	mol%
Absorber	61	60	60	53	55	57	m3
Stripper	51	153	170	348	585	823	m3
Inlet Knockout Drum	14	15	15	17	19	21	m3
Three Phase Flash (Dry)	61	184	204	419	704	990	m3
Reboiler	19	56	62	127	213	299	m3
Reclaimer	19	56	62	127	213	299	m3
Reflux Drum	6	19	22	44	74	104	m3
Total Volume	231	543	594	1134	1864	2593	m3

Note that Pumps are not listed in this table, partly because they are not the main contributors to installed volume and partly because there are many types and sizes of pumps. For an idea of the size of the pumps it's better to consider the kilowatts of power required by them, shown in Table 3.6.

Table 3.6 Pump Electrical Power Consumption

CO2 content in gas field	5%	13,6%	15%	30%	50%	70%	Mol%
Lean Amine Pump	500	1499	1662	3406	5730	8055	kW
Steam Condensate Pumps	2	5	5	10	17	24	kW
Reflux Pump	0	1	1	1	2	3	kW
Reclaimer Feed Pump	1	2	2	4	7	10	kW
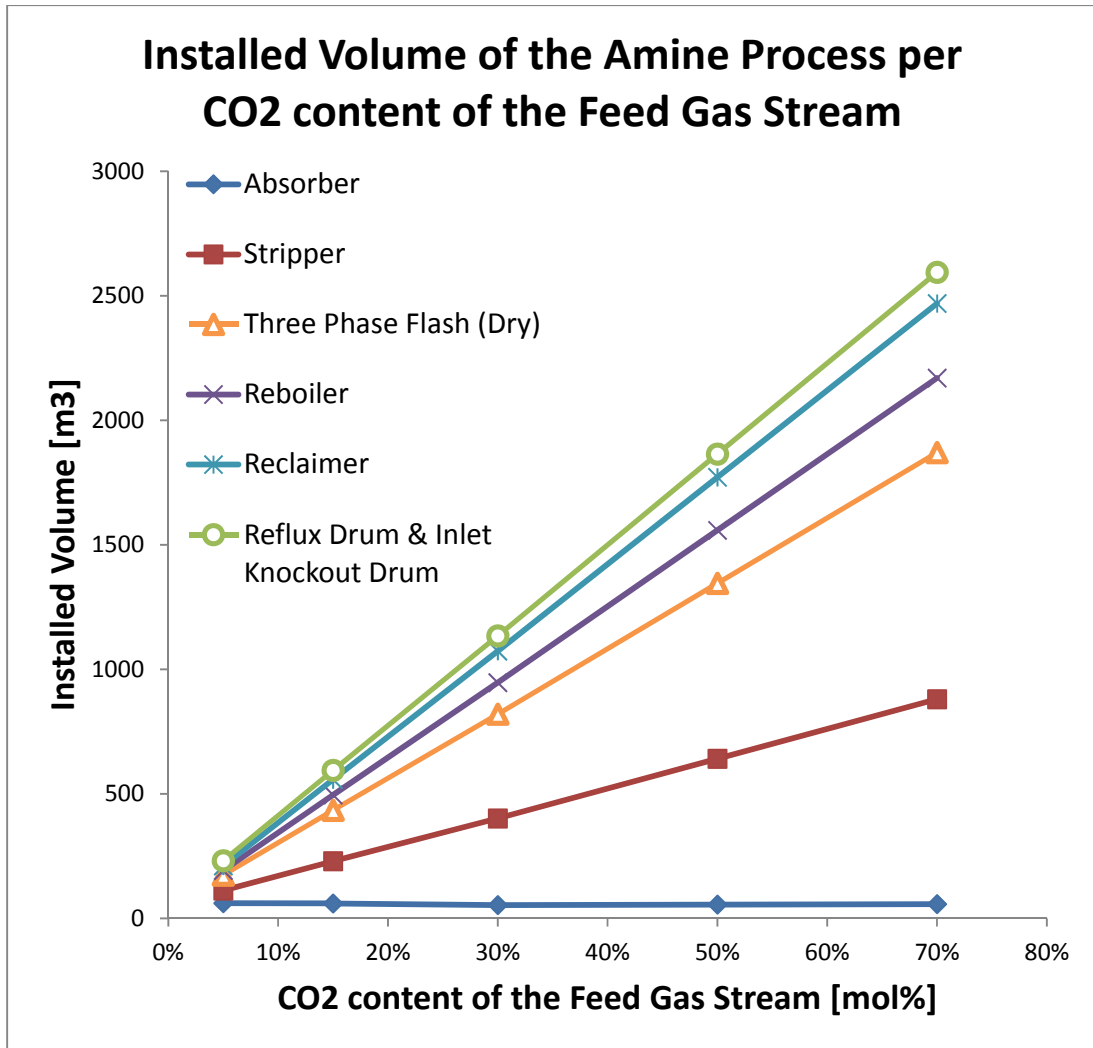
Figure 3.1 Installed Volume of the Amine Process per CO₂ content of the Feed Gas Stream
Note: the values are cumulative, therefore the distance between lines represents the volume of the (upper) component at a given CO₂ concentration.

4 Condensed Rotational Separation

Condensed Rotational Separation, abbreviated by CRS, is a novel separation method for mixtures of gases, which uses elements of cryogenic distillation (Brouwers et al., 2006), (van Wissen et al., 2007). A mixture of gases is cooled by expansion through a valve or turbine to a temperature at which one of the components condenses into micron-sized droplets. This development is enabled by the availability of efficient cryogenic expanders that are able to work in the condensing area (e.g. GE, Atlas-Copco, Cryostar, Petrogas). These droplets are subsequently removed by centrifugal separation using the invention of the Rotational Particle Separator, abbreviated by RPS (Brouwers, 1994), (Brouwers and Hoijtink, 2007). CRS is particularly applicable to systems where reduction in size and weight is advantageous, like floating LNG production, or the removal of contaminants like CO2 and H2S from natural gas (van Wissen, 2006), (Willems, 2009). See Appendix D for more information on the process' advantages over fractional cryogenic distillation.

4.1   CRS as bulk separator in combination with an Amine Absorption plant.

As shown in the previous chapter, the energy demand of the classic amine absorption process increases rapidly with the contamination level. Therefore it is interesting to use a bulk separation process prior to the amine absorption process to reduce the size and energy consumption of the latter. CRS is an excellent candidate, as it is able to separate CO_2 from a binary CO_2-CH_4 mixtures of up to 70% CO_2 concentration to achieve a remaining 13,60% CO_2 content in the gas stream towards the amine absorber, see section D.1 for the thermodynamic principles governing these limits.

As explained in the section on absorber sizing, separating CO_2 from the gas stream to bring the CO_2 content down removes a significant portion of the total flow. From the remaining mass flow shown at the gas outlet in Figure A.5 and the composition of 13,6% CO_2 one can calculate the corresponding MMscf/day that are fed to the Amine absorption plant. These values are shown in Table 4.1.

Table 4.1 Volume flow to Amine at 13,6% CO_2 content after the CRS bulk separation step. Note: at 13,6% CO_2 content no CRS is used and the full flow is delivered to the amine process.

Original CO2 Content	13,6%	15%	30%	50%	70%	mol%
Volume Flow Rate	125	122	100	71	42	MMscf/day

This smaller flow has a significant impact on the volume and energy cost of the amine plant, as is shown in section 5, "Comparison Results".

4.2   Methane Loss

At the liquid outlet of the CRS process, shown in Figure A.5, 1,7 volume percentage of the flow is CH_4. This methane is considered 'lost', as there is no easy way of recovering it from the flow. This amounts to a certain % of the original CH_4 flow that is considered lost, shown in Table 4.2.

Table 4.2 Percentage of CH$_4$ lost in the solute stream of CRS

Original CO2 Content	13,6%	15%	30%	50%	70%	mol%
CRS Methane Loss	0,0%	0,03%	0,5%	1,5%	3,8%	mol%

4.3 Energy

In the flow scheme presented in Figure A.5, the compressor is the only energy consumer that contributes to the total energy consumption of the process. The pressure loss across the system is not considered as energy loss, as the 40 bar remaining is more than adequate for further processing. The heat exchangers in the system do not require extra cooling in any of the 4 cases presented, as explained in section D.3.3.

Compressor

The work done by the compressor scales with the mass flow, which in turn scales with the CO$_2$ content as explained in section 2. The specific work done per kg of mass flow is calculated as in section D.4. Taking efficiency of the compressor and the electromotor into account, one can calculate the power consumption in kW of electricity. This required electrical energy is converted into equivalent gross heating value of natural gas using a value for the heat rate of natural gas fired power plants, see section C.10. Table 4.3 shows the power consumption of the compressor for each of the 4 CO$_2$ contents considered.

Table 4.3 Compressor Power Consumption in electric power and equivalent Gross Heating Value of natural gas.

CO2 content in gas field	15%	30%	50%	70%	mol%
Electric Power	400	4781	10694	16602	kW
Equivalent GHV (Natural Gas)	929	11089	24806	38509	kJ/s

4.4 Volume

There are four main types of components in the CRS process. There are expansion valves, heat exchangers, separation devices (referred to as RPS) and a compressor. Figure A.5 shows an overview of the process, for 4 values of CO$_2$ content of the inlet gas stream.

Heat Exchangers

Estimation of the dimensions of the heat exchangers used in the CRS process is based on a multi-stream, spiral-wound-type (Linde, 2012b) as commonly applied in LNG plants. The size of the heat exchangers depends on the overall heat exchange coefficient between the two streams for each heat exchanger, of which the calculation is shown in section D.3. The optimum flow scheme applies maximum heat integration, whilst avoiding the use of the liquid CO$_2$ stream as cooling medium as much as possible, as liquefied CO$_2$ is much easier to handle in later uses, for instance for carbon sequestration. This offsets the increase in size of the heat exchangers resulting from using the gas stream as cooling medium instead of the liquid stream and is definitely an advantage for the CRS process over other processes. The result of the calculation is shown in Table 4.4.

Table 4.4 Heat exchanger volume calculated for each CO$_2$ stream

CO2%	15%	30%	50%	70%	mol%
Heat Exchanger Volume	9,7	22,2	31,5	32,6	**m3**

Note: The overall heat exchange coefficients found ranged from 100 to 300 W/(m^2 K).

Rotating Particle Separators

The RPS is sized by considering a working prototype, as built and tested by (Buruma et al., 2012). Using relations derived in section D.2.2, one can then size the different components of the RPS with the relative flow rate and relative density of the gas. In order to keep the size within acceptable boundaries, as the device contains rotating elements, the choice was made to limit the height of the RPS (without engine) to about 3 meters and the diameter to about 1 meters. When 1 of these values was exceeded the flow was divided over multiple parallel devices. The results are shown in Table 4.5.

Table 4.5 Number and Total Combined Volume of RPS devices for each CO$_2$ stream

CO2 content	Device name	# of devices	Tot. Vol. [m^3]	Device name	# of devices	Tot. Vol. [m^3]
15%	**RPS1**	2	1,0	**RPS2**	1	0,2
30%	**RPS1**	2	1,5	**RPS2**	3	4,7
50%	**RPS1**	6	1,7	**RPS2**	6	11,1
70%	**RPS1**	8	2,3	**RPS2**	9	17,6

In terms of volume, the expansion valves are considered negligible. Also note that the compressor installed volume is not considered, just like the pumps in the amine calculation and for the same reasons. For an idea of the size of the compressor it's better to consider the kilowatts of power required, shown in the previous section.

5 Comparison Results

This section will compare the Amine Absorption Process to the combination of CRS as bulk separator (down to 13,6% CO_2 concentration) and Amine Absorption used to bring the CO_2 content down to pipe-line specification. First the energy cost will be compared.

5.1 Energy

In order to place the energy cost data into perspective, the Available Energy in the flow from the gas field has to be calculated.
In the flow of 125 MMscf/day a certain percentage is CH_4 and a certain percentage CO_2. The methane has a heating value, as it can be burned, and the CO_2 doesn't. The available energy per second is the gross heating value that the flow represents. This is calculated by dividing the amount of moles/sec of CH_4 in the flow by the mol% of CH_4 in the pipe specification of natural gas to obtain the total molar flow. After that this total molar flow becomes a volumetric flow in nm^3/sec using the molar volume. Multiplying this volumetric flow with the gross heating value in kJ/nm^3 of natural gas gives one the available energy per second that the flow possesses when it leaves the gas field. Pipeline specification of Natural Gas and the Gross Heating Value can be found in Table A.1.

The amine process is modeled on the basis that none of the CH_4 is entrained in the amine, as there is a three phase flash tank present to recover entrained CH_4. Therefore there are no methane losses in the amine process. The CRS process does have a methane loss, as stated before, which is included in the energy cost as lost methane accounts for lost Gross Heating Value of the natural gas.

All energy cost calculations have been calculated to represent the equivalent amount of energy in Gross Heating Value of Natural Gas at pipeline specification that has to be burned to sustain the process. For steam-linked processes this equals the Gross Heating Value required in the steam furnaces and for electric powered processes this corresponds to the Gross Heating Value of natural gas required in the power plant.

Table 5.1 lists the absolute values of available energy content of natural gas coming from the process and the energy cost of the amines and the CRS+amines process. Furthermore it lists the percentage obtained by dividing energy cost by available energy.

This percentage is a measure of the operating cost and possible return on investment of the process. If one divides the total amount of available energy by the Gross Heating Value per m^3 of natural gas, one obtains the amount of m^3 of natural gas that can be sold. This has a direct value. The percentage burned therefore represents the direct cost of the energy required to remove the CO_2 from the gas field.
With increasing CO_2 content, the amount of Available Energy and thus recoverable Natural Gas decreases. Therefore, for high CO_2 content, there is an even stronger incentive to keep the cost of separation down.

Table 5.1 Absolute values of Available Energy content in the feed gas stream and the Energy costs of each process, both in listed in equivalent Gross Heating Value of Natural Gas. The percentages are the Energy costs divided by the total Available Energy.

CO2 content	5%	13,6%	15%	30%	50%	70%	mol%
Avail. Energy	1401537	1274661	1254006	1032711	737651	442590	*kJ/s*
Amine Only	35558	106645	118250	242289	407674	573059	*kJ/s*
Amine Only	3%	8%	9,43%	23%	55%	129%	*mol%*
CRS	0	0	929	11089	24806	38509	*kJ/s*
CH$_4$ loss	0	0	349	4780	10718	16616	*kJ/s*
Amine(CRS)	35558	106645	104326	85706	60650	35970	*kJ/s*
CRS+Amine	35558	106645	105604	101575	96174	91095	*kJ/s*
CRS	0,0%	0,0%	0,1%	1,1%	3,4%	8,7%	*mol%*
CH$_4$ loss	0,0%	0,0%	0,03%	0,5%	1,5%	3,8%	*mol%*
Amine(CRS)	2,5%	8,4%	8,3%	8,3%	8,2%	8,1%	*mol%*
CRS+Amine	2,5%	8,4%	8,4%	9,8%	13,0%	20,6%	*mol%*

Note: The Amine(CRS) denotes the energy cost of the amine plant cleaning the natural gas after bulk separation down to 13,6% CO$_2$ content has been done by the CRS process.

In Figure 5.1 a plot is shown of the absolute value of the Available Energy and the energy cost of the processes. Amine behaves as expected, its energy cost rising linearly with the CO$_2$ content of the gas field, even consuming more than 100% of the Available Energy for CO$_2$ concentrations over 65%. It can be clearly seen why amine treating is very limited in its potential to process high contents of CO$_2$ (and H$_2$S), as the linear rise in cost with CO$_2$ content combined with the linear decrease in available energy causes a quadratic increase in % of available energy burned, as shown in Figure 5.2. This means that even significant improvements to process efficiency will be moot for the high CO$_2$ content gas fields.

Then there is the curve of the CRS+Amine process. As stated before, CRS is used as a bulk separator, using amine to clear the remaining CO$_2$ content. In a binary CH$_4$-CO$_2$ system the process is limited to an optimum 13,6% CO$_2$ in the gas phase by the position of the vapor-liquid boundary at 40 bar and -64,2 °C. For other systems CRS can achieve higher purities of methane, for instance in the presence of H$_2$S. (van Kemenade et al., 2011). This would mean that even smaller amine plants are needed to bring the gas up to pipeline specification.

However, in this case CRS starts from 13,6% upwards and the effect is immediately noticeable. The main difference between CRS and Amine is the energy cost per mole% of CO$_2$ removed. For amine this is a linear relation, as shown in equation (5.1):

$$\text{Cost/mol\%}_{\text{amine}} = \text{Energy Cost}/\left(CO_2\% - \text{pipeline spec } CO_2\%\right) \qquad (5.1)$$

Which amounts to $\pm 8250 \left(kJ/s\right)/mol\% \ CO_2$ increase in energy cost for each mol% above pipeline specification.
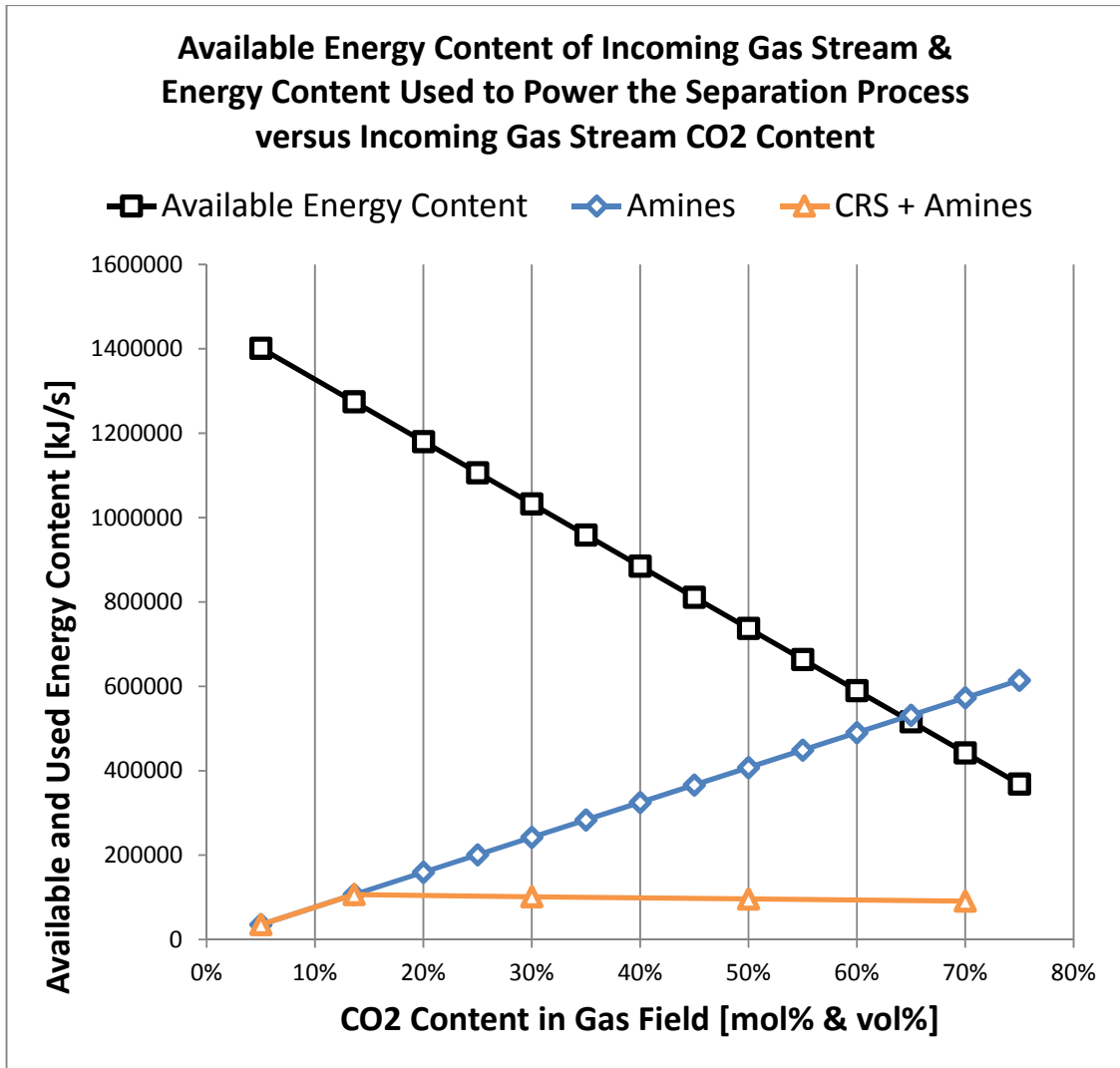
Figure 5.1 A plot of the Available Energy Content in the incoming gas stream and the energy cost of the amines process and the CRS+amines process. This is plotted as a function of the CO2 content of the gas stream coming from the gas field.
Note: Valid for a flow of 125 MMscf/day and binary composition of CO2 and CH4

Although the CRS energy costs and the savings of amine(CRS) are not entirely linear, Figure 5.1 shows that an approximate linear fit should be possible.

In this model the CRS process only has 2 energy costs. Methane loss in the waste stream and the compressor which sizes with the mass flow of the reflux of gas from the second stage. Using the following relation

$$\text{Cost/mol\%}_{\text{CRS}} = \text{Energy Cost}\big/\big(\text{CO}_2\% - 13{,}6\%\big) \qquad (5.2)$$

This amounts to $\pm 680\,\big(kJ/s\big)\big/mol\%\,\text{CO}_2$ increase in energy cost for the compressor and $\pm 280\,\big(kJ/s\big)\big/mol\%\,\text{CO}_2$ increase in energy lost due to extra methane loss, both for each mol% above 13,6%. Combined this amounts to $\pm 960\,\big(kJ/s\big)\big/mol\%\,\text{CO}_2$ a factor 8,5 lower than Amine absorption.

However, because CRS also removes part of the flow, the volumetric flow to the amine plant is lower with each mol% in the original CO_2 concentration higher than 13,6%. When the decrease in energy cost of the Amine(CRS) plant is calculated this amounts to $-1350\left(kJ/s\right)/mol\%$ CO_2 resulting in a net decrease of $-390\left(kJ/s\right)/mol\%$ CO_2 for each mole above 13,6% CO_2 content from the absolute value for a 125MMscf/day, 13,60% CO_2 cleaning amine plant.

Finally the Available Energy content of the gas stream comes down with $-14750\left(kJ/s\right)/mol\%$ CO_2 for all percentages. As this value is larger than the savings of CRS Figure 5.2 still shows an increase in % of available energy content used in the process.
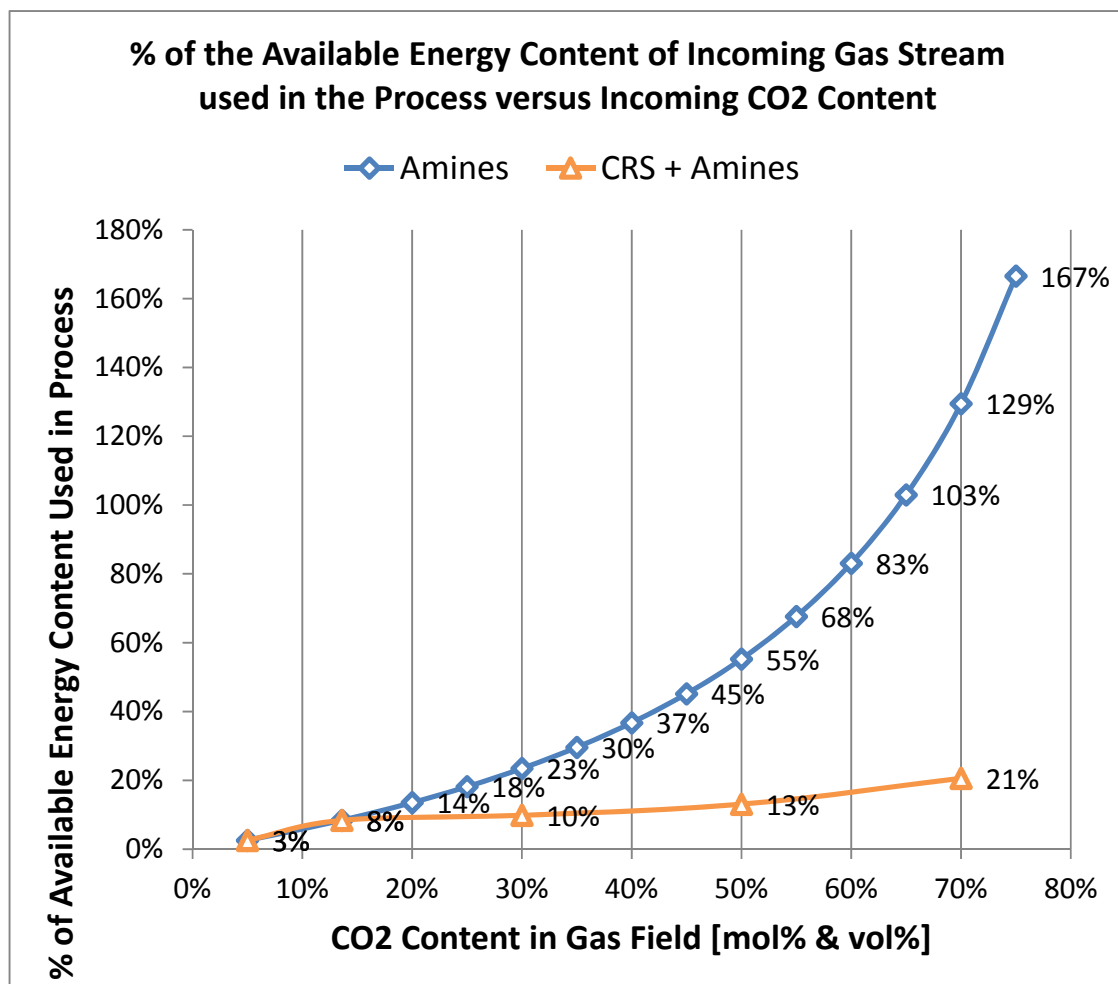
Figure 5.2 Plot of the percentage of the Available Energy Content available in the gas stream coming from the Gas Field which is required to separate the CO2. This is plotted as a function of the CO2 content of the gas stream coming from the gas field.
Note: Valid for a flow of 125 MMscf/day and binary composition of CO2 and CH4

5.2   Volume

The graph of the installed volume of both processes shows a similar behavior as the graph for the energy cost. As the volume for the components of the Amine process were already given in section 3.2, only the volumes of the CRS+Amine process are given in Table 5.2. The total volumes for both processes are plotted in Figure 5.3.

Table 5.2 Total Volume of the Amine process, combined CRS+Amine process and the contribution of CRS listed separately

CO2 Content	5%	13,6%	15%	30%	50%	70%	mol%
Amine(CRS)	231	543	531	437	309	183	m3
CRS	0	0	11	28	44	53	m3
CRS+Amine	231	543	542	465	353	236	m3
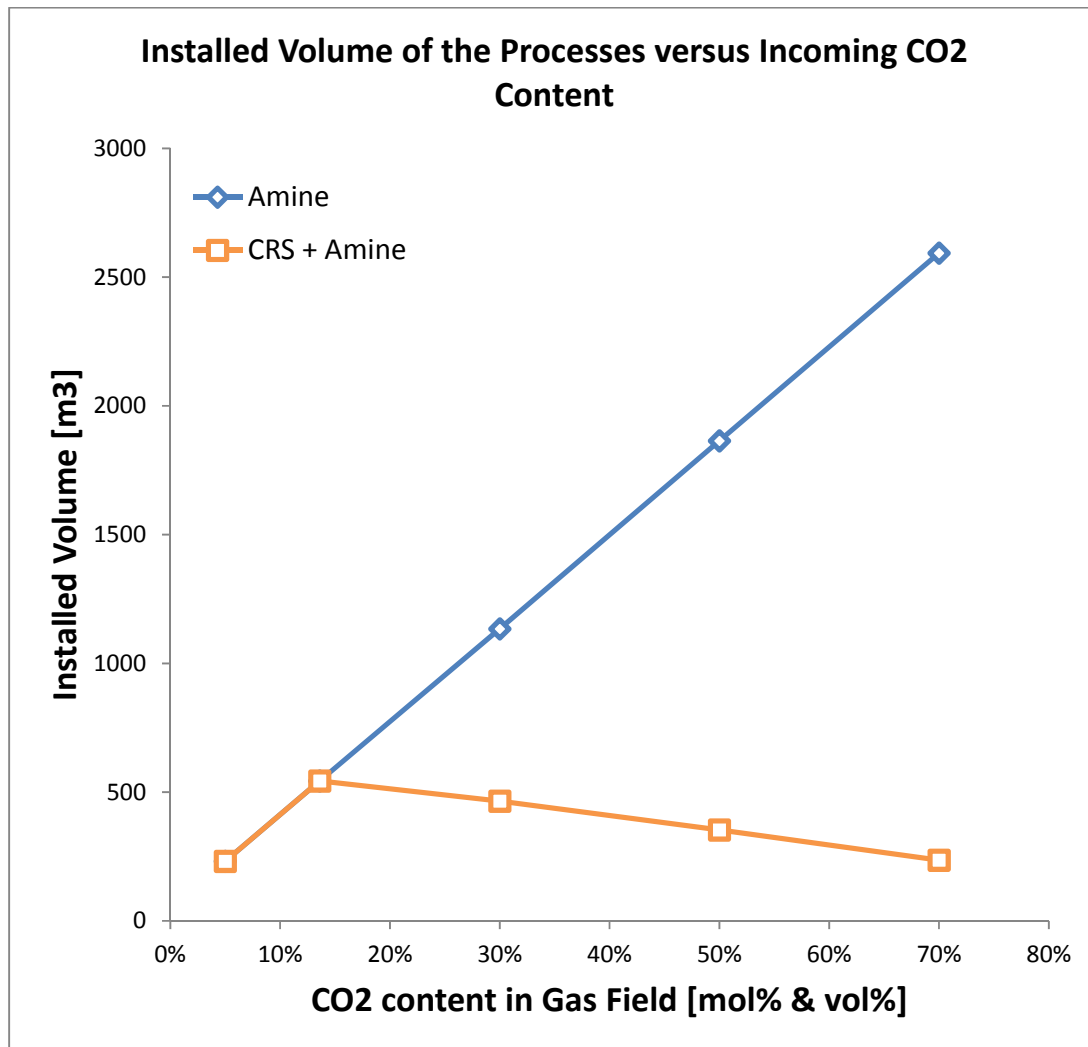
Figure 5.3 Total Volume of the Amine process and the combined CRS+Amine process

Again increases and decreases per % of CO_2 can be calculated as both graphs shown an almost linear trend. The amine process increases its volume with a quite steady 36,3 m^3/mol% . From 15% to 70% the CRS equipment increases its volume at a rate of 0,4 to 1,2 m^3/mol% while the amine(CRS) plant decreases in size at a rate of -6,3 to -8,5 m3/mol% resulting in a net decrease in size at a rate of -5,1 to -5,8 m^3/mol% from the size of a 125 MMscf/day & 13,6%.CO_2 cleaning amine plant.

6 Conclusions and recommendations

The main conclusion that can be drawn from this report is that CRS and amine absorption complement each other very well. Amine absorption has the capability to bring the gas purity up to pipeline specification, while CRS has a resounding advantage over amine in terms of energy cost and equipment size. The combination of both technologies allows the exploitation of previously uneconomical gas fields and CRS even replaces some of the gas pre-treatment necessary for a stable amine absorption process.

There is a lot of room for improvement, both in optimization of the process and in expanding the model. As mentioned earlier, the CRS process can manage even better methane purities when the system is allowed to work in a vapor-liquid-solid region. Each gas field composition requires its own optimization in order to use the CRS process to its full potential, therefore it would be a good idea to assess the boundaries of the practical use of the CRS process and be able to quickly asses if a gas field is eligible for the CRS process.

The model presented here incorporates the most important aspects of both technologies. The main components of each technology are simulated and the behavior of the energy and volume curve is well represented. The defining factor for amine systems is that the amount of circulated amine is directly proportional to the amount of moles of sour gas in the gas stream. Energy consumption scales directly with this fact and most of the volume calculations do as well.

For CRS the defining factor is that it works with vapor-liquid equilibria which are valid, no matter the size of the mass flow. The CRS process can handle high liquid loads and as such can instantly remove large quantities of sour gas from the gas stream. The main reason for its low energy consumption is the fact that the heat exchanging streams do not require extra cooling, as most of the cooling is supplied by expansion of the gases. A low pressure gas field would make the economical use of CRS more difficult.

There is, of course, room for improvement. First of all, many of the world's sour gas fields are laden with CO_2 ánd H_2S, therefore expansion of the model to allow for a gas composition of 3 or more types will be required. The model can also be adapted to include different amines, including physical solvents to compare CRS with for instance Selexol or Flexsorb. Perhaps a certain amount of selectivity is also possible with CRS. However, by far the most challenging and important question is if CRS will hold its own against Sprex, CFZ and the other cryogenic distillation processes which are trying to demonstrate their worth in unlocking highly contaminated sour gas fields for exploration.

Appendix A   Tables and Graphs

Figure A.1 Typical Amine System
Source (RefiningOnline, 2007)

Note: This work does not incorporate an Amine Surge Tank, LPG contactor, LPG-Amine Coalescer, NH_3 scrubber, Sulfur Recovery Unit (SRU) and Overhead Knock-Out Drum (OH KO Drum)

Table A.1 Chemical Composition of Natural Gas in American Gas System
Source: (NAESB, 2010)

Component	Typical Analysis (mole %)	Range (mole %)
Methane	94.9	87.0 - 96.0
Ethane	2.5	1.8 - 5.1
Propane	0.2	0.1 - 1.5
iso - Butane	0.03	0.01 - 0.3
normal - Butane	0.03	0.01 - 0.3
iso - Pentane	0.01	trace - 0.14
normal - Pentane	0.01	trace - 0.04
Hexanes plus	0.01	trace - 0.06
Nitrogen	1.6	1.3 - 5.6
Carbon Dioxide	0.7	0.1 - 1.0
Oxygen	0.02	0.01 - 0.1
Hydrogen	trace	trace - 0.02
Specific Gravity	0.585	0.57 - 0.62
Gross Heating Value (MJ/m^3), dry basis *	37.8	36.0 - 40.2

Note: * The gross heating value is the total heat obtained by complete combustion at constant pressure of a unit volume of gas in air, including the heat released by condensing the water vapor in the combustion products (gas, air and combustion products taken at standard temperature and pressure).

Table A.2 Selected Country-Specific Gross Calorific Values for Natural Gas
Source: (IEA, 2012)

Country	kJ/m^3
Russian Federation	38 232
United States	38 192
Canada	38 520
Qatar	41 400
Islamic Rep. of Iran	39 356
Norway	39 620
People's Rep. of China	38 931
Saudi Arabia	38 000
Indonesia	40 600
Netherlands	33 339

Note: For the top-ten producers in 2011. To calculate the net calorific value, the gross calorific value is multiplied by 0,9. The gross heating value is the total heat obtained by complete combustion at constant pressure of a unit volume of gas in air, including the heat released by condensing the water vapor in the combustion products (gas, air and combustion products taken at standard temperature and pressure).

Table A.3 Physical Properties of Alkanolamines
Source: (Sheilan et al., 2009)

	MEA	DEA	DGA	MDEA	DIPA
Molecular Weight	61.08	105.14	105.14	119.16	133.19
Specific gravity, 20/20 °C (* 30/20 °C)	1.0179	1.0919*	1.0550	1.0418	0.989 *
Weight, kg/liter	1.016 @ 15 °C	1.09 @ 15 °C	1.06 @ 15 °C	1.04	0.995
Boiling point @ 760 mm Hg, °C	171	269	221	247	249
Freezing point, °C	10.6	27.8	-12.2	-22.8	42.2
Vapor pressure, mm Hg @ 20 °C	0.36	0.01	0.01	0.01	0.01
Heat of vaporization, Btu/lb @ 760 mm Hg	355	288 (23 mm)	219	223	185
Heat of reaction, Btu/lb					
H$_2$S	550 – 670	500 – 600	674	450 – 520	-
CO$_2$	620 – 700	580 – 650	850	570 - 600	-
Viscosity, cp @ 20 °C	24.1	380 (30 °C)	26 (24 °C)	101	198 (45 °C)
Specific heat @ 15.5 °C, Btu/lb/°F	0.608 @ 68 °F	0.600	0.571	0.335	0.69 @ 30 °C
Thermal conductivity Btu/[(hr•sq ft•°F)/ft] @ 20 °C	0.148	0.127	0.121	0.159	-
Critical constants					
Pressure, kPa	5989	3280	3776	-	3776
Temperature, °C	350	442	403	-	399

Table A.4 Exothermic Heat of Reaction of certain Alkanolamines with CO$_2$.
Source: (Vaidya and Mahajani, 2006) & (Kohl and Riesenfeld, 1985)

Alkanolamine	Exothermic Heat of Reaction [kcal/kg]
MEA	454,5
DEA	359,7
TEA	347,1
DGA	468,3

The choice of K-value

The Gas Processing Suppliers Association Engineering Data Book, (GPSA, 1987), recommends the following K-values for vertical drums with horizontal mesh pads (at the denoted operating pressures).

Table A.5 K-values for several operating pressures

Gauge Pressure [bar]	K-value [m/s]
0	0,107
7	0,107
21	0,101
42	0,092
63	0,083
105	0,065

GPSA Notes:

1. K= 0,107 m/s at a gauge pressure of 7 bar. Subtract 0,003 for every 7 bar above a gauge pressure of 7 bar.
2. For glycol or amine solutions, multiply above K-values by 0,6 – 0,8
3. Typically use one-half of the above K-values for approximate sizing of vertical separators without mesh pads
4. For compressor suction scrubbers and expander inlet separators, multiply K by 0,7 – 0,8

Table A.6 Energy Content of burned product required to create 1 kWh of Electrical Energy
Source: NATIONAL PETROLEUM COUNCIL, (Bellman et al., 2007)

Product Burned	Heat Rate [btu/kWh]	Heat Rate [kJ/kWh]
Natural Gas (with Carbon Sequestration)	7920	8350,45
Natural Gas	7200	7591,32

Note: Data taken in 2007, valid for power plants in America.
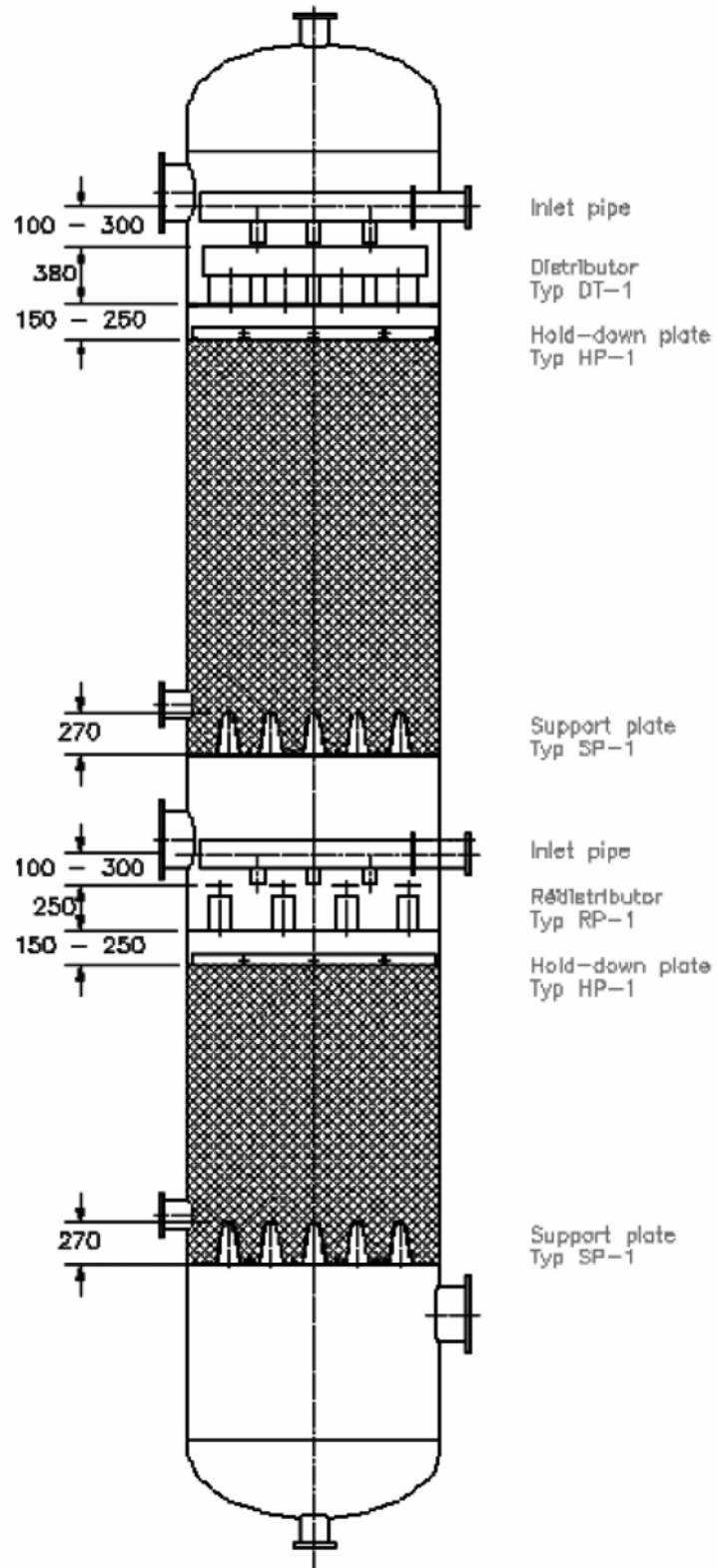
Figure A.2 Column internals for packed columns with a diameter greater than 700 mm
Source: (Schultes and Halbirt, 2010)
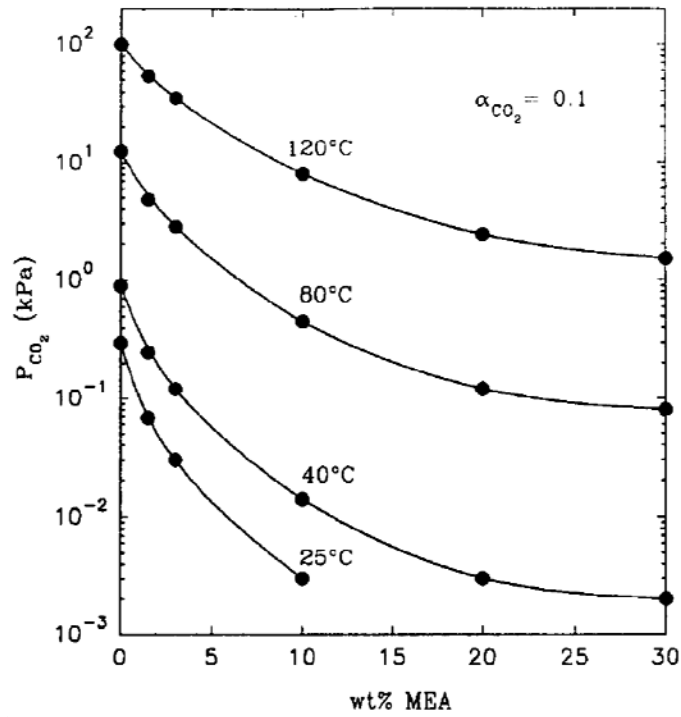
Figure A.3 Partial pressure of CO₂ as a function of composition at a_{co2}, = 0.1.
Source: (Jou et al., 1994)
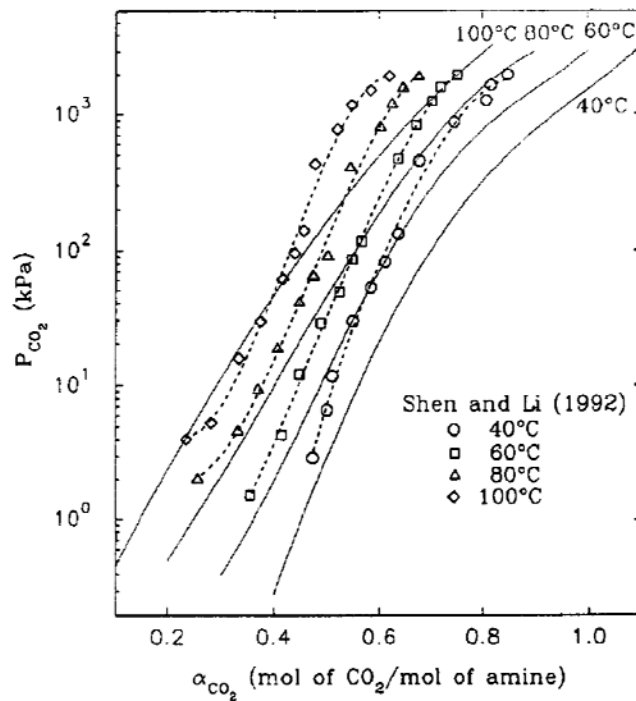
Figure A.4 Comparison of the solubility of CO₂ in 24 wt % MEA + 6 wt % MDEA solution.
Points and lines, Shen and Li (1992); solid lines, interpolation from this work.
Source: (Jou et al., 1994)
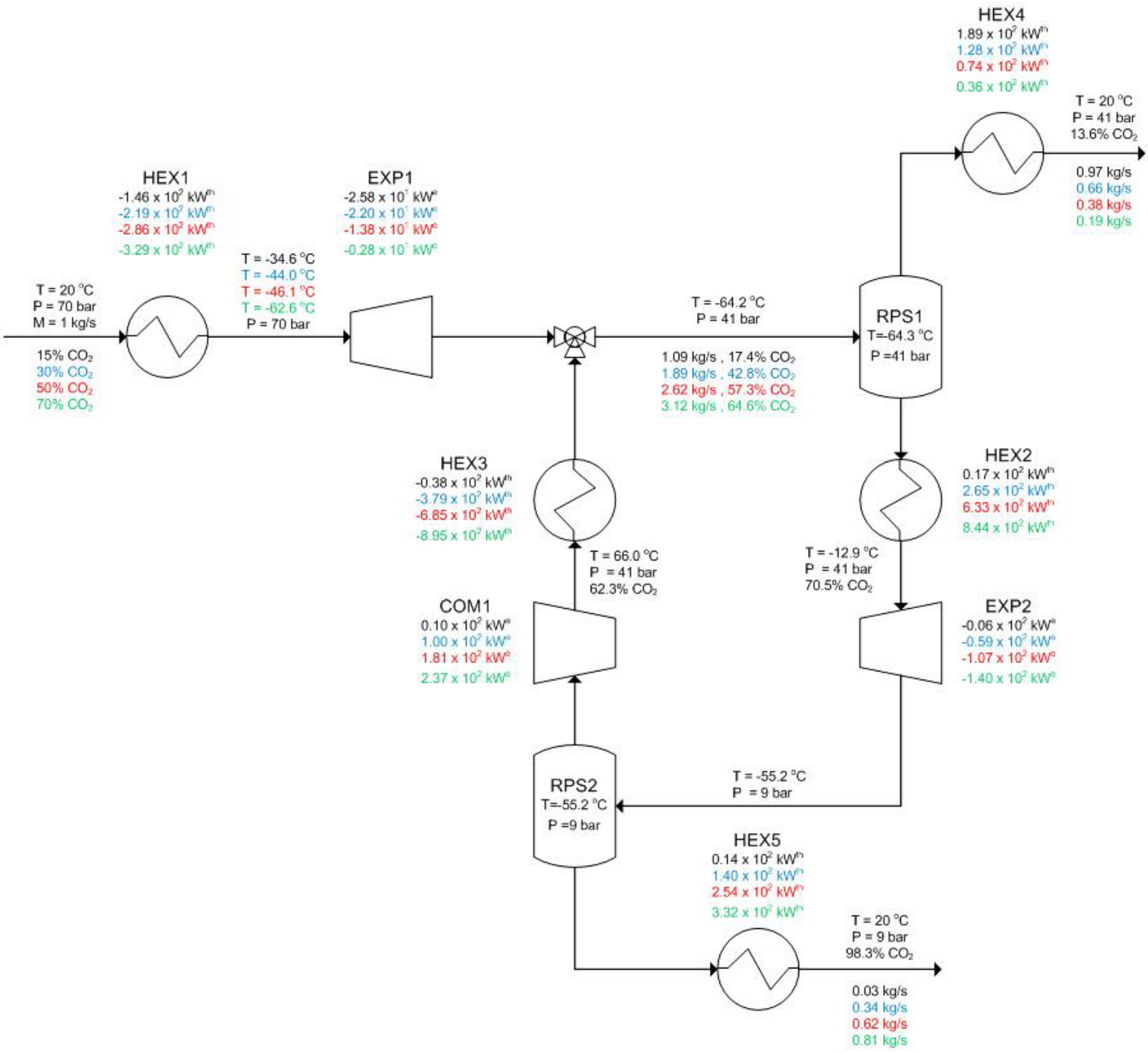
Figure A.5 Process flow diagram of the CRS process for 4 cases of CO2 concentration

Appendix B Amines treating – Process Description and Components
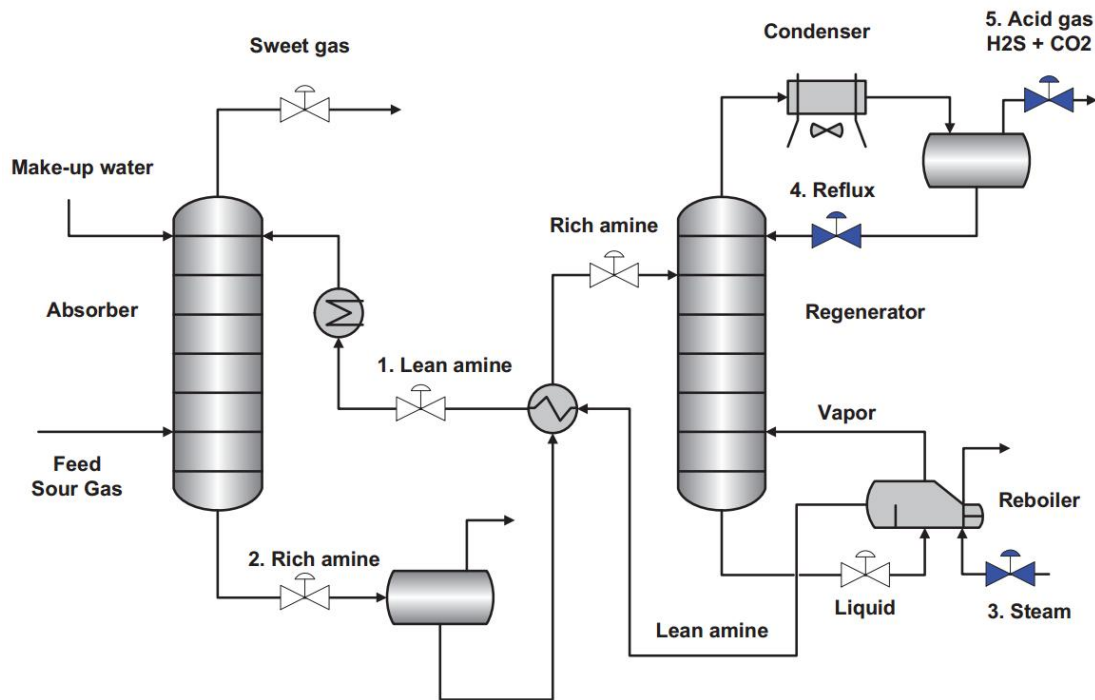
Figure B.1 Typical Amine Gas Sweetening Process Diagram

Amine gas treating, also known as gas sweetening and acid gas removal, refers to a group of processes that use aqueous solutions of various alkanolamines (commonly referred to simply as amines) to remove hydrogen sulfide and carbon dioxide from gases. H_2S and CO_2 are known as acid-(or sour-)gases, because in water or an aqueous solution they dissociate to form weak acids. The alkanolamines are weak organic bases. When the sour gas stream is contacted counter-currently with the aqueous solution, the acid gas and amine base react to form and acid-base complex, a salt. This salt is broken apart in the stripper when the acid gas rich amine is stripped by steam. It is a common unit process used in refineries, and is also used in petrochemical plants, natural gas processing plants and other industries.

B.1   Process Overview

A typical amine gas treating process (as shown in Figure B.1) includes an Absorber unit and a Stripping unit as well as accessory equipment. Varying terminology is used in the industry, the Absorber is also known as Treater, Contactor or Scrubber, while the Stripper is also known as Regenerator, Reactifier, Tower, Still, Still tower.

The inlet gas is contacted counter-currently with 'lean' solvent in the Absorber, containing multiple trays or packing. H_2S and CO_2 are removed from the gas by absorption into the solution. Rich solution from the absorber flows into a flash tank that is operated at lower pressure permitting the venting of any entrained light hydrocarbons from the system. The rich solution is then preheated and acid gases stripped from the solution, in the stripper and reboiler. This is done by heating the fluid (and vapor) in the reboiler to a temperature at which the bond between the solute and the amine breaks. The reboiler is essentially a heat-exchanger in which steam condensates and the tower bottom liquid is heated. The CO_2 and H_2S escapes from the liquid, leaving a lean amine solution behind. The lean solution is cooled and sent back to the absorber, while the vapor re-enters the tower and exchanges heat with the down coming liquid.

Many plants have multiple amine absorbers and a common amine regeneration unit.

B.2   Absorption Operating Principles

Absorption refers to the transfer of a gaseous component from the gas phase to a liquid phase. The opposite operation, known as stripping, involves the transfer of the contaminant from the liquid to the gas phase. Absorption occurs into liquid droplets dispersed in the gas stream, sheets of liquid covering packing material, or jets of liquid within the vessel. The liquid surface area available for mass transfer and the time available for diffusion of the gaseous molecules into the liquid are important factors affecting performance.

Absorption can be divided into two broad classifications:

1. Straight dissolution of *absorbate* (contaminant gas) into *absorbent* (liquid)
   - The gaseous contaminant being absorbed (absorbate) must be at least slightly soluble in the scrubbing liquid (absorbent). Mass transfer to the liquid continues until the liquid approaches saturation. At saturation, equilibrium is established between the two phases. In other words, the mass transfer rate of the contaminant into the liquid is equal to the mass transfer rate of the dissolved species back into the gas phase. Accordingly, the solubility of the contaminant in the liquid creates a limit to the amount of pollutant removal that can occur with a given quantity of liquid.
2. Dissolution accompanied by irreversible chemical reaction
   - The chemical reaction provides a means to overcome the solubility limit, by providing reactants in the liquid phase that react with the dissolved gas contaminant, forming a dissolved compound that cannot exit the liquid.

The amine process uses the latter type of absorption, but for completeness both processes are discussed in the next paragraphs.

B.2.1 Straight Dissolution of Absorbate
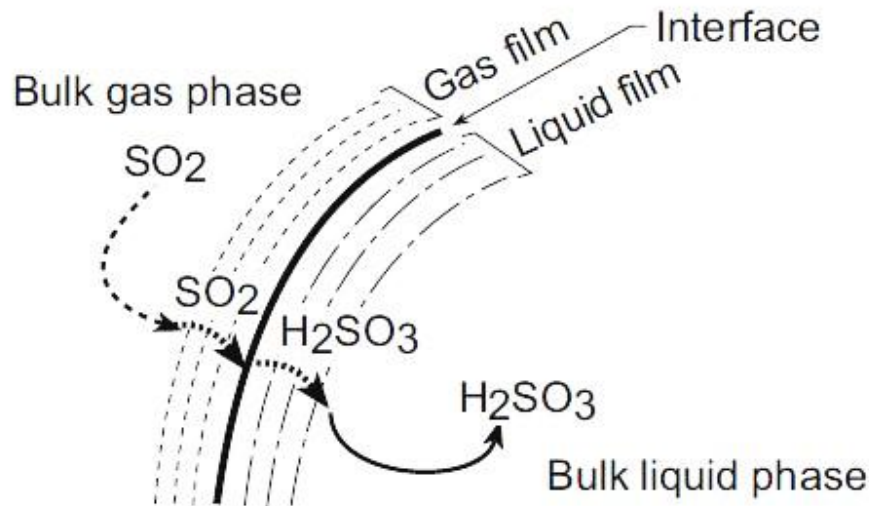
Figure B.2 Two Film Theory of Absorption

The gaseous contaminant (*solute*) in the bulk gas stream passing through the absorber is transported by turbulent diffusion to the boundary layer immediately adjacent to the liquid interface, as seen in Figure B.2 The contaminant then diffuses through this thin gas boundary layer, across the interface and then through the liquid boundary layer adjacent to the interface. Finally, the pollutant diffuses into the bulk portion of the liquid droplet.

If the dissolved form of the pollutant does not react, it can move in the direction opposite to the liquid phase; therefore, mass transfer goes in both directions. When the dissolved contaminant species reaches its saturation limit, the rates of mass transfer are equal in both directions. This is termed equilibrium. No additional contaminant removal occurs once equilibrium is established. Accordingly, it is important to design and operate absorbers so that equilibrium conditions are not reached. There are two ways to achieve this goal

1. Provide sufficient liquid so that the dissolved contaminants do not reach their solubility limit.
2. Chemically react the dissolved contaminants so that they cannot return to the gas phase.

B.2.1.1 Solubility

Solubility is the property of a solid, liquid, or gaseous chemical substance called solute to dissolve in a solid, liquid, or gaseous solvent to form a homogeneous solution of the solute in the solvent. The solubility of a substance fundamentally depends on the used solvent as well as on temperature and pressure. The extent of the solubility of a substance in a specific solvent is measured as the saturation concentration, where adding more solute does not increase the concentration of the solution.

Solubility is a function of the temperature of the liquid. Solubility of gases increases as the liquid temperature decreases. Gas phase pressure also influences solubility.

The solubility of a given solute in a given solvent typically depends on temperature. For many solids dissolved in liquid water, the solubility increases with temperature up to 100 °C. Gaseous solutes exhibit more complex behavior with temperature. As the temperature is raised, gases usually become less soluble in water, but more soluble in organic solvents.

The solubility of gases does not always decrease with increasing temperature. For aqueous solutions, the solubility usually goes through a minimum. For most permanent gases, the minimum is below 120 °C. It is often observed that the smaller the gas molecule (and the lower the gas solubility in water), then the lower the temperature at which the minimum occurs. Thus, the minimum is at about 30 °C for helium, 92 to 93 °C for argon, nitrogen and oxygen, and 114 °C for xenon. (Cohen, 1989)

The solubility of a specific gas in a given liquid is defined at a designated temperature. For example, Table B.1 presents data concerning the solubility of SO2 gas in water at various temperatures (atmospheric pressure). The units used to express the solubility are often the partial pressure of the contaminant in millimeters of mercury versus the quantity of the contaminant dissolved in the liquid in grams of per 100 grams of liquid. The data in Table B.1 is taken from the International Critical Tables.

Table B.1 Partial Pressure of SO$_2$ [mm Hg] Above Aqueous Solutions

gm SO$_2$ per 100 gm H$_2$O	10°C	20°C	30°C	40°C	50°C	60°C	70°C
0.0	0	0	0	0	0	0	0
0.5	21	29	42	60	83	111	144
1.0	42	59	85	120	164	217	281
1.5	64	90	129	181	247	328	426
2.0	86	123	176	245	333	444	581
2.5	108	157	224	311	421	562	739
3.0	130	191	273	378	511	682	897
3.5	153	227	324	447	603	804	-
4.0	176	264	376	518	698	-	-
4.5	199	300	428	588	793	-	-
5.0	223	338	482	661	-	-	-

B.2.1.2   Gas and Liquid Concentration Equilibrium lines - Henry's Law

The most common method of analyzing solubility data is to use an equilibrium diagram. This is a plot of the mole fraction of solute (contaminant) in the liquid phase, denoted as x, versus the mole fraction of solute in the gas phase, denoted as y. Equilibrium data for the SO2 and water system given in Table B.1 are plotted in Figure B.3. This figure illustrates the temperature dependence of the absorption process. At a constant mole fraction of solute in the gas (y), the mole fraction of SO2 in the liquid (x) increases as the liquid temperature decreases.
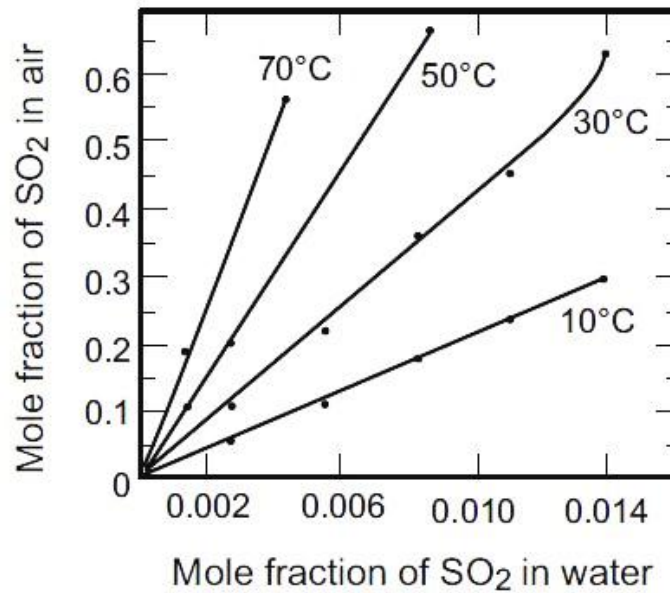
Figure B.3 SO₂ & Water System

Figures such as Figure B.3 are often created by acquiring experimental data on the gas-liquid concentration equilibrium.

In this particular case, the equilibrium lines are (approximately) straight. This means that the relationship between the gas phase concentration and the liquid phase concentration of the contaminant at equilibrium can be expressed by Henry's law, which states that the solubility of a gas in a liquid is directly proportional to the partial pressure of the gas above the liquid.

$$p^* = Hx \qquad (8.1)$$

Where:

      p^* = partial pressure of contaminant in gas phase at equilibrium
      H = Henry's law constant
      x = mole fraction of contaminant dissolved in the liquid phase at equilibrium

Henry's law can be written in a more useful form by dividing both sides of equation (8.1) by the total pressure, P, of the system. The left side of the equation becomes the partial pressure divided by the total pressure, which equals the mole fraction in the gas phase, y^*. It is important to express the contaminant concentrations in mole fraction as indicated in equation (8.2).

$$y^* = Hx \qquad (8.2)$$

Where:

      y^* = mole fraction of the contaminant in the gas phase at equilibrium
      H = Henry's law constant
      x = mole fraction of contaminant dissolved in the liquid phase at equilibrium

(Note: *H* is now dependent on the total pressure.)

Equation (8.2) is the equation of a straight line, where the slope (m) is equal to H. Henry's law can be used to predict solubility only in the range in which the equilibrium line is straight. This is the case when the contaminant concentrations are very dilute, as is the case in many air pollution control applications.

B.2.2 Dissolution accompanied by irreversible chemical reaction

A chemical reaction of the solute with a component in the liquid phase has the effect of increasing the liquid-film absorption coefficient over what would be observed with simple physical absorption. This results in an increase in the overall absorption coefficient in packed towers or an increase in tray efficiency in tray towers.
With very slow reactions, such as between carbon dioxide and water, the dissolved molecules migrate well into the body of the liquid before reaction occurs so that the overall absorption rate is not appreciably increased by the occurrence of the chemical reaction. In this case the liquid film resistance is the controlling factor, the liquid at the interface can be assumed to be in equilibrium with the gas, and the rate of mass transfer is governed by the molecular CO_2 concentration-gradient between the interface and the body of the liquid.
At the other extreme are very rapid reactions (such as those of ammonia with strong acids) where the dissolved molecules migrate only a very short distance before reaction occurs. The location of the reaction zone (and the value of the absorption coefficient) will depend primarily upon the diffusion rate of reactants and reaction products to and from the reaction zone, the concentration of solute at the interface and the concentration of the reactant in the body of the liquid.

B.2.2.1 Chemical reaction with Amines

The flow scheme for all amine sweetening units is similar.
The fundamental underlying principle is the exothermic, reversible reaction between a weak acid (e.g., CO_2) and a weak base (e.g., amine) to form a soluble salt.
For instance, MEA reacts with CO_2 and H_2S as:

$$2\left(RNH_2\right)+CO_2 \underset{T_{high}}{\overset{T_{low}}{\rightleftharpoons}} RNHCOONH_3R \qquad (8.3)$$

$$2\left(RNH_2\right)+H_2S \underset{T_{high}}{\overset{T_{low}}{\rightleftharpoons}} \left(RNH_3\right)_2 S \qquad (8.4)$$
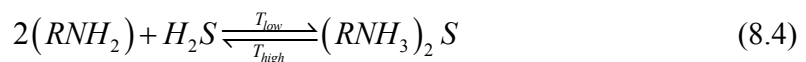
This reaction is a lot faster than e.g. the reaction of CO_2 with H_2O. Also the reaction can only be reversed by adding heat to break the bonds between the amine and the solute.

B.3   Stripping Operating Principles

Stripping refers to breaking the bond between the amines and the solute (CO_2 and/or H_2S) by heating the rich amine stream. The other name of this tower, regenerator, refers to regenerating the lean amine from the rich amine by stripping it of the solute.
As amines are costly, it's common practice to use a stripper to regenerate the rich amine into lean amine.

The amine is stripped from the solute with heat added to the solution in the reboiler. The reboiler boils the solution, supplying heat to break the bond between amine and solute and creating steam from the solution, which flows upward through the tower, in counter-current with the rich amine solution, heating the solution before it enters the reboiler. The heated steam also lowers the partial pressure of H_2S and CO_2 in the gas stream, enhancing the driving force of the acid gases from the amine solution.
Once the bond between amine and solute is broken the solute becomes a gas once again and flows upward with the steam towards the top of the tower, also exchanging heat with the down coming rich amine. The vast majority of the stripping should occur in the stripper column rather than in the reboiler itself. If substantial stripping occurs in the reboiler, excessive corrosion and premature reboiler failure is likely, especially in applications with substantial CO_2 contamination. A detailed explanation of the reboiler and its heat duty is given in section B.6.

On the top of the tower, the overhead gas passes through a condenser to recover water and the small amount of amine that is vaporized in the stripper. The regeneration requirement to reach a typical lean loading is a reflux ratio of 1,0 to 3,0. This value is found in (Sheilan et al., 2009), (RefiningOnline, 2007) & (Kohl and Nielsen, 1997). This refers to the number of moles of steam per mole of sour gas in the stripper. A reflux ratio of 1,0 should be considered as a practical minimum. In some low pressure or tail gas treating applications, higher reflux ratios may be required to meet the product specifications.

The overhead condenser, the reboiler tube bundle, and the upper third of the stripping column shell are all susceptible to high corrosion rates, and may need to be manufactured out of stainless steel. Thermal degradation, which can contribute to corrosion, can be minimized by designing the reboiler to use a low temperature heating medium such as low pressure steam.

B.4 Amines

There are several types of amines available, which are introduced in this section. Also some information is shown on the solution concentration of amines and the preferred loading of these amines. The choice of amine, concentration and loading is of great impact on the efficiency and energy use of the process and the amount of corrosion in the installation.

B.4.1 Alkanolamine Solvents

Alkanolamines have three functional groups: an amino nitrogen, an alcohol(hydroxyl group and an alkane (hydrocarbon) arm. In general, the hydroxyl group serves to reduce vapor pressure, modify base strength and increase water miscibility, while the amino group provides the necessary alkalinity in water solutions to promote the reaction with acid gases. Also, all the alkanolamines have at least one alkane (hydrocarbon) arm that separates the hydroxyl and amino group and provides a degree of chemical stability. The alkanolamines are classified by the degree of hydrocarbonhydroxyl substitution on the central nitrogen;

- a single substitution denoting a primary amine
- a double substitution denoting a secondary amine
- a triple substitution denoting a tertiary amine
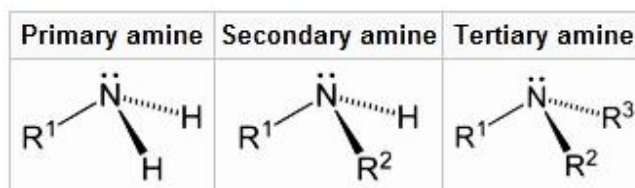
Figure B.4 Types of Amines

It is readily apparent, by looking at the molecular structures of the alkanolamines in Figure B.4, that the non-fully substituted alkanolamines have hydrogen atoms at the non-substituted valent sites on the central nitrogen, whereas the tertiary amines are fully substituted on the central nitrogen. This structural characteristic plays an important role in the reaction chemistry and thus the acid gas removal capabilities of the various gas treating solvents. The number, size and type of alkane groups attached to the central amino group determine the different physical and chemical properties of the solvent.

Some examples of alkanolamine solvents include:
- Monoethanolamine (MEA)
- Diethanolamine (DEA)
- Diglycolamine Agent (DGA)
- Methyldiethanolamine (MDEA)
- Diisopropanolamine (DIPA)

Whilst all alkanolamine solvents are within the same classification, available ranges of concentration and loading per amine varies quite a lot.

This work will focus on Monoethanolamine, because the use of MEA in gas treating applications is well established and the subject of a tremendous amount of literature.

The advantages of MEA include, according to (Sheilan et al., 2009):

- Low Cost
- Good Thermal Stability
- Partial Removal of COS and CS_2, which does however require a reclaimer to be added to the process.
- High reactivity due to its primary amine character, a 4 ppmv H_2S specification can usually be achieved and CO_2 removal to 100 ppmv for applications at low to moderate operating pressures
- Easily reclaimed to concentrate irreversible degradation products.

Some of the disadvantages of MEA are:

- High solvent vapor pressure, which results in higher solvent losses than the other alkanolamines
- Higher corrosion potential than other alkanolamines
- High energy requirements due to the high heat of reaction with H_2S and CO_2
- Nonselective removal in a mixed acid gas system
- Formation of irreversible degradation products with CO_2, COS and CS_2, which requires continuous reclaiming. The MEA-CO_2 degradation reaction produces the following: oxazolidone-2, 1-(2-hydroxyethyl) imidazolidone-2, N-(2-hydroxyethyl) ethylenediamine (HEED) and higher polyamines which accelerate corrosion in addition to representing a loss of MEA.

B.4.2   Other solvents used in gas treating

In addition to the alkanolamines, there are a number of other solvents which utilize a process scheme very similar to the basic gas treating plant process flow used in gas treating applications. The other solvent technologies can be segmented in to the following categories:

- Hindered amines
- Physical Solvent Processes
- Mixed Chemical/Physical Solvent Processes

In some refinery processes only H_2S needs to be eliminated from a gas stream which contains both CO_2 and H_2S. Because the amount of circulated amine has a strong effect on the cost, it's interesting to decrease the amount of amine required to separate the H_2S from the stream. Therefore a selective amine is used. Selectivity means that the amine is more likely to bond with a certain contaminant than to bond with another type of contaminant (e.g. twice as likely to bond with H_2S as with CO_2).

B.4.2.1   Hindered amine technology

Hindered amine technology is an example of a selective amine and a prime example of hindered amine technology is the Flexsorb® family of solvents. (Goldstein et al., 1986). These solvents are designed with a bulky hydrocarbon-hydroxyl arm on the central amino group which physically prevents reaction of CO_2 due to the steric hindrance. Extremely high levels of selectivity have been exhibited in some applications. The Flexsorb® technology has carved out a niche in the industry in applications that require acid gas enrichments. The principal disadvantage of the technology is the high cost of the solvent which can be 5 to 10 times that of other amines.

B.4.2.2   Physical Solvent Processes

Physical solvent processes such as Selexol®, Rectisol® and Morphysorb® are based on physical adsorption of the acid gases and operate with a flow scheme significantly different than the basic alkanolamine process flow. Through the basic process scheme for a physical solvent process is more complex; these processes can be economically attractive because less energy is required for regeneration. These solvents are regenerated by:

- Multi-stage flashing to low pressures.
- Regeneration at low temperature with inert stripping as.
- Heating and stripping of solution with steam/solvent vapors in the conventional manner.

In general, these processes should be considered when:

- The partial pressure of the acid gas in the feed is greater than 50 psi.
- The hydrocarbon content of the feed gas is low
- Selective removal of H_2S is desired.

The principal disadvantages of the physical solvent processes are:

- Very high solubility for heavy hydrocarbons, particularly: aromatics(BTEX) and olefinic hydrocarbons
- Not viable at low acid gas partial pressures.

B.4.2.3   Mixed Chemical/Physical Solvent Processes

Mixed chemical/physical solvent processes such as the Sulfinol® process, utilize a mixture of a chemical solvent, typically DIPA or MDEA, with a physical solvent, Sulfolane®. The process combines the advantages of both solvents; using the physical solvent to achieve bulk acid gas removal while employing the chemical solvent to achieve specification product. The advantages of a mixed chemical/physical solvent process include:

- Applicability for a wide range of H_2S and CO_2 removal applications
- High degree of trace sulfur removal
- Low energy requires
- Low circulation rate

The disadvantages of a mixed chemical/physical solvent process include

- Higher co-adsorption of heavier hydrocarbons (especially aromatics)
- Probable requirement for a solvent reclaimer
- Expensive chemical costs
- License fee required

B.4.3   Amine Concentration

The choice of amine concentration may be quite arbitrary and is usually made on the basis of operating experience.

Typical concentrations of monoethanolamine range from 12 wt% to a maximum of 32 wt%. On the basis of operating experience in five plants, (Feagan et al., 1954) recommended the use of a design concentration of 15 wt% monoethanolamine in water. The same solution strength was recommended by (Conners, 1958). (Dupart et al., 1993) recommends a maximum MEA concentration of 20 wt%. However, it should be noted that higher amine concentrations, up to 32 wt% MEA, may be used when corrosion inhibitors are added to the solution and when CO_2 is the only acid gas component. (Sheilan et al., 2009) states that MEA is typically used at 15-20 wt% concentration.

Diethanolamine solutions that are used for treatment of refinery gases typically range in concentration from 20 to 25 wt%, while concentrations of 25 to 30 wt% are commonly used for natural gas purification.

Diglycolamine solutions typically contain 40 to 60 wt% amine in water
MDEA solution concentrations may range from 35 to 55 wt%.
(Kohl and Nielsen, 1997)

It should be noted that increasing the amine concentration will generally reduce the required solution circulation rate and therefore the plant cost. However, the effect is not as great as might be expected, the principal reason being that the acid-gas vapor pressure is higher over more concentrated solutions at equivalent acid-gas/amine mole ratios. In addition, when an attempt is made to absorb the same quantity of acid gas in a smaller volume of solution the heat of reaction results in a greater increase in temperature and a consequently increased acid-gas vapor pressure over the solution.

B.4.4   Amine Loading

Rich/Lean Amine Loading, in other words the amount of acid gases contained within a given amount of amine, is critical in the operation, maintenance and performance of an amine plant.

Rich Amine Loading, (RAL), is determined by measuring the amount of acid gas contained in the amine stream exiting the Absorber. This is typically represented in a molar ratio [(mol of CO_2 + mol of H_2S)/mol amine]. Generally speaking, this measurement is almost impossible to accurately measure in the field or in a lab, so plant simulations are often times used to determine the RAL and adjust amine circulation rates and concentrations to meet desired results. As RAL increases above a value of 0.40 mol AG/mol amine, several detrimental effects may be encountered, especially in an all CO2 acid gas system. These effects may include higher corrosion rates, higher temperature bulges within the Contactor and lower recovery of the acid gases, due to slower reaction kinetics and capacity. Thus, if the Rich Amine Loading exceeds recommended limits, acid gas breakthrough may occur, process piping may erode/corrode (resulting in piping failures) and equipment may fail. For these reasons regular audits of amine plant operation are recommended, while also employing corrosion inhibitors and stainless steel materials in the most critical areas of the plant.(Kohl and Nielsen, 1997)

Lean Amine Loading (LAL) is determined by measuring the amount of acid gas contained in the amine stream exiting the stripper/reboiler and is measured in the same manner as the RAL described above. This is a much easier and more reliable measurement, though simulation results can still be used to check the collected data. LAL values will vary, depending on the type of amine being used. For MEA, which is one of the most corrosive amines, a LAL of up to 0.18 mol/mol may be seen, while in an MDEA system (one of the weakest and least corrosive amines) a LAL of 0.005 mol/mol is not uncommon. Lean Amine Loading will be affected by the reboiler duty, reflux ratio and the number of fractionation stages within the Amine Still. If the lean amine is not properly stripped of the acid gases corrosion may be encountered in the hot portions of the plant, specifically the Amine Still Reboiler and associated piping. Also, if the LAL is too high, the ability of the amine to remove the acid gases from the inlet gas stream in the Amine Contactor may be diminished and product specifications may not be met. This is especially true of MDEA systems that try to meet a very low level H2S specification.

Therefore, when designing and operating an amine plant, care should be given to making sure the system is large enough to avoid overloading the amine with acid gases (high RAL) and ensuring that the stripper has sufficient capabilities to properly strip the acid gases from the amine (low LAL)

B.5　Absorber and stripper columns

Cutaway section of a plate column
a) Downcomer; b) Tray support;
c) Sieve trays; d) Manway; e) Outlet weir;
f) Inlet weir; g) Side wall of downcomer;
h) Liquid seal

Cutaway section of a packed column
with a structured wire gauze packing
(Sulzer)
a) Liquid distributor; b) Liquid
collector;
c) Structured packing; d) Support
grid;
e) Manway; f) Liquid redistributor
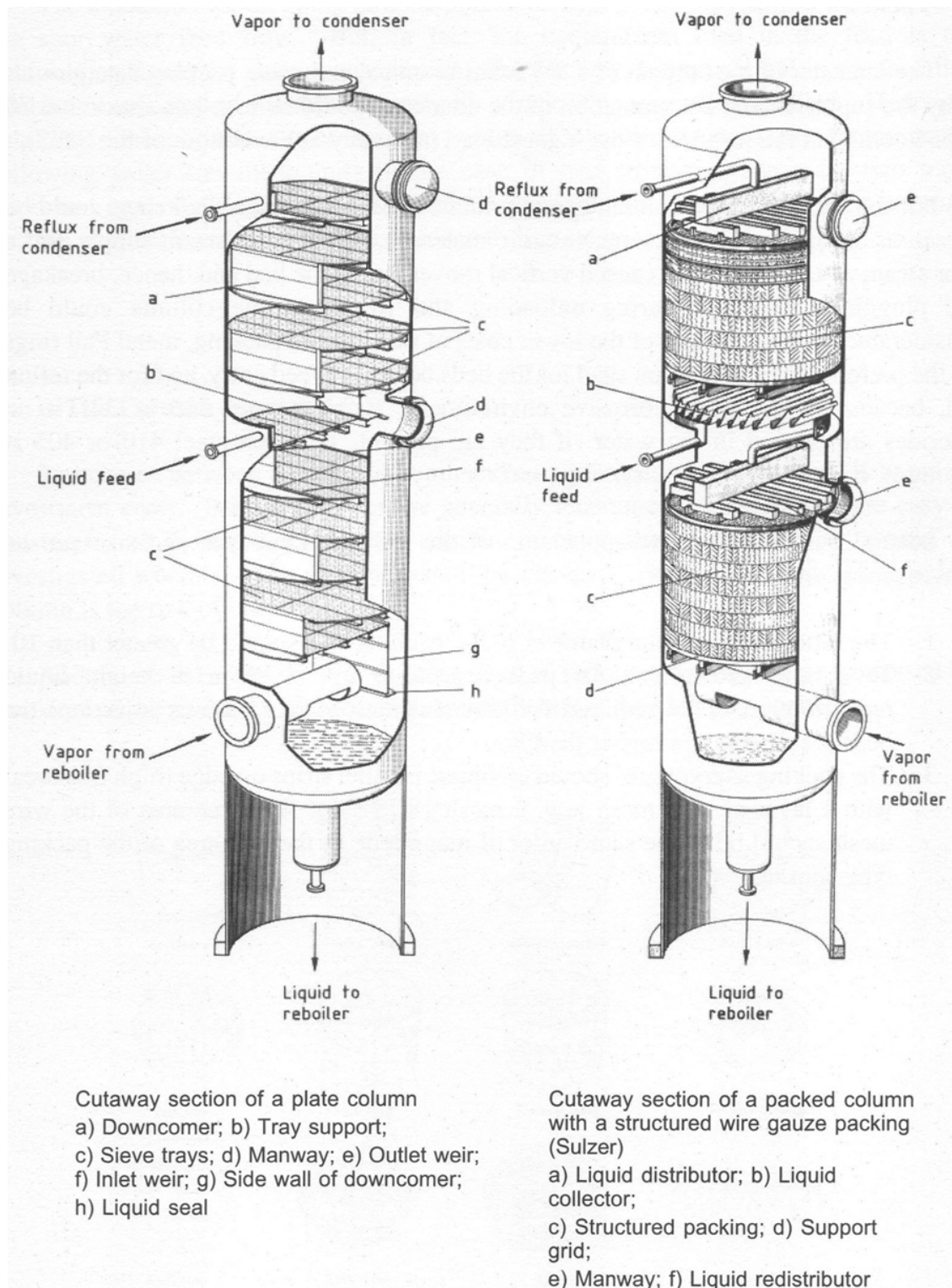
Figure B.5 Cutaway sections of tray and packed columns used for stripping.
Source: (Sheilan et al., 2009)

Three types of devices are commonly used for liquid contacting with alkanolamines. These devices are Packed Bed (Random and Structured Packing), Sieve Tray and Spray Tower columns. Of these, the Random Packed and Sieve Tray Columns are the most prevalent, but structured-packed columns are being used effectively in more and more applications. The selection of equipment depends on the treating requirement and the specific needs of the operation. Each type of device offers its own unique advantages and disadvantages which will be discussed in detail.

B.5.1   Packed Bed Columns

Packed bed columns are the most common columns used for gas removal. Packed columns disperse the scrubbing liquid over packing material, which provides a large surface area for gas-liquid contact. Packed beds are classified according to the relative direction of gas-to-liquid flow.

The most common packed bed column is the **counter-current flow** tower shown in Figure B.5 (on the right). The gas stream being treated enters the bottom of the tower and flows upward through the bed of packing material.
Liquid is introduced at the top of the packed bed by sprays or weirs and flows downward over the packing material, resulting in the highest theoretically achievable efficiency.
In an absorber, the most dilute gas is put into contact with the least saturated absorbing liquor. Accordingly, the maximum concentration difference between the gas phase contaminants and the dissolved concentration of the contaminant in the liquid is at the top of the packed bed. This concentration difference provides a driving force for continued absorption.

In a **cross-flow** packed bed vessel, the gas stream flows horizontally through the packed bed, which is irrigated by the scrubbing liquid flowing down through the packing material. A typical cross-flow set-up is shown in Figure B.6. Inlet sprays aimed at the face of the bed (not shown in Figure B.6) may also be included. The leading face of the packed bed is often slanted in the direction of the in-coming gas stream. This ensures complete wetting of the packing by allowing the liquid at the front face of the packing enough time to drop to the bottom before being pushed back by the entering gas. Cross-flow absorbers require complex design procedures because concentration gradients exist in two directions in the liquid: from top to bottom and from front to rear. More importantly, the cross-flow process cannot reach the values of enrichment of counter-flow. However it is a more compact design.
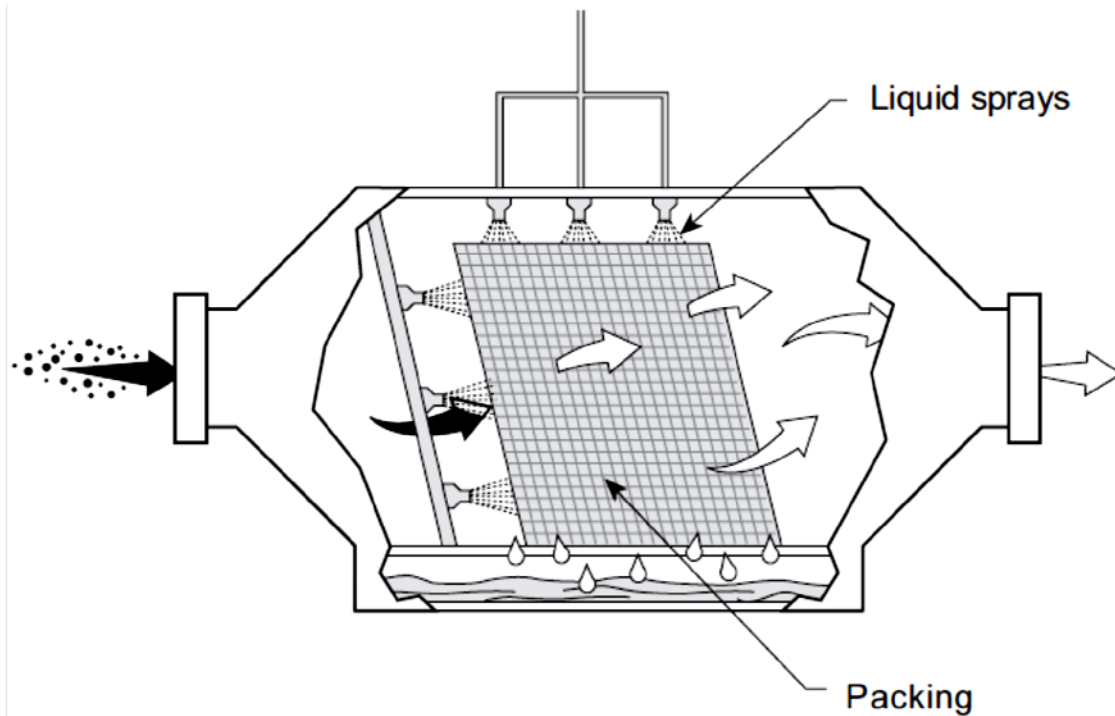
Figure B.6 Flowchart of cross-flow scrubber

Large variations in liquid or gas flow rates cause loading and flooding of this type of absorber, see section C.1.2.1. Packed bed absorbers are most suited to applications where high gas removal efficiency is required and the exhaust stream is relatively free from particulate matter.

Packing material may be arranged in an absorber in either of two ways. The packing may be dumped into the column randomly or stacked as structured material. Randomly packed towers provide a higher surface area (m^2/m^3), but also cause a higher pressure drop than stacked packing. In addition to the lower pressure drop, the stacked packing provides better liquid distribution over the entire surface of the packing. This work will focus on random packing.

B.5.1.1 Types of Random Packing

Packing serves a number of purposes. (Strigle, 1987). First and foremost, packing increases the gas-liquid interfacial area. Secondly packing reduces the likelihood of back mixing of the solvent within the column. Third, the packing distorts, coalesces and disperses the droplets to enhance internal circulation and refresh the film surface for mass transfer.

There are several types of random packing available. Figure B.7 illustrates some of the most commonly used packing types. These packing types are usually made of plastic, but can be ceramic or metal. A specific packing is described by its trade name and overall size. For example, a column can be packed with 2-inch (5-centimeter) Raschig™ rings or 1-inch (2.5-centimeter) Tellerettes™. The overall dimensions of packing materials normally range from 1 to 4 inches (2.5- to 10.1-centimeter).
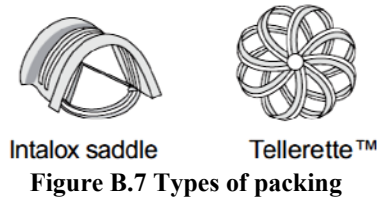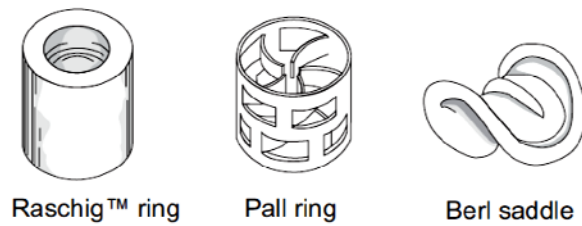
Figure B.7 Types of packing

Figure B.8 Example IMTP-packing manufactured by Koch-Glitsch

The specific packing selected depends on the nature of the corrosiveness of the contaminants and scrubbing liquid, the size of the absorber, the static pressure drop and the cost.

Specific considerations involved in the selection of packing materials are summarized below.

- **Cost.** Plastic packings are generally cheaper than metal, with ceramic being the most expensive.
- **Low-pressure drop.** Pressure drop is a function of the volume of void space in a tower when filled with packing. Generally, the larger the packing size, the smaller the pressure drop.
- **Corrosion resistance.** Ceramic or porcelain packing is commonly used in a very corrosive atmosphere.
- **Structural strength.** Packing must be strong enough to withstand normal loads during installation, service, physical handling, and thermal fluctuations. Ceramic packing is subject to cracking under sudden temperature changes.
- **Weight.** Heavier packing may require additional support materials or heavier tower construction. Plastics are much lighter than either ceramic or metal packings.
- **Void Fraction**. Packing that has a low void fraction leaves less space for the gas and liquid to flow through, resulting in larger columns.
- **Design flexibility.** The efficiency of a scrubber changes as the liquid and gas flow rates are varied. Packing material must be able to handle the process changes without substantially affecting the removal efficiency.

B.5.1.2   Liquid Distribution.

One of the requirements for efficient absorption is good gas-liquid contact throughout the entire packed bed. The performance of the liquid distributors in the absorber is important to achieve good gas-liquid contact.

Liquid should be distributed over the entire upper surface of the packed bed. This is commonly achieved by weirs or feed tube arrangements as shown Figure B.9. Arrays of spray nozzles are also used. However, distributors similar to the units are more flexible with respect to variations in the liquid recirculation rate.

(a) Riser orifice

(b) Notched riser

(c) Trough and weir type

(d) Perforated pipe
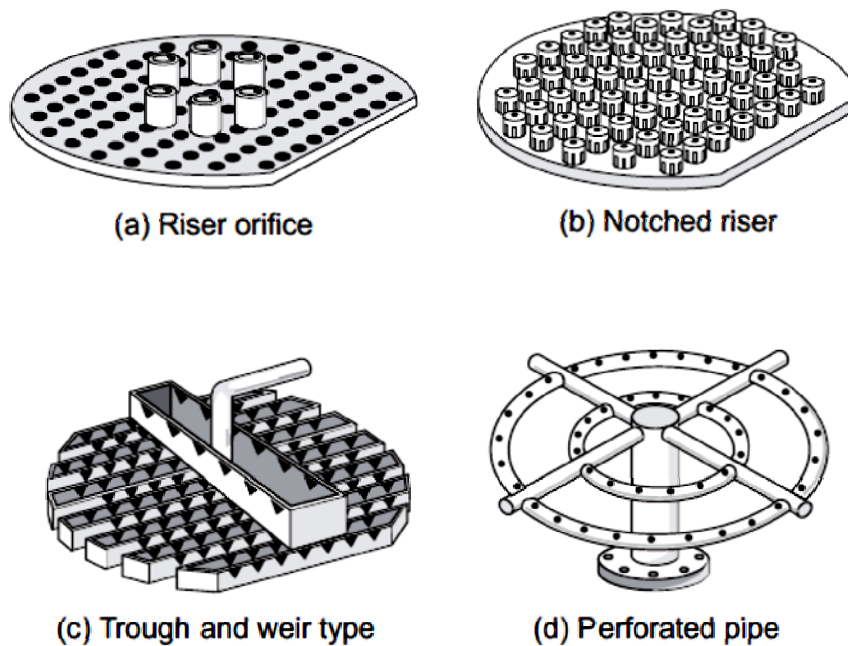
Figure B.9 Types of liquid distributors for packed bed absorbers
Source: (APTI, 1999)

Once the liquid is distributed over the packing, it flows down by the force of gravity through the packing, following the path of least resistance. The liquid tends to flow toward the tower wall where the void spaces are greater than in the center. Once the liquid hits the wall, it flows straight down the tower (channels).

It is necessary to redirect the liquid from the tower wall back to the center of the column. Liquid redistributors are used to funnel the liquid back over the entire surface of packing. Redistributors are usually placed at intervals of no more than 10 feet (3.1 meters), or 5 tower diameters, whichever is smaller. (APTI, 1999)

Another reason to limit the continuous height of packing is the deformability of the packing under its own weight. (Kohl and Nielsen, 1997) state that for every form of random packing the maximum height of packing is 20-25 feet (6-7,5 meters) for metal packing and 10-15 feet (3-4,5 meters) for plastics.

Uniform distribution of the inlet gas stream is also very important for achieving good gas-liquid contact. This is accomplished by properly designing the inlet gas ducts and the support trays that hold the packing material.

B.5.2   Tray Columns

A tray tower absorber is a vertical column with one or more trays mounted horizontally inside for gas-liquid contact. The gas stream enters at the bottom and flows upward, passing through openings in the plates. Liquid enters at the top of the tower and travels across each tray, then through a downcomer to the tray below until it reaches the bottom of the tower. Mass transfer occurs in the liquid spray created by the gas velocity through the openings in the tray. Figure B.10 illustrates a typical tray tower unit.
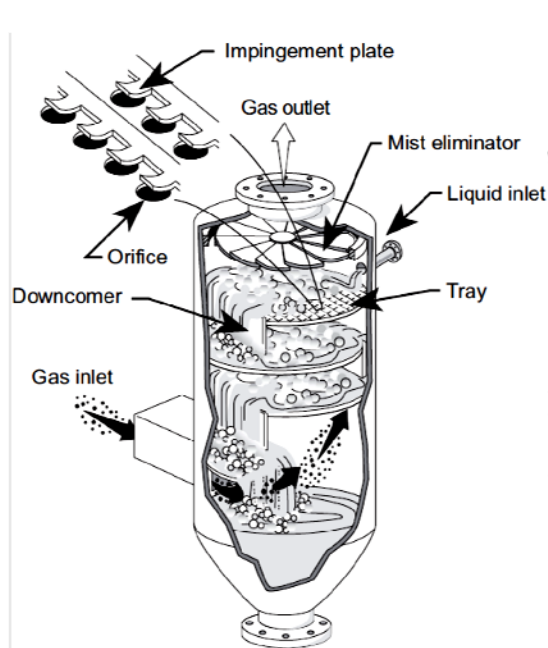
Figure B.10 Impingement Tray Tower   **Figure B.11 Bubble Cap Tray Tower**
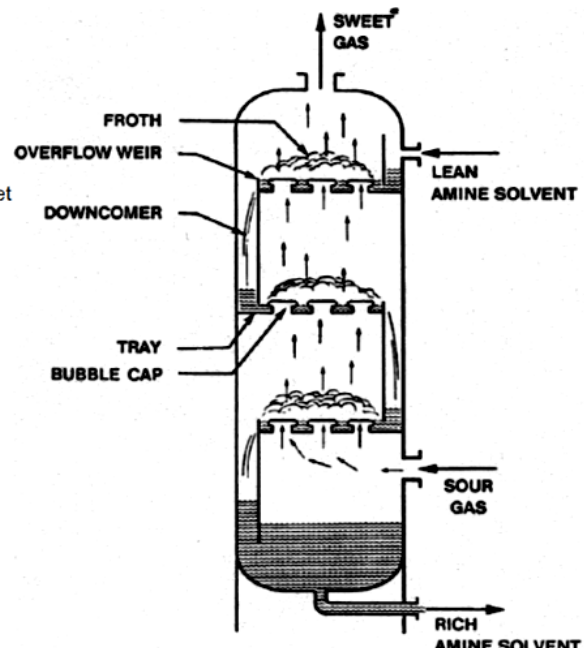
The function of the trays is to disperse the liquid into droplets and the gas into bubbles, thereby creating large gas-liquid interface areas for mass transfer. The gas passes up from underneath the trays through openings in the trays such as perforations, bubble caps, or valves, and disperses into bubbles through the liquid, forming a froth.

The gas disengages from the froth, travels through a vapor space, providing time for the entrained amine solution to fall back down to the liquid on the tray, and passes through the next tray above. Nearly all absorption of H_2S and CO_2 takes place on the trays, and not in the vapor space between the trays.

A variety of different tray designs are available. The most common types are impingement trays and sieve trays.

- **Impingement Trays**. The gas stream passes through orifices in the impingement tray that are usually 3/16 in. (0.48 cm) in diameter. Due to high gas velocities, the liquid passing across the tray is atomized. Small impingement targets above each orifice are used to enhance gas-liquid contact immediately above the tray. The liquid layer across the impingement tray is maintained at 0.75 to 1.5 in. (1.9 to 3.8 cm) by means of an overflow weir on the discharge side of the tray. Most impingement tray absorbers have two to three trays in series.
- **Sieve Trays**. The orifices in sieve tray absorbers range from 0.25 to 1 in. (0.64 to 2.5 cm) in diameter. Because of these relatively large openings, the sieve trays are less prone to solids accumulation and pluggage of the orifices than the impingement tray units that have smaller orifices. Mass transfer in sieve tray absorbers occurs because of mass transfer from gas bubbles to the liquid layer and from the bulk gas stream to liquid droplets formed above the orifices.
- **Bubble Cap Trays**. The gas stream enters the liquid layer through bubble caps mounted on the trays. This type of unit can handle wide ranges of gas and liquid rates without adversely affecting efficiency. Because bubble caps are liquid tight, this type of tray can use very low liquid rates.
- **Float Valve™ Trays.** The gas stream flows up through small holes in the tray and lifts up metal valves or caps that cover the openings. The valves are restrained by legs that limit vertical movement. The liftable caps act as variable orifices and adjust the opening for gas flow proportional to the gas flow rate through the absorber.

High removal efficiencies are possible because of the good gas-liquor contact that can be achieved on a tray. The use of several trays in series also ensures that gas-liquid maldistribution on a single tray does not severely limit the efficiency of the overall absorber.

B.5.3 Spray Tower Absorbers

Spray towers are the simplest devices used for gas absorption. They consist of an open vessel and a set of liquid spray nozzles to distribute the scrubbing liquid (absorbent). Typically, the contaminant gas stream enters the bottom of the tower and passes upward through the vessel. Figure B.12 is a typical co-current flow-type spray tower absorber. Source: (APTI, 1999)
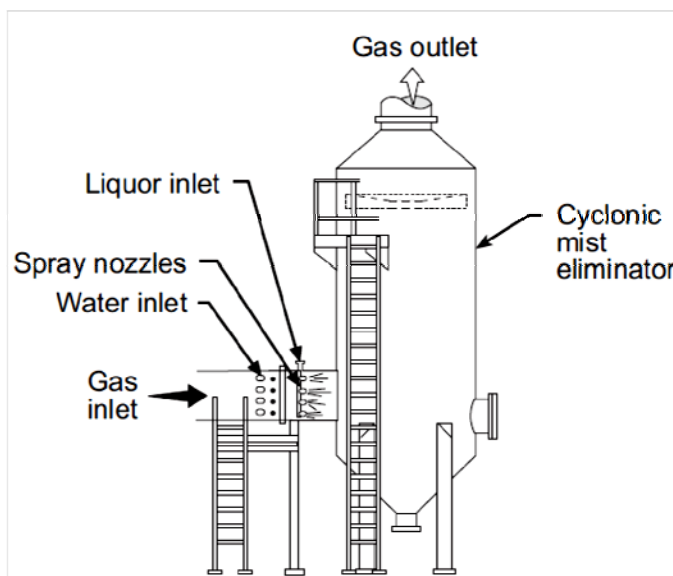
Figure B.12 Co-current Gas Flow Spray Tower Scrubber   **Figure B.13 Full cone nozzle**
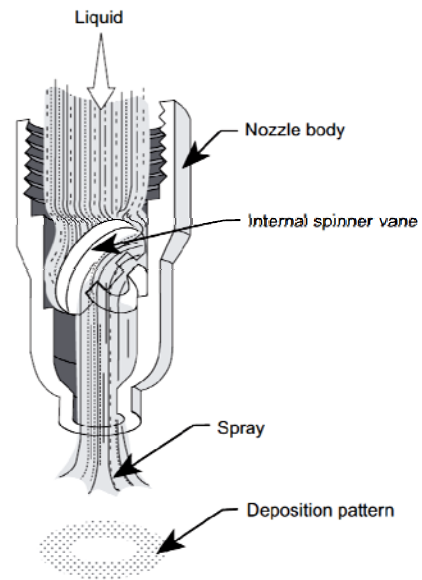
Spray chambers can operate in cross-current or co-current flow arrangements when there is limited space in an industrial facility, because higher gas velocities can be achieved. However, counter-current units remain the most efficient. One of the main components of spray tower absorbers is the spray nozzle. Various types of full cone nozzles are often used. A full cone nozzle, as shown in Figure B.13, generates a spray pattern that completely fills the target area.

The main advantage of spray tower absorbers is that they are completely open. They have no internal components except for the spray nozzles and connecting piping. Therefore they have a very low gas stream static pressure drop.

However because of the limited contact between the liquid droplets and the gas stream, spray tower absorbers can have very limited capability for removing pollutants. They are used primarily in applications where the gases are extremely soluble in the absorbent, where high pollutant removal efficiency is not required, or where the chemical reactions in the absorbing liquid could result in salts that could cause plugging in other types of absorber vessels. They have been used to control SiF_4 and HF generated in fertilizer plants during the production of superphosphate. Spray towers are also used in a number of flue gas desulfurization systems. (APTI, 1999)

B.6 Kettle Reboiler

The Kettle Reboiler is used to heat the tower bottoms (lean amine) stream to vaporize the last of the captured CO_2 and H_2S from the liquid. The vapor returns to the stripper, while the lean amine is pumped from the bottom of the Reboiler. A schematic of a typical Kettle Reboiler is given in Figure B.14.
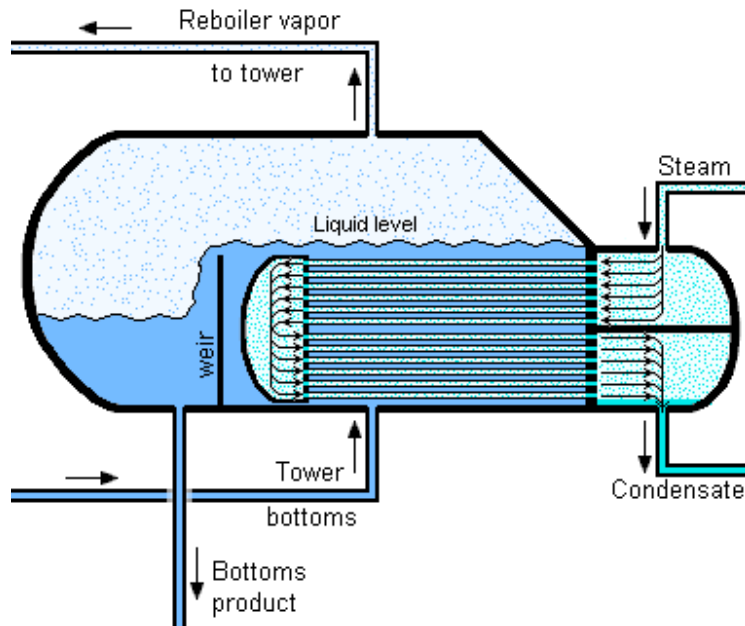
Figure B.14 Schematic of a Kettle Reboiler

The reboiler heat duty includes
- The sensible heat required to raise the temperatures of the rich amine feed, the reflux, and the makeup water to the temperature of the reboiler,
- The heat of reaction to break chemical bonds between the acid gas molecules and the amine
- The heat of vaporization of water to produce a stripping vapor of steam.

$$
\underbrace{\dot{m}_{steam} \cdot \dot{Q}_{cond} (T_{steam}, P_{steam})}_{\text{Steam Condensation}} =
$$

$$
\underbrace{\dot{m}_{vapor} \cdot \dot{Q}_{vaporisation} (T_{liquid}, P_{liquid})}_{\text{Water Vaporization}}
$$

$$
+ \underbrace{\dot{Q}_{reaction} \cdot \dot{m}_{CO_2}}_{CO_2 \text{ stripping}} + \underbrace{\dot{Q}_{reaction} \cdot \dot{m}_{H_2S}}_{H_2S \text{ stripping}}
$$

$$
+ \underbrace{\dot{m}_{rich} \cdot c_p \cdot \Delta T}_{\text{Heating Rich Stream}} + \underbrace{\dot{m}_{reflux} \cdot c_p \cdot \Delta T}_{\text{Heating Reflux}}
$$

(8.5)

In order to strip the Rich Amine stream from its CO_2 and/or H_2S this stream has to be heated to a certain temperature in the tower and reboiler. This temperature is the temperature at which the bond between the amine and the CO_2 and/or H_2S breaks. The value of this temperature depends on the type of amine used.

"For a MEA absorption system, a consensus exists that the reboiler temperature should be approximately 120 to 125 °C in order to prevent solvent degradation and corrosion. Assuming a 124 °C temperature in the reboiler and ten degree pinch, the reboiler should use saturated steam at 134 °C and approximately 3 bar." (Bashadi and Herzog, 2011) "To prevent thermal degradation of the amine solvent, steam or hot oil temperatures providing heat to the reboiler should not exceed 350 °F (177 °C). Superheated steam should be avoided. 50 psig (350 kPa) saturated steam is recommended. The maximum bulk solution temperature in the reboiler should be limited to 260 °F (127 °C) to avoid excessive degradation." (Sheilan et al., 2009)

B.6.1 Operating Principles
The steam condensates in the horizontal tubes, giving off the heat of condensation to the liquid. The liquid comes in from the bottom of the stripper and will have a temperature very similar to the vapor entering the bottom of the tower.
In order to have an efficient vaporization at the desired temperature of (in the case of MEA) 125 °C, the pressure on the liquid is designed to be ±2.3 bar. In other words, the liquid is kept at the pressure and temperature combination at which water boils. This ensures that the heat transferred is efficiently put into vapor production and freeing amine from solute.

B.6.2 Combination with Reclaimer
When an amine reclaimer is used in the process, (see section B.7), a vapor flow at the operating temperature of the reclaimer (300 °F) enters the stripper bottom. This vapor has the same composition as the lean amine flow and exchanges heat with the down coming liquid. Therefore the total reboiler heat duty reduces with the heat duty delivered by the reclaimer to the reclaimer solution, which is described in section C.4.

B.7   Amine Reclaimer
Over time the used amine is contaminated by reactions with impurities in the gas stream, specifically strong acids, as an amine is a base. The result of these reactions are Heat Stable Salts, such as formic acid, acetic and sulfuric acid. The amine cannot be released from these strong acids under the conditions in the stripper and reboiler; however, with the addition of a stronger base than the amine, the amine can be recovered. This is done using an Amine Reclaimer, of which schematics can be seen in Figure B.15 and Figure B.16.
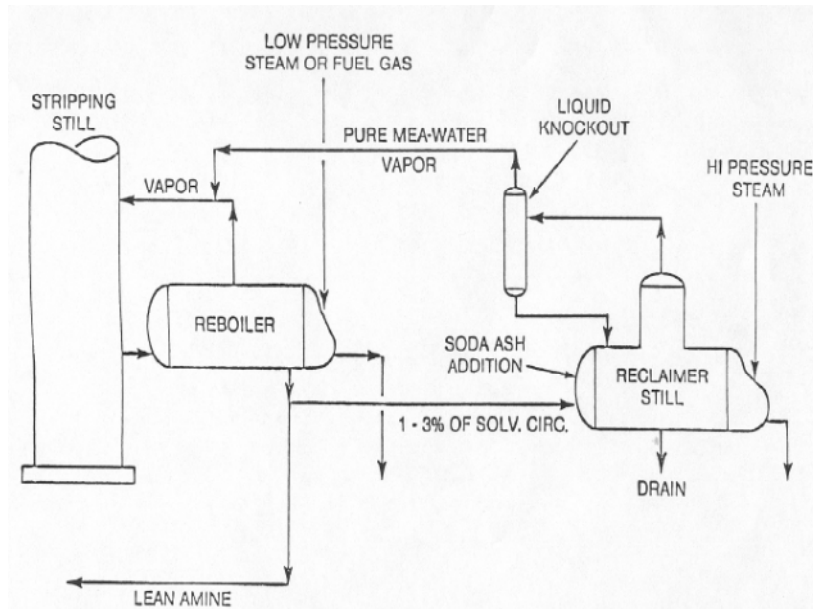
Figure B.15 Reboiler & Reclaimer Flow Diagram
Source: (Dow, 1998)
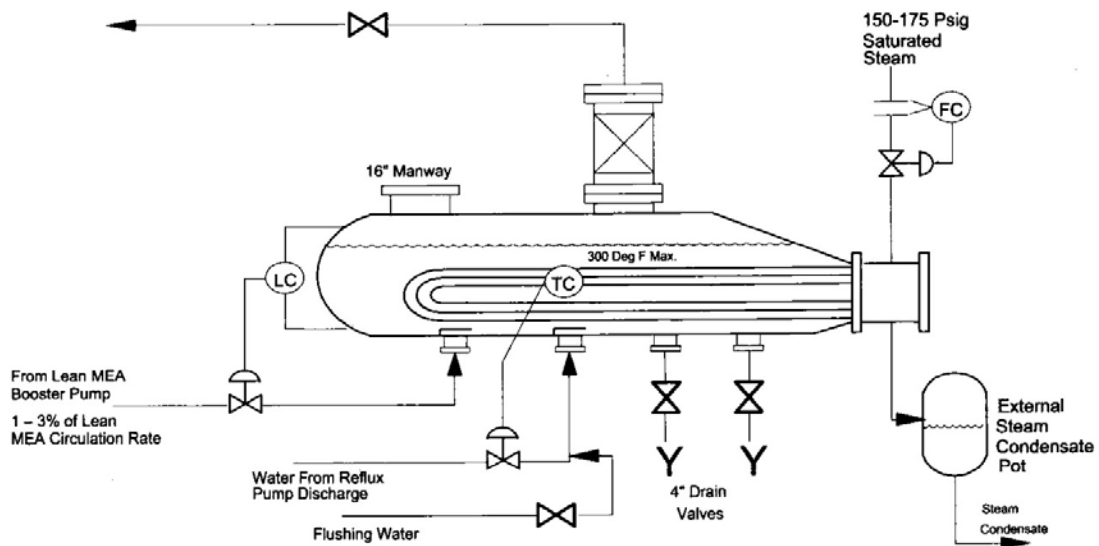
Figure B.16Typical Process Flow Diagram for a MEA reclaimer
Source: (Sheilan et al., 2009)

A reclaimer is shaped somewhat like a kettle reboiler. It is designed to reclaim MEA and remove non-reclaimable salts and thermal degradation products from the MEA solution.

The removal is done by a semi-batch process which boils a slipstream of the lean MEA coming from the reboiler in the presence of a strong base (caustic or soda ash). The strong base causes a replacement reaction between the MEA heat stable salt and the caustic, forming a non-volatile sodium salt and liberating the volatile MEA so it can be vaporized and returned to the stripper via the overhead vapor line. The flashed vapors may be passed through a small packed column for removal of any entrained liquids. A 3-5 feet [0,91-1,52 meter] high section of random packed column is satisfactory.

The operation of the reclaimer begins with charging of the reclaimer with caustic. After charging, the reclaimer is filled with a slipstream of hot lean amine solution from the reboiler (fed under level control). This slipstream is usually between 1 and 3% of the total lean amine flow. (Sheilan et al., 2009)

B.7.1   Mea concentration step
The kettle is brought up to the operating temperature using 1035 -1205 kPa saturated steam as the heating medium. At the start of each cycle, most of the overhead vapor will be water. As the cycle progresses, the amine will become more concentrated in the reclaimer bottoms and the amine content of the overhead stream will increase. The temperature of the liquid in the reclaimer will increase as the solution becomes more concentrated in MEA and other compounds of higher boiling point than MEA. Increments of fresh feed are added via the level controller to maintain the liquid level in the kettle. The amine concentration will increase until the vapor composition approximates the composition of incoming lean amine stream.

B.7.2   Steady-State Boiling Step
Steady-state equilibrium is reached where the rates of MEA and water vapors leaving the reclaimer equal the rates of MEA and water entering the reclaimer. With a 20 wt% lean MEA solution feed stream entering the reclaimer and a 20 wt% MEA vapor stream leaving the reclaimer, the liquid phase in the reclaimer will contain about 76wt % MEA. If there are no impurities present in the circulating MEA solution, the liquid in the reclaimer will continue to boil indefinitely at the same steady state equilibrium conditions. If there are impurities present, they will accumulate in the reclaimer causing the boiling temperature of the reclaimer to gradually rise. When the reclaimer liquid temperature reaches an absolute maximum of 300 °F, fresh lean solution feed to the reclaimer must be discontinued. Above 300 °F, for EMA, appreciable thermal degradation of the MEA begins and undesirable impurities could be distilled back to the stripper.

B.7.3   MEA Recovery Step
When the lean amine solution feed to the reclaimer is discontinued at the end of the steady-state boiling cycle, the reclaimer is full of contaminated solution containing a high MEA concentration. The quantity of MEA in the reclaimer is a significant fraction of the total MEA content in the circulating amine solution (10% of the total is not unusual). Therefore it's uneconomical to simply dump the contents of the reclaimer.

This recovery step is basically the reverse of the concentration step at the start of the cycle. With the lean solution feed line blocked, water is added to the reclaimer from the reflux pumps under level control as the solution is boiled. Gradually the MEA concentration in the reclaimer liquid and the vapors leaving the reclaimer decrease, as well as the reclaimer boiling temperature. At the very end of this water dilution step, further stripping with live steam sparging recovers additional MEA and is helpful in cleaning the residue from the reclaimer tube bundle. After a few hours, the live steam sparger can be shut off.

The water dilution / steam sparging is stopped when essentially all the MEA has been removed from the reclaimer. When the reclaimer liquid temperature stops falling, most of the MEA has probably been recovered. Normally the reclaimer liquid temperature should fall below the temperature of the solution in the reboiler. A small injection of caustic into the reclaimer at this stage may be useful to help liberate additional MEA from the HSS in the reclaimer. If the laboratory analyzes <5 wt% MEA in the reclaimer sludge then the cycle is completed. If not, continue boil-off on the reclaimer while adding reflux water.

The residue remaining in the reclaimer is discarded by flushing with fresh (not salt) water. If the residue is a thick, concentrated sludge, then the reclaimer efficiency is satisfactory. If only a small amount of sludge is present, then the reclaimer operation has been poor (the reclaimer cycle length was too short and the MEA lost with the reclaimer residue is unnecessarily wasted.

As a general guideline, typical times for each of these steps are
- Concentration step: 1-2 days
- Steady-State Boiling Step   ~2 weeks
- MEA Recovery Step   16 hours – 1 week

These times are only for guidance; the actual times will vary widely depending on many factors including level of impurities, steam rate to the reclaimer, MEA concentration, etc.

B.7.4   Reclaimer Cleaning / Shutdown Procedure

Once most of the MEA has been recovered, the steam flow is stopped. The reclaimer is isolated from the stripper & reboiler and utilities and drained with a valve at the bottom of the reclaimer. The manholes at the top of the reclaimer are opened and the internals are flushed thoroughly with a jet of fresh (not salt) water. Afterwards the reclaimer is ready for another start-up

B.8   Other Components Common to Most Amine Systems

Usually the amine gas sweetening process also makes use of the system components listed in this paragraph. Most of the information given here is taken from Dow Chemical, (Dow, 1998) and (Sheilan et al., 2009).

B.8.1   Inlet Gas Knockout Drum

A general rule for amine treating is that the cleaner the inlet feed gas into the absorber tower is, the better the system operates. Many of the contaminants that cause poor performance enter the amine system via the inlet feed gas. Liquid hydrocarbons and well-treating chemicals can cause foaming, brine can lead to corrosion and iron sulfide can contribute to foaming and plugging.

Before entering the absorber, the gas is passed through an inlet separator where entrained droplets or slugs of liquid are removed from the gas stream by impaction devices, as seen in Figure B.17. Baffles remove a portion of the liquids. Mist eliminator pads, located near the gas outlet of the tank, trap the rest. Standard mist elimination pads common in inlet separation vessels have 99% efficiency down to about 10 microns, but efficiency drops to low values quickly for smaller particles. (Sheilan et al., 2009)

Aerosols, which may be as small as ½ micron, are not removed effectively by standard mist elimination pads. (van Benthum et al., 2011). If aerosols are determined to be present, high technology coalescing filtration systems are available which can remove aerosols in the sub-micron range. A water wash system in the inlet feed gas consisting of small trayed (4-5 trays) or packed column is also effective in the pre-treatment of FFC gas and coker off-gas that can contain substantial amounts of heat stable salt precursors. The water wash will remove these compounds and prevent the formation of heat stable salts in the amine solution.
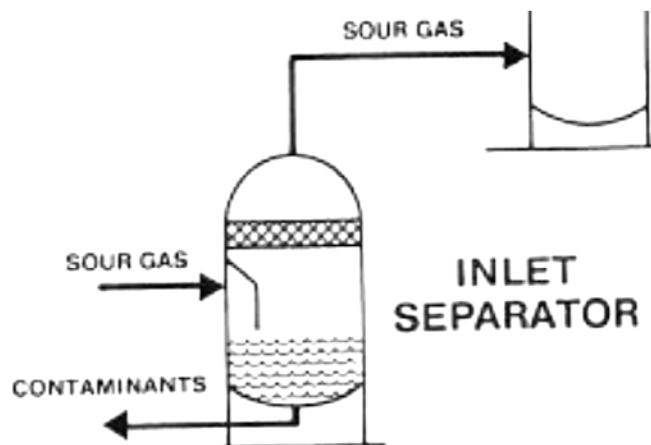
Figure B.17 Inlet Separator
Source: (Dow, 1998)

B.8.2   Three Phase Flash Tank

In many units the rich amine solution is sent from the absorber to a flash skimmer tank to recover hydrocarbons that may have dissolved or condensed in the amine solution in the absorber. The pressure of the solution is dropped as it enters the tank, allowing the lightest of the hydrocarbons to flash. The heavier hydrocarbons remain as a liquid, but separate from the aqueous amine, forming a separate liquid layer. Because the hydrocarbons have a lower density than the aqueous amine, they form the upper liquid layer A flash tank should incorporate an internal baffle system, as shown in Figure B.18, that allows the hydrocarbon collected in the tank to be routinely skimmed off.
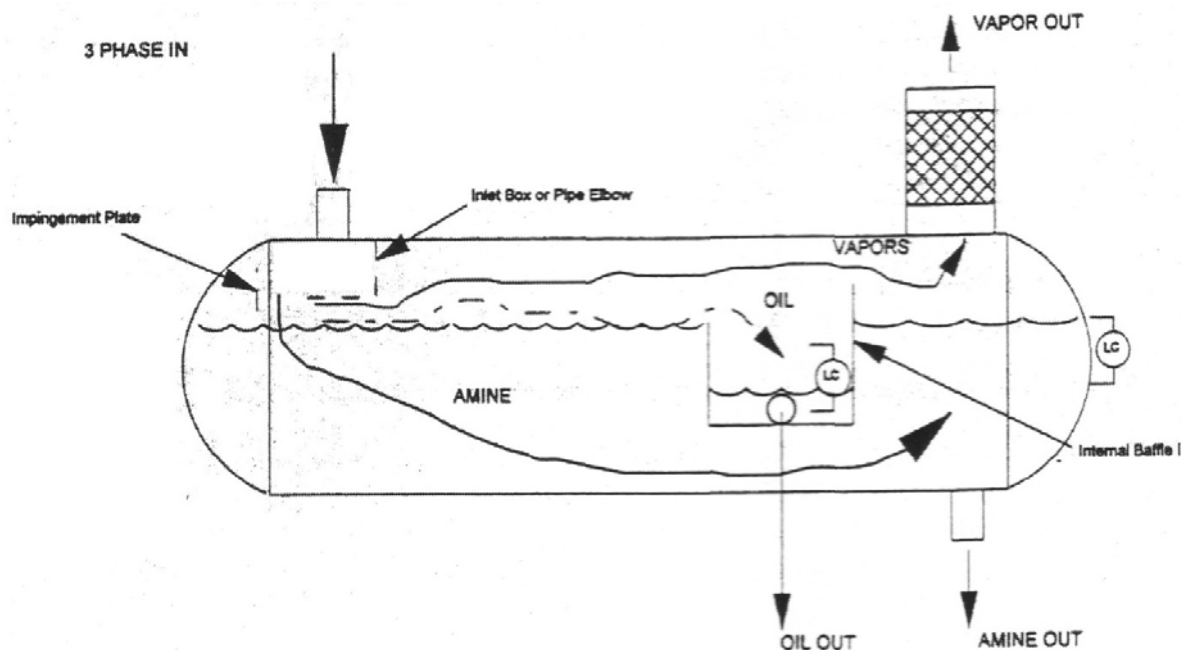
Figure B.18 Three Phase Flash Tank Schematic
Source: (Sheilan et al., 2009)

The aqueous amine, freed from the hydrocarbon, is drained from the bottom of the tank. Not only is the flash tank valuable in recovering lost hydrocarbon product, it is also beneficial in maintaining the condition of the amine solution and the amine sweetening system. Hydrocarbon contamination in aqueous amine solutions often promote foaming. Equipment fouling may be more severe and occur at a faster rate in the absence of a flash separator. Sulfur plant operations may be hindered if hydrocarbons are volatilized in the stripper.

A flash tank is typically used in application where the contact pressure exceeds 500 psi (3,500 kPa). The normal operating pressure of the flash tank ranges from 5 psig to 75 psig (35 to 525 kPa) depending upon the disposition of the flash tank vent stream. (Sheilan et al., 2009) & (RefiningOnline, 2007). When the flash tank operates at low pressure, 0-50 psig (up to 350 kPa)., a rich amine pump is usually required, because of the pressure drop over the lean/rich cross exchanger the height of the stripper inlet and the operating pressure of the stripper column.

A flash tank should be considered a process requirement in refinery gas treating applications and should be strongly considered in gas plant applications treating wet natural gas (>8% C_2^+) or where a considerable amount of hydrocarbons may be present due to condensation of pipeline slugging. If significant quantities of H_2S & CO_2 are present in the hydrocarbon gases flashed from the amine solution in the flash tank, an absorber with 4-6 trays or an equivalent amount of packing is installed on the top of the flash tank. A slipstream of lean amine is fed to this absorber to remove H_2S and CO_2 from the hydrocarbon flash gas. Flash gas at less than fuel gas header pressure can be disposed of to the vapor recovery system, flare, incinerator or heater firebox.

A minimum residence time for a three phase flash tank of 20 minutes is recommended, based on the flash tank operating half full. Amine systems treating very dry natural gas (<2% C_2^+) or syngas streams with very little hydrocarbon content can utilize a lower flash tank residence time of 5 minutes if a flash tank is incorporated into the amine unit design.(Sheilan et al., 2009)

B.8.3   Lean/Rich Heat Exchanger

Incorporating a lean/rich cross exchanger into the amine process flow decreases the reboiler heat duty by as much as 30-40% by recovering the heat contained in the hot lean amine solution exiting the reboiler. Historically, a shell and tube configuration (rich amine on the tube side and lean amine on the shell side) has been used, but plate/frame exchangers have come into use more frequently in recent years.

The most common problem encountered in the lean/rich cross exchanger is corrosion due to flashing acid gases at the outlet of the exchanger or in the rich amine feed line to the stripper. Adequate pressure should be maintained on the rich solution side of the exchanger to reduce acid gas flashing and two-phase flow through the exchanger. A recommended maximum velocity to minimize corrosion in the tubes is about 1 m/s (3-3,5 feet/sec). (Kohl and Nielsen, 1997)

B.8.4   Filtration

Installation of a good filtration system has become one of the key components of amine system design. A good filtration design includes both a particulate and a carbon filter. The cleaner the amine solution, the better the amine system operates. The particulate filter is used to remove accumulated particulate contaminants from the amine solution that can enhance foaming and aggravate corrosion. Carbon filtration removes surface active contaminants and hydrocarbons that contribute to foaming. With proper inlet gas separation and pre-treatment, filtering a 10 to 20 percent slipstream of the total lean solution has usually proven adequate. (Sheilan et al., 2009). Where practical, total stream filtration should be considered. However, in large refinery applications, this is usually not practical.

The filtration system is typically installed on the cool lean amine stream (absorber feed). Recirculation of a slipstream from the discharge side of the charge pump to the filtration system with a return to the suction side of the pump is a common arrangement. If combined in series, the particulate filter should be installed upstream of the carbon filter to protect the carbon filter. A second post-filter or screen should be installed down-stream of the carbon filter to keep carbon fines out of the circulating system. If the carbon filter is installed independent of the particulate filter, a pre-filter should be installed on the carbon filter inlet to protect the carbon bed.

In systems that are extremely contaminated with particulate due to inadequate feed preparation, excessive corrosion, or if the inlet gas CO_2/H_2S ratio is high, particulate filtration of the rich amine exiting the absorber may be required. The concern is that FeS in the rich amine can dissociate in the stripper under certain conditions to soluble iron

products which lean side filtration will not remove. These soluble iron products can then react with H_2S in the contactor to form additional FeS, fouling the absorber trays or packing. If components of the filtration systems are installed on the rich amine stream, extreme care should be taken when performing maintenance to control the risk of exposure to H_2S.

B.8.5   Mist Eliminators

In every process involving contact between liquid and flowing gas, tiny mist droplets are carried away with the gas. This phenomenon is called entrainment. In order to recover the entrained particles devices were developed to remove mist from gas streams. Now known as mist eliminators, or demister pads (Demister is a registered trademark of Koch-Glitsch) these devices provide a large surface area in a small volume to collect liquid without substantially impeding gas flow. Unlike filters, which hold particles indefinitely, mist eliminators coalesce (merge) fine droplets and allow the liquid to drain away. Gas typically flows upward through a horizontal mist eliminator.
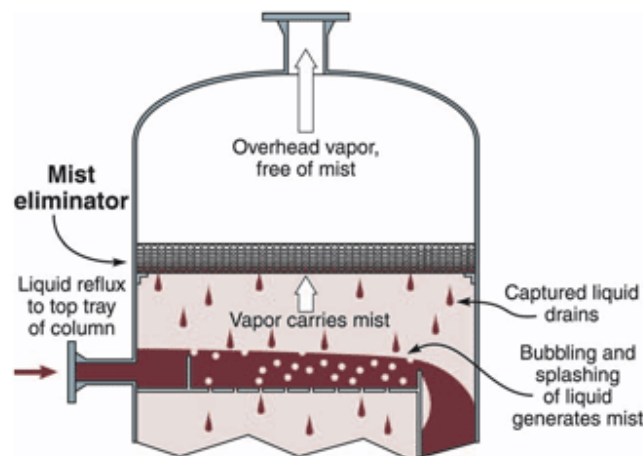
Figure B.19 Typical mist eliminator application in distillation column

B.8.5.1   Operating principle

Vane and mesh devices both employ the same mechanism, known as inertial impaction, and thus are subject to the same basic design rules.

Vane-type mist eliminators consist of closely spaced corrugated plates that force mist-laden gas to follow serpentine paths. Also known as chevron or plate type, these devices are generally not efficient for mist droplets smaller than about 20 microns, but they are sturdier than mesh pads and impose less pressure drop. Vane arrays can be mounted horizontally or vertically. They are preferred in applications involving high vapor velocities, low available pressure drop, viscous or foaming liquids, lodging or caking of solids, slugs of liquid, or violent upsets. Like mesh pads, vane units are usually round or rectangular. They are sometimes used in combination with mesh pads for optimum performance in special situations.

Mesh-type mist eliminators are the most widely applicable type and are made of metal or plastic wire, loosely knitted in a form resembling a cylindrical net. This tube is flattened to form a two-layer strip typically 12 inches wide, which is then crimped in a diagonal pattern with ridges. When these strips are laid together, the ridges slant in alternate directions, forming an open structure through which gas flows freely. Such mesh can efficiently capture mist droplets as small as 5 microns (micrometers). For eliminating droplets down to 1 micron in diameter, multi-filament yarns of various plastics or glass are knitted into the mesh. The result is called a composite or co-knit mesh, which is also more expensive. (AMISTCO, 2004)

As shown in Figure B.20 (Left), vanes bend the path of mist-laden gas into relatively tight curves. As the gas changes direction, inertia or momentum keeps mist droplets moving in straighter paths, and some strike adjacent vanes. There, they are held by surface forces and coalesce (merge) with other droplets, eventually trickling down. If the vane material is wettable, a surface film promotes coalescence and drainage. In the case of upward flow, coalesced liquid disengages from the bottom of the vanes as droplets large enough to fall through rising gas. In the case of horizontal flow, the liquid trickles down vanes to a drain below.
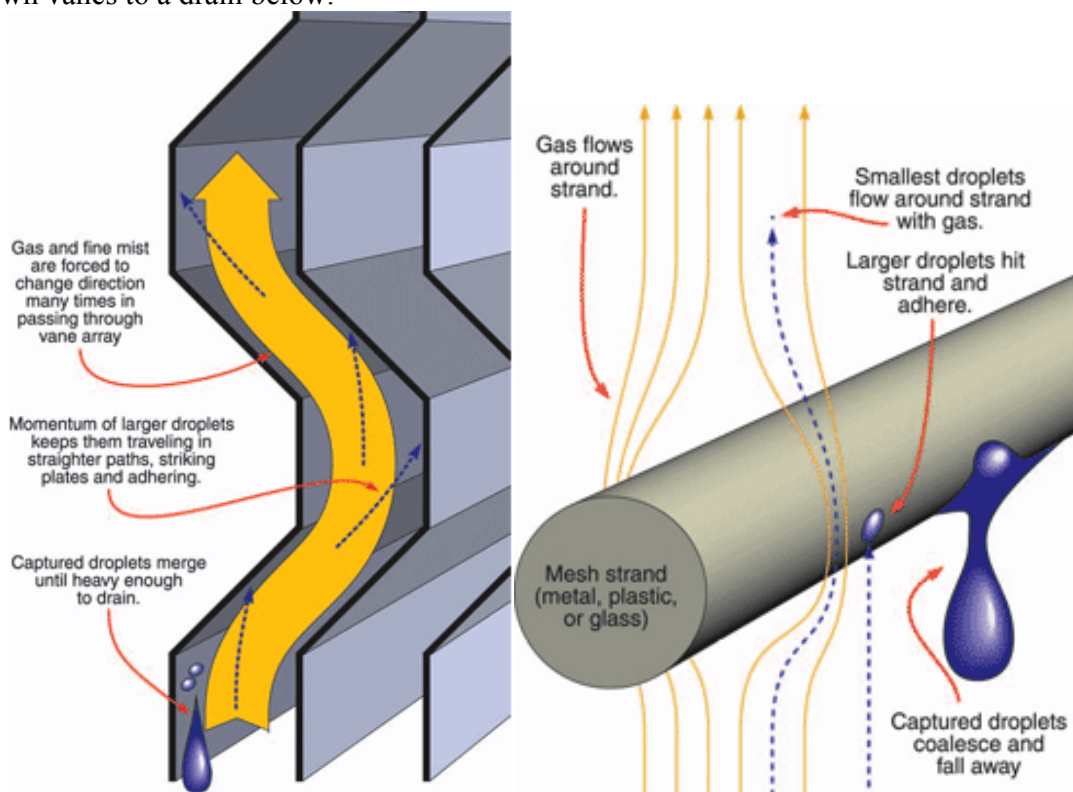
Figure B.20 (Left) Capture of mist droplets in a vane array with vertical flow.
(Right) Droplet capture in a mesh-type mist eliminator

In a mesh-type mist eliminator, each strand acts as an obstruction around which gas must flow, shown in Figure B.20 (Right). Within a very short distance upstream of a filament, the gas turns aside sharply, but some mist droplets are unable to follow. They strike the

filament, adhere, and coalesce to form droplets that are large enough to trickle down and fall away.

In Table B.2 the typical size range of mist droplets created by various processes is shown.
An example of a mesh-type mist eliminator pad is given in Figure B.21.
An example of a special curved, non-metallic vane type mist eliminator is given in Figure B.22.

Table B.2 Typical size range of mist droplets created by various processes
Source: (AMISTCO, 2004)

Mechanical	
Column (Packing or Trays)	5 to 800 μm
Sprays	10 to 1000 μm
Surface evaporation	3 to 1000 μm
Chemical	
Acid Mists	0,1 to 15 μm
Condensation	
Blown off heat exchanger surface	3 to 500 μm
In saturated vapor	0,1 to 50 μm

Figure B.21 Typical mesh-type mist eliminator pad

Figure B.22 Vane-type mist eliminator with curved non-metallic vanes

B.8.5.2   Capacity Limits

The throughput capacity of a mesh or vane mist eliminator is limited by either of two related phenomena: flooding (choking with liquid) and re-entrainment (dislodging, suspension, and escape of coalesced droplets). In some low-pressure applications, the pressure drop across the device can also be an important consideration.
These limiting factors are illustrated in Figure B.23 and Figure B.24.

Figure B.23 is based on experimental data for a typical horizontal mesh pad (Amistco mesh type TM-1109), using water sprayed at various rates into rising air. It shows how pressure drop varies with velocity and mist load in the vicinity of the typical operating range. The mist droplets are assumed to be within a size range suitable for capture by a pad of this sort—larger than 10 microns. In Figure B.23, notice that the pressure drop would be considered small in most applications, only about 2 or 3 inches of water column even at the most extreme velocity and load combination. Also notice that pressure drop increases markedly with mist load. At 10 feet per second, the pressure drop for 1 GPM/ft2 is more than three times that for a dry pad.
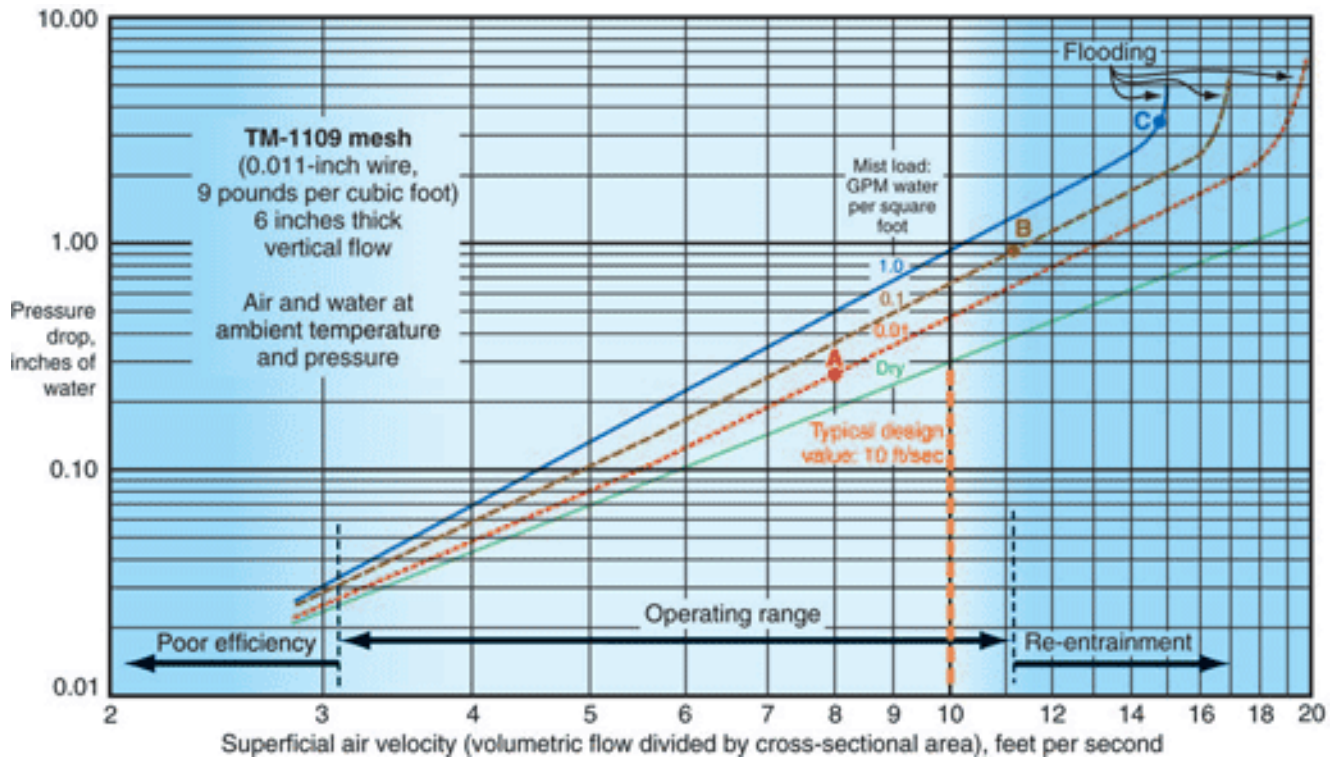
Figure B.23 Pressure drop, flooding and re-entrainment in a typical horizontal mesh pad
Source (AMISTCO, 2004)

Figure B.24, in turn, provides a subjective impression of what happens in a typical horizontal mesh pad at three different conditions of flow rate and mist load indicated as Points A, B, and C in Figure B.23.
Point A represents a light mist load and a velocity of about 8 feet per second (2,44 m/s). Nearly all the incoming mist is captured well below the middle of the pad. The rest of the

pad remains dry. In the active zone, coalesced droplets slip rapidly down the mesh wire. At the bottom, however, surface tension makes water accumulate on and between wires before falling away as streams and large drops. The result is a thin flooded layer agitated by rising gas, generating a small amount of additional mist that is immediately captured again.

Point B, in turn, lies on a "moderate" load line at the velocity where a few re-entrained droplets begin to blow upward from the pad—about 11 ft/sec (3,35 m/s), under these conditions. Re-entrainment is roughly indicated by the darker background at the right side of the plot. (The darker area on the left, in turn, signifies poor capture efficiency.) The higher the liquid load, the lower the velocity at which re-entrainment occurs.

At **Point B**, velocity is high enough to detach coalesced droplets and lift some of them against the force of gravity. Most re-entrained droplets are relatively large— up to 1,000 microns (1 millimeter). Because of the higher liquid flow rate in the approaching mist and greater upward drag on captured liquid due to higher air velocity, the flooded zone fills an appreciable layer. Incoming mist rises higher in the pad before being captured.

Finally, at **Point C**, the velocity is high enough not only to lift even the largest re-entrained droplets, but also to slow drainage within the pad virtually to zero. The mesh is entirely choked with agitated liquid, generating mist droplets downstream across a wide range of sizes. Flooding has caused the pressure-drop curve to begin turning up sharply. If flow were increased beyond this point, the line would become almost vertical. For lower liquid loads, flooding occurs at higher velocities. Similar behavior governs capacity limits also for vane mist eliminators and for horizontal flow through vertical mist eliminators of both types.

Considering operating variables, flooding is promoted by high liquid load, high gas velocity and high liquid viscosity and surface tension (inhibiting drainage). At very light liquid loads, re-entrainment can occur without appreciable flooding. However, with or without flooding, re-entrainment is promoted by higher gas velocity, smaller strand diameter or vane corrugation spacing, sharper corrugation angles, greater liquid load, lower liquid density relative to gas, lower liquid surface tension, and lower wettability of the mesh or vane surface.
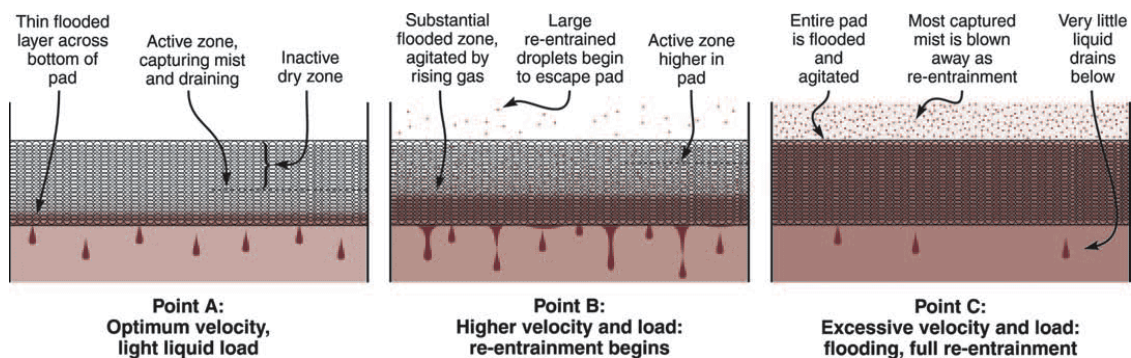
Figure B.24 Effect of high velocity and load on mist eliminators

B.8.6   Pumps

Pumps increase the pressure for a liquid flow, either to match the pressure of the next destination of the liquid, compensate for the static pressure due to height difference and/or overcome pressure loss due to friction in the piping/equipment. The calculations on this subject are in section C.9.

A list of pumps used in the amine process is given below:

Lean amine pump: Used to pump the lean amine solution from the reboiler through the lean/rich exchanger, the lean amine cooler and into the absorber tower top.
Rich amine pump: Necessary when the three phase flash tank operates at 350 kPa or less, to overcome the pressure drop over the lean/rich cross exchanger the height of the stripper inlet and the operating pressure of the stripper column.
Steam Condensate Pump: Used to pump the condensate from the reboiler (& reclaimer) to (their respective) steam furnace(s).
Reflux Drum bottoms Pump Used to pump the reflux drum bottoms to the stripper tower.
Reclaimer Feed Pump Used to pump a portion of the lean amine from the reboiler to the reclaimer.

B.9   Operating Difficulties

Amine gas sweetening plants can experience operating difficulties including foaming, failure to meet sweet gas specification, high solvent losses, corrosion, fouling of equipment and contamination of the amine solution. Often one operating difficulty is the cause of another. Below are some of the most common problems that occur in amine gas sweetening plants.

B.9.1   Foaming

Pure aqueous amine solutions do not foam. It is only in the presence of contaminants such as condensed hydrocarbons, small suspended particulate matter, or other surface-active agents such as some pipeline corrosion inhibitors or compressor oils, that a foaming problem may develop. Foaming usually occurs in the absorber or the stripping tower, and is accompanied by a sudden noticeable increase in the differential pressure across the column. Other indications of a foaming condition may be a high solvent carryover, a drop in liquid levels, and the detection of off-specification gas.

An immediate method to control a foaming problem is the addition of an antifoam at a location just upstream of the foam. Effective foam inhibitors for amine sweetening systems are silicone antifoams and polyalkylene glycols. Also widely used are high-boiling alcohols such as oleyl alcohol and octylphenoxyethanol. (Kohl and Nielsen, 1997). It is advisable to test the antifoam on a plant sample in the laboratory before applying it in the field to verify that it will break the foam. In the event that one antifoam is ineffective, switching to another antifoam may solve the problem.
The silicone antifoams have proven to be quick and effective in controlling foaming problems in the gas treating industry. When using a silicone antifoam, the antifoam

should be added downstream of the carbon filters because carbon filters will adsorb the silicone.

Care should be exercised with respect to the amount of silicone antifoam added to a system. The silicone antifoams should be used only in small quantities, as recommended by the manufacturer. It is important to be aware that silicone antifoams used in excessive quantities have the potential to promote the formation of foam.

The use of an antifoam may only be a temporary solution to a continuing problem. The objective in controlling foaming should be to minimize the level of contaminants in the amine solution. Of critical importance is the prevention of entrained contaminants in the feed gas from entering the amine system. The inlet separator, equipped with a demister pad and possibly filters, is instrumental in trapping most contaminants, and should be monitored to ensure that it is operating efficiently and not being overloaded. Mechanical and carbon filters are necessary in maintaining a clean solution. In order to prevent hydrocarbons from condensing in the absorber, the lean amine feed temperature should be held between 10'F and 20'F above the temperature of the feed gas. (Sheilan et al., 2009)

B.9.2   Failure to meet gas specifications

Difficulty in meeting the sweet gas specification may be the result of poor contact between the gas and the amine solvent, which may in turn be caused by foaming or mechanical problems in the contacting equipment.

In the case of foaming, the gas remains trapped in bubbles, unable to contact the rest of the solvent, resulting in poor mass transfer of acid gas from the gas to the amine solution. In terms of mechanical damage, if trays are broken or have fallen, there may not be enough contact zones (trays) for adequate sweetening. If the trays are plugged, there is less contact between the gas and liquid on each tray, resulting in poorer sweetening. Other explanations for off-specification gas may be related to the amine solution: the circulation rate may be too low, the amine concentration too low, the lean solution temperature may be too high, or the acid gas loading in the lean solution may be too high.

B.9.3   Solvent Losses

Amine losses are largely through entrainment, caused by foaming or excessive gas velocities, and by leakage an inefficient mist eliminator. In MEA units the reclaimer bottoms disposal significantly adds to the makeup requirement. On a much smaller scale are vaporization losses from the absorber, the overhead condenser, and the flash tank and degradation losses by chemical and thermal degradation.

B.9.4   Corrosion

Corrosion is a problem experienced by many alkanolamine gas sweetening plants. When loaded with CO_2 and H_2S, aqueous amine solutions can become corrosive to carbon steel. Corrosion rates are increased by high amine concentration, high acid gas loading, high temperatures, degradation products, and foaming. The acid gases flashed from solution are also corrosive.

Monoethanolamine is more reactive than diethanolamine and similarly more corrosive. As a result, the concentration of MEA is restricted to 10 to 20 weight percent, while DEA strengths range from 20 to 30 weight percent. Rich solution loadings are normally limited to the range of 0.25 to 0.45 moles acid gas/mole MEA, while in DEA systems loadings may range from 0.5 to 0.6 moles acid gas/mole DEA. The corrosiveness of a loaded amine solution is strongly influenced by the relative proportion of CO_2 to H_2S in the feed gas.

CO_2 is more corrosive to carbon steel than H2S, in aqueous systems. Thus, for gases containing a higher ratio of CO_2 to H_2S, the rich acid gas loading should be maintained at the lower end of the recommended loading range. In cases where the feed gas is predominantly H_2S, loadings at the higher end of the loading range may be acceptable.

In terms of design, a number of measures can be taken to minimize corrosion. Solution velocities should not exceed 1 m/s (3 to 3.5 ft/sec) (Kohl and Nielsen, 1997). The rich solution should be on the tube side of the lean/rich heat exchanger, and pressure should be maintained on the exchanger to prevent acid gases from flashing, creating an erosion/corrosion cycle. A low temperature heating medium should be used in the reboiler, thereby preventing accelerated corrosion rates and thermal degradation of the amine. All equipment should be stress relieved.

There are certain areas of amine sweetening plants which are more susceptible to corrosion than others, and, as a result, are often constructed of corrosion-resistant materials such as Type 304 stainless steel. These areas include
1) the lean/rich heat exchanger tube bundle
2) the reboiler tube bundle
3) the stripping column, particularly the upper section and overhead gas line
4) the reflux condenser
5) the rich solvent let-down valve and subsequent piping to the stripper.

Appendix C Derivation of the Volume and Energy calculation methods for the Amine Process

The design of amine plants centers around the absorber, which performs the gas purification step, and the stripping system which must provide adequately regenerated solvent to the absorber. After selecting the amine type and concentration, as discussed earlier, key items which need to be determined by the designer are the required solution flow rate; the absorber and stripper Column parameters (heights, diameters) and the thermal duties (heating and cooling) of all heat transfer equipment.
In this chapter the volume and energy calculation methods for several components of the amine process are given

Component	Volume Calculation	Energy Calculation
Absorber	YES	YES
Stripper	YES	YES
Reboiler	YES	YES
Steam Furnace	Not Included	YES
Reclaimer	YES	YES
Three Phase Flash Tank	YES	Does not apply
Condenser & Reflux Drum	YES	YES
Pumps	Negligible	YES
Lean/Rich Exchanger	Negligible	YES

C.1 Absorber
The first step in designing an absorber is calculating the amount of amine solution that has to be circulated to lower the sour gas concentration in the incoming gas stream to the desired values in the outgoing gas stream.

The conditions at the gas inlet are usually known:
- Chemical Composition
- Total flow
- Pressure & Temperature

Gas outlet composition is a design choice. The gas outlet flow equals the gas inlet flow minus the absorbed sour gas.
> For example, according to The North American Energy Standards Board, natural gas sold to customers should have a mole concentration of CO_2 of 0,1 to 1mol% (NAESB, 2010), see Table A.1.

The required flow of amine solution is given by the amount of amine required to bind the desired amount of CO_2. The amount of CO_2 bound per mole of amine is found by subtracting the Lean Amine Loading (LAL) from the Rich Amine Loading (RAL).

For MEA a normal lean amine loading is 0,1 mol CO_2/mol MEA and a normal rich amine loading is 0,45 molCO_2/mol MEA. (Kohl and Nielsen, 1997).

The total amount of MEA required to bind the CO_2 follows from equation
Error! Reference source not found.

$$\frac{molesCO_2}{(RAL - LAL)} = molesMEA \tag{9.1}$$

Using the concentration in the amine solution and the respective solution density, one can calculate the mass and volume flows of the lean and rich amine streams.
For MEA commonly a concentration of 15 wt% is employed (Kohl and Nielsen, 1997), with a density of 1004,8 kg/m^3 (Ko et al., 2008)

C.1.1   Operating Pressure and Temperature

The gas inlet pressure and temperature of gas into the absorber is usually a given parameter. This pressure is considered to be the pressure at which the entire absorber operates, as this work considers the pressure loss over the absorber to be negligible.

There is, however, a temperature difference present in the absorber, mainly due to the fact that the CO_2-alkanolamine reaction is exothermic. The heat of reaction (ΔH_R) is listed in Table A.4. Typically, in an industrial absorber, the liquid phase temperature rises 20 °C from top to bottom. The heat generated in the liquid phase due to chemical reaction (ΔH_R) can be dissipated in three ways:

1. Direct heat transfer between the gas and liquid phase
    - Due to the relatively low heat transfer coefficient of the gas phase and the relatively small temperature difference (±20°C), this is assumed to be negligible in the model.
2. Saturation of the gas phase by vaporization of water
    - The model assumes that the gas phase is already saturated with water. Therefore this effect is also considered negligible
3. Heat loss to the surroundings.
    - In large-scale industrial absorbers, the heat loss to the surroundings is negligible. Thus the entire system is considered to be adiabatic.

Therefore this work assumes that the heat released by the amine-bonding is assumed to result in a rise of temperature of the liquid phase only.

According to (Sheilan et al., 2009), the amine solution temperature entering the absorber should be 6 to 8 °C higher than the inlet feed gas temperature to prevent condensation of hydrocarbons in the contactor, which can cause foaming. As a practical maximum, though dependent upon the particular amine and absorber application, the lean amine solvent temperature should generally not exceed 57 °C. High lean solvent temperatures can lead to poor solvent performance due to H_2S equilibrium problems on the top tray of the absorbed or increased solution losses due to excessive vaporization losses.

This liquid inlet temperature, combined with the rise in temperature due to the exothermic reaction, allows the liquid outlet temperature to be calculated as well, see equation (9.2).

$$T_{liquid,out} = \frac{\left[molCO_{2,absorbed} \cdot \Delta H_R \right]}{\dot{m}_{liquid} \cdot cp_{liquid}} + T_{liquid,in} \qquad (9.2)$$

With cp written in [kJ/(kg K)] and ΔH_R in [kJ/kg]
This leads to a known pressure and temperature at all inlets and outlets over the tower.

C.1.2   Absorber diameter
In many processes practical limitations such as available 'footprint', weight, layout or production limitations determine the size of a scrubber. When the size of the vessel is not determined by some of the listed factors, the K-value is the most common design parameter. This value is a measure of the terminal velocity of a droplet in a upward flowing gas flow. The K-value dawns from the expression developed by (Souders and Brown, 1934), for sizing of fractionating columns. This expression involves an empirical factor known as the Souders Brown value, K-value, C-factor, λ or Gas Load Factor (GLF). In this publication, the term K-value will be used. The basis of the expression is the force balance on a droplet in an upwards-flowing gas field as shown in Figure C.1.
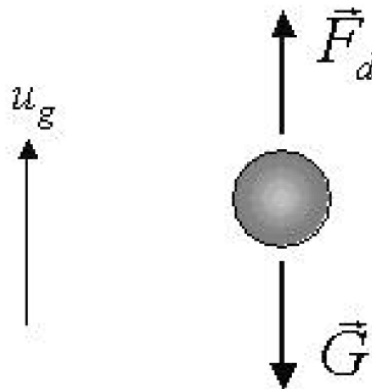
Figure C.1 The relevant forces acting on a droplet flowing in an upwards-flowing gas

The gravitation force on the droplet adjusted for buoyancy when resolved in vertical direction is:

$$G_d = \frac{\pi}{6} d^3 g \left(\rho_l - \rho_g \right) \qquad (9.3)$$

The resistance of a droplet in a moving fluid resolved in the vertical direction can be expressed as

$$F_r = K \mu_g \frac{\sqrt{\pi}}{2} d \cdot u_g + C_d * A_d \frac{1}{2} \rho_g u_g^2 \qquad (9.4)$$

Souders and Brown argued that the viscosity of the gas phase was very small so that the viscous term could be neglected. The vapor velocity they sketched for a fractionating column was in the range 0.01 to 0.001 cP. This is also a relevant estimation for a typical

natural gas in a gas scrubber. This leaves us only with the drag force F_d as the relevant force acting upwards as sketched in Figure C.1. Assuming that the droplet has the shape of a sphere, the drag force therefore can be expressed as

$$F_d = C_d * A_d \frac{1}{2} \rho_g u_g^2 = C_d * \frac{\pi}{4} d^2 \frac{1}{2} \rho_g u_g^2 \tag{9.5}$$

The terminal settling velocity is found when the drag force equals the gravitation

$$u_{g,set} \sqrt{\frac{\rho_g}{\rho_l - \rho_g}} = \sqrt{\frac{4gd}{3C_d}} \tag{9.6}$$

If the droplet size and drag force coefficient is constant the right hand side of the expression also is a constant and this is the definition of the K-value:

$$K = \sqrt{\frac{4gd}{3C_d}} \tag{9.7}$$

The "critical" K-value is usually determined experimentally. "Critical" in this sense, means the value of K where the gas velocity equals the terminal velocity of the mean droplet size, in a vessel without internals. The K-value is proportional to the superficial gas velocity from which the size of the vessel is determined by the following procedure. Values for the K-value can be found in Table A.5

The maximum velocity is calculated based on the critical K-value:

$$u_{s,g} = K \sqrt{\frac{\rho_l - \rho_g}{\rho_g}} \tag{9.8}$$

The calculated maximum velocity is then used to calculate the necessary diameter D of the vessel for the actual gas volume rate:

$$A = \left(\frac{\dot{Q}_g}{u_{s,g}} \right) \cdot \frac{1}{\varepsilon} = \pi \left(\frac{D}{2} \right)^2 \tag{9.9}$$

Note that the void fraction of packing ε is also incorporated, as the presence of packing decreases the flow area. Equation (9.9) can be rewritten to give the formula for the vessel diameter

$$D = \sqrt{\frac{4\dot{Q}_g}{\pi u_{s,g}} \cdot \frac{1}{\varepsilon}} \tag{9.10}$$

This paragraph is based on work by (Austrheim, 2006).

C.1.2.1 Flooding Consideration

The flow through a specific packing is subject to three main problems. All three are characteristic of fluid flow and are almost always independent of mass transfer itself. The first of these, called 'channeling' occurs when the gas or liquid flow is much greater at some points than at others. Such channeling is undesirable, for it can substantially reduce mass transfer. It can be severe in stacked packing. It is usually minor in crushed solid packing and is minimal in commercially purchased random packing.

The other two flow problems affecting packed towers are called 'loading' and 'flooding. The amount of liquid flowing downward through a tower can be reduced when a large upward gas flow is introduced in the tower. This condition is called 'loading'. At very high gas flow, the liquid stops flowing altogether and collects in the top of the column. This condition is called 'flooding'. (Cussler, 1997)

Flooding dramatically reduces mass transfer. It is avoided by reducing the liquid and gas fluxes. Of course, the total amounts of liquid and gas involved depend on how large a gas-absorption process is needed. The fluxes, that is, the flows per area, are reduced by increasing the cross-sectional area of the tower. This area is usually found using an empirical correlation like that in Figure C.2.
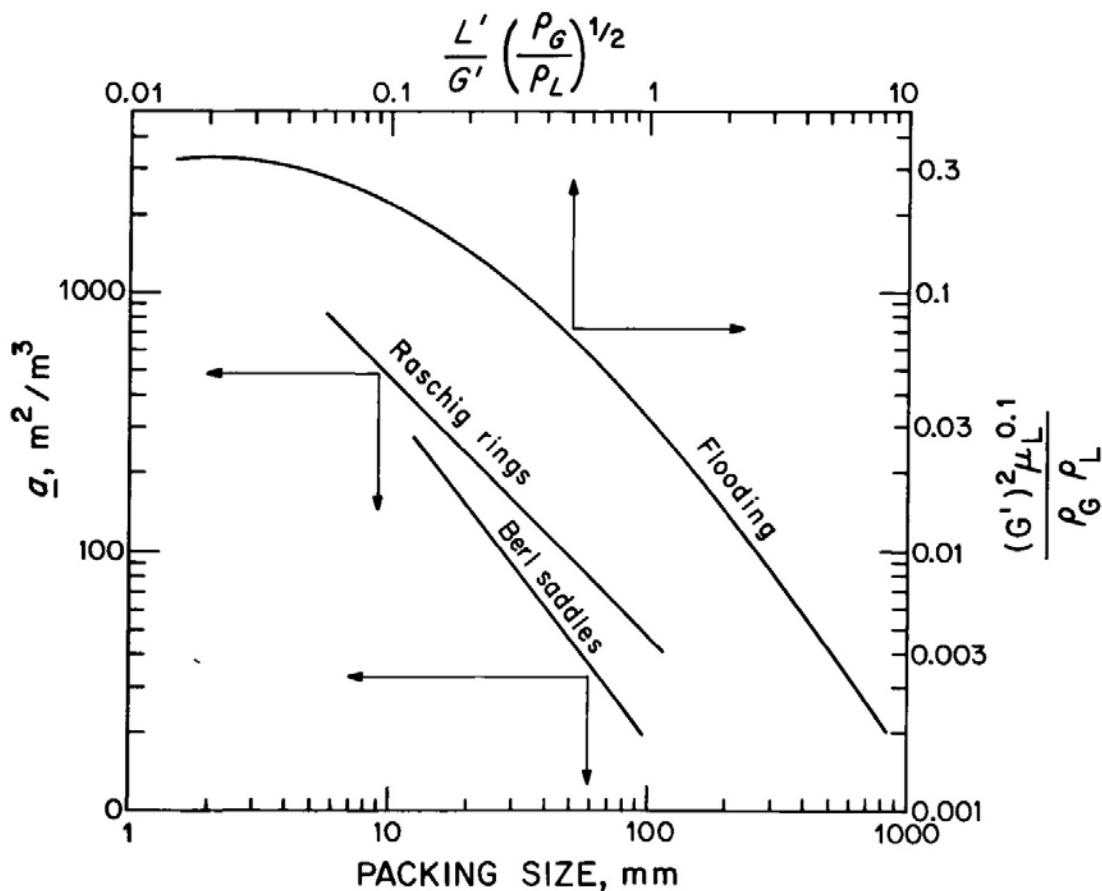
Figure C.2 Flooding and surface areas in a packed tower.
The upper curve gives the flooding velocity in a packed tower as a function of the ratio of liquid and gas fluxes. Note that these fluxes L' and G' are written in mass units, not molar ones; this is because flooding is the result of fluid mechanics, not chemical factors. Note also that the ordinate in this figure is not dimensionless, but is written in SI units. The two lower curves give the surface area per packing volume for two common tower packings. [Adapted from (Treybal, 1980)]

This correlation gives the liquid flux at flooding as a function of the ratio of liquid and gas flows used. Because this ratio is usually specified, the flux at flooding is easily calculated. One can design the tower to operate at fluxes equal to half this flooding condition. This empirical choice of one-half flooding represents a balance of two factors:

a lower flux implies an unnecessarily large tower, and a much higher flux requires an unnecessarily large pump. Thus the tower's cross-sectional area can be chosen on the basis of fluid mechanics, and it includes the choice of appropriate flows

In this work this calculation has been used as a check to ensure that no flooding would occur when calculating the diameter based on the superficial gas velocity. Usually that calculation yielded a larger diameter.

C.1.3 Packed Tower Absorber Height

The height of a packed tower absorber directly scales with the depth of packing material needed to accomplish the required removal efficiency. The more difficult the separation, the larger the packing height required. Determining the proper height of packing is important because it affects both the rate and efficiency of absorption.

As suggested by (Vaidya and Mahajani, 2006), the absorption rate of CO_2 in the tower can be used to calculate the required height. In order to understand what the rate of absorption represents, one first has to look at the mechanism of absorption, as described in the next paragraph.

C.1.3.1 Mass transfer across interfaces

In Figure C.3 one can see an interface between gas and liquid.
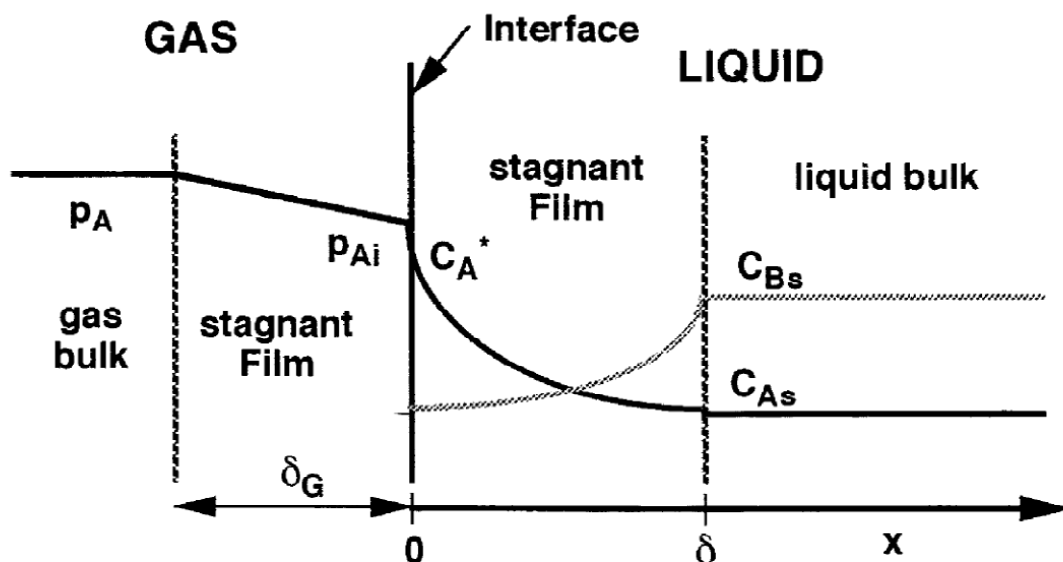
Figure C.3 Concentration profiles in the diffusion film,
for Mass transfer with chemical reaction. Source (Roizard and Wild, 2002)

In order to react with an amine-molecule, a CO_2-molecule has to diffuse towards the gas-liquid interface (diffusion), go through the interface (mass transfer), diffuse in the liquid towards an amine-molecule and react with that molecule.

One can quantify the amount of molecules CO_2 moving through the interfacial area as a flux. The flux in the gas is

$$R = k_G \left(p_{CO_2,G} - p_{CO_2,i} \right) \qquad (9.11)$$

Where K_G is the gas-phase mass transfer coefficient (typically in mol/(m^2-sec-bar)), $p_{CO2,G}$ is the bulk (partial) pressure of CO_2 and $p_{CO2,i}$ is the interfacial pressure, both in bar. Because the interfacial region is thin, the flux across it will be in steady state, and the flux in the gas will equal that in the liquid. Thus,

$$R = k_G \left(p_{CO_2,G} - p_{CO_2,i} \right) = k_L \left(c_{CO_2,i} - c_{CO_2,L} \right) \qquad (9.12)$$

Where K_L is the liquid-phase mass transfer coefficient (typically in m/sec) and $c_{CO2,i}$ and $c_{CO2,L}$ are the interfacial and bulk concentrations, respectively, both in mol/m^3.
Thus the rate of absorption is given as moles of CO_2 absorbed per m^2 of gas-liquid interface and per second.

Packing exists to increase the interfacial area between gas and liquid. All types of packing come with a value of a, which indicates the surface area on the packing per m^3 of packing. From this value a value for $\underline{a}$ can be derived, which indicates the amount of gas-liquid interface created per m^3 of packing, see paragraph C.1.3.6 for the formula. Both a and $\underline{a}$ have a unit of m^2/m^3. Please note however that $a \neq \underline{a}$.
Thus, the volumetric rate of absorption $R\underline{a}$ can be expressed as

$$R\underline{a} = k_G\underline{a} \left(p_{CO_2,G} - p_{CO_2,i} \right) = k_L\underline{a} \left(c_{CO_2,i} - c_{CO_2,L} \right) \qquad (9.13)$$

Finally the CO_2 reacts in the liquid with the amine molecules, speeding the rate of absorption on the liquid side. In order to quantify this increase, the dimensionless Enhancement Factor (E) is added to the right hand side of the equation.

$$R\underline{a} = k_G\underline{a} \left(p_{CO_2,G} - p_{CO_2,i} \right) = k_L\underline{a} \left(c_{CO_2,i} - c_{CO_2,L} \right) E \qquad (9.14)$$

In order to eliminate the unknown interfacial concentrations from these equations, one can assume an equilibrium exists across the interface, which is valid for almost all cases:

$$p_{CO_2,i} = \frac{c_{CO_2,i}}{H} \qquad (9.15)$$

Where H is a type of Henry's law or partition constant (here in mol/(cm^3-atm)). Combining equations (9.14) and (9.15) one can find the volumetric rate of absorption to be

$$R\underline{a} = \frac{\left(p_{CO_2,G} - p_{CO_2,L} \right)}{\dfrac{1}{k_G\underline{a}} + \dfrac{1}{k_L\underline{a}HE}} \qquad (9.16)$$

Equation (9.16) offers an interesting analogy between absorption and electricity, as described by (Cussler, 1997). In this analogy the concentration difference is the driving factor, and thus resembles voltage. The rate of absorption is the current and the gas and liquid mass transfer coefficients can be seen as 2 resistances placed in series. Note

however that the resistances $1/k_G$ and $1/k_L$ are not directly added, but always weighted by partition coefficients like H.

In order to make equation (9.16) more practical, the top half of the equation, the "voltage" is expressed in mole fractions, as seen in equation (9.17)

$$\left(p_{CO_2,G} - p_{CO_2,L} \right) = P_T \left(y_{CO_2,G} - y_{CO_2,L} \right) \tag{9.17}$$

The mass transfer coefficients, the "resistances", can be expressed in 1 parameter, as suggested by (Vaidya and Mahajani, 2006). This parameter is given the symbol β, defined by

$$\beta = \left[1/k_G + 1/\left(k_L \cdot H \cdot E \right) \right]^{-1} \tag{9.18}$$

Substituting equation (9.17)&(9.18) in equation (9.16) gives

$$R\underline{a} = \beta P_T \left(y_{CO_2,G} - y_{CO_2,L} \right) \tag{9.19}$$

The value of β remains practically constant throughout the length of the column, variations due to temperature are usually in the order of 10%. However, when absorption is accompanied by a chemical reaction, the rate of absorption varies along the column height due to change in the enhancement factor E and hence the value of β is not constant.

C.1.3.2 Mass balance over a small volume

One can consider a small section of height of the absorber tower, as shown in Figure C.4,
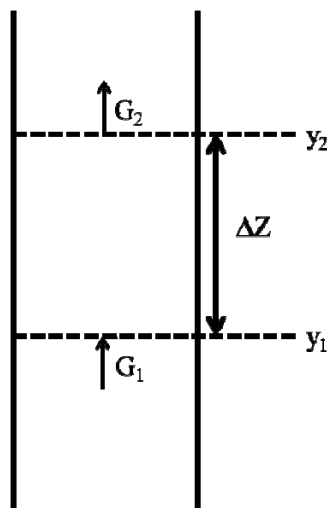
Figure C.4 Schematic of a small section of height of the absorber tower

Where the molar flow rates G_1 and G_2 in [mol/s] is given by equation (9.20)

$$G_i = \frac{G_s}{1 - y_i}, i = [1, 2] \tag{9.20}$$

In which y_i denotes respective the mole fraction of CO_2 and G_s the molar flow rate of inerts in [kmol/s]. The molar flow rate lost to absorption is then given by equation (9.21)

$$\Delta G = G_s \left(\frac{1}{1 - y_1} - \frac{1}{1 - y_2} \right) = G_s \left(\frac{\Delta y}{(1 - y_1)(1 - y_2)} \right) \tag{9.21}$$

with $\Delta y = y_1 - y_2$.

The volumetric rate of absorption $R\underline{a}$ multiplied with the cross-sectional area of the column, S gives the rate of absorption per meter of packing height, $R\underline{a}S$, in [mol/(m s)].

The change in molar flow rate is caused by the absorption over the height ΔZ, thus

$$\Delta G = R\underline{a}S \cdot \Delta Z \tag{9.22}$$

Combining equation (9.21)&(9.22)

$$\Delta Z = \frac{G_s}{R\underline{a}S} \frac{\Delta y}{(1 - y_1)(1 - y_2)} \tag{9.23}$$

When $\Delta y \rightarrow 0$, $y_1 \approx y_2 \approx y_{CO_2,G}$ and by taking the integral over dy, equation (9.23) becomes equation (9.24)

$$\Delta Z = \int_{y_2}^{y_1} \frac{G_s}{R\underline{a}S} \frac{dy_{CO_2,G}}{(1 - y_{CO_2,G})^2} \tag{9.24}$$

Which is the equation for the height of packing.

Substituting equation (9.19) in equation (9.24) yields

$$\Delta Z = \frac{G_s}{S\underline{a}P_T} \int_{y_2}^{y_1} \frac{dy_{CO_2,G}}{\beta \left(y_{CO_2,G} - y_{CO_2,back} \right)(1 - y_{CO_2,G})^2} \tag{9.25}$$

Equation (9.25) is the general design equation for calculating the height of packing. The reaction between CO_2 and alkanolamine is, in true sense, reversible. This always results in equilibrium partial pressures of CO_2, also known as backpressure, denoted by $y_{CO_2,back}$.

At the tower bottom, the solute CO_2 exerts equilibrium backpressure. The mole fraction of CO_2 in the gas is relatively high in comparison with the mole fraction of CO_2 in the liquid, therefore:

$$\left(y_{CO_2,G} - y_{CO_2,back} \right) \approx y_{CO_2,G} \tag{9.26}$$

Therefore, the effect of reversible reaction can be neglected. In other words, the reaction is pseudo irreversible. In the control volume under consideration, the change in mole fraction of CO_2 is assumed such that the variation in enhancement factor E and hence β over the volume is very small.

Thus, an average value of β can be safely used for finding the height of packing. Equation (9.25) then takes the form

$$\Delta Z = \frac{G_s}{S \underline{a} P_T \beta} \int_{y_2}^{y_1} \frac{dy_{CO_2,G}}{y_{CO_2,G}(1-y_{CO_2,G})^2} \tag{9.27}$$

At the tower top the solute CO_2 exerts a very low but finite backpressure over the absorbent, the mole fraction of CO_2 is nonzero. Also the mole fraction of the CO_2 in the gas is very small. Therefore, the assumption in equation (9.26) isn't valid here. Thus, the effect of backpressure (equilibrium) becomes dominant and here, the reversible nature of the reaction needs to be considered. The value of $y_{CO2,back}$ is taken as the mean value of the equilibrium mole fraction calculated at the top and bottom of the control volume. The equation used for the top section of the tower is

$$\Delta Z = \frac{G_s}{S \underline{a} P_T \beta} \int_{y_2}^{y_1} \frac{dy_{CO_2,G}}{\left(y_{CO_2,G} - y_{CO_2,\underline{back}}\right)(1-y_{CO_2,G})^2} \tag{9.28}$$

Stacking all calculated ΔZ's on top of each other should yield the required height of packing for removing the required amount of CO_2.

C.1.3.3 Backpressure and equilibrium concentration of CO_2 over an aqueous amine solution

The backpressure of CO_2 in the top of the column corresponds to the equilibrium pressure of CO_2 over an amine solution.(Jou et al., 1994) published data on this, shown in Figure A.3 and Figure A.4. The data is considered at 40°C, and the values of 24wt% MEA + 6wt% MDEA are assumed to be the same as 30%MEA. It is also assumed that the relative difference in partial pressure between 15wt% MEA and 30wt% MEA solution is the same for all loading factors a.

This leads to the values shown in Table C.1. Obtaining $y_{CO_2,back}$ is as simple as dividing the equilibrium partial pressure by the total pressure in the column.

Table C.1 Equilibrium Partial pressure of CO_2 over an aqueous MEA solution

mol CO₂ / mol MEA	Partial Pressure @ 30 wt% MEA solution and 40°C [kPa]	Partial Pressure at 15 wt% MEA solution and 40°C [kPa]
0,00	0,0	0
0,10	0,002	0,006
0,15	0,020	0,06
0,20	0,040	0,12
0,30	0,100	0,3
0,40	0,2	0,6
0,50	2,0	6,0
0,60	20,0	60,0
0,70	100,0	300,0
0,80	300,0	900,0

C.1.3.4 Correlations for Solubility, Diffusivity and the Reaction Rate constant

Solubility

The solubility of CO_2 in a MEA solution can be calculated with a correlation. This solubility is represented by the variable H, which is Henry's law constant.

The ionic strength in a 2,5 M MEA solution varies from 0,375 to 1 [g ion L^{-1}] and hence H varies from $10^{-(0,07 \cdot 0,375)} = 0,94$ to $10^{-(0,07 \cdot 1)} = 0,85$ times that in pure water. The solubility of CO_2 in pure water was found using the following correlation. (Versteeg and Van Swaaij, 1988b).

$$H_{CO_2,H_2O} = 3,54 \cdot 10^{-7} \exp(2044/T) \tag{9.29}$$

In this case the unit of H is $kmol/(m^3 \cdot kPa)$

Reaction Rate Constant

The second order reaction rate constant for CO_2-MEA systems was found using the following correlation. (Versteeg and Van Swaaij, 1988a)

$$\ln k_2 = pK_a + 16.26 - (T_a/T) \tag{9.30}$$

With $T_a = 7188K$ and pK$_a$ ranging from 9,66 for 293 K to 9,51 for 298 K and to 9,36 for 303 K. This gives an approximate equation $pK_a = 9,66 - 0,03(T - 293)$.

Therefore one can write for equation (9.30):

$$k_2 = e^{(9,66-0,03(T-293))+16,26-(7188/T)} = e^{34,71-0,03T-(7188/T)} \tag{9.31}$$

Diffusivity

CO_2 in solution

In order to obtain the diffusivity of CO_2 in an amine solution, one can first look at the diffusivity of CO_2 in pure water. The diffusivity of CO_2 in water was found using the following correlation. (Versteeg and Van Swaaij, 1988b)

$$D_{CO_2,H_2O} = 2,35 \cdot 10^{-6} \exp(-2119/T) \tag{9.32}$$

One can then assume that the ratio of diffusivity of CO_2 in a 2,5 M MEA solution to that in pure water at 298 K is 0,64 and that this ratio remains unchanged throughout the length of the column.

MEA in solution

Values for the diffusivity of MEA in a solution are taken from (Ko et al., 2008).

In order to make this diffusivity suitable for the model, i.e. be able to change with the temperature of the solution the temperature coefficient of diffusivity of amine, D_{MEA}, in the solution was assumed to be the same as that of CO_2 in water.

For a 2,5 M MEA solution at 313,2 K the diffusivity given by (Ko et al., 2008) is 9,75E-10 m^2/s. This leads to a base value of

$$\frac{9,75 \cdot 10^{-10}}{e^{-2119/313,2}} = 1,064 \cdot 10^{-6} \tag{9.33}$$

And a formula for $D_{MEA,H2O}$

$$D_{MEA,H_2O} = 1,064 \cdot 10^{-6} \exp\left(-2119/T\right) \tag{9.34}$$

This formula shows ±1% error over a variation of 10K from the 313,2K, and thus gives acceptable results.

CO_2 in gas
For the diffusivity of CO_2 in the gas mixture one can take values from literature which are generally measured/calculated at 1 atm and 273 to 298 K.

However, because our model has to be useable at arbitrary temperatures and pressures a correlation incorporating these factors is preferred.
The most common method for theoretical estimation of gaseous diffusion is that developed independently by Chapman and by Enskog. (Chapman and Cowling, 1991). This theory, accurate to an average of about 8%, leads to equation (9.35),

$$D = \frac{1,86 \cdot 10^{-3} T^{3/2} \left(1/\tilde{M}_1 + 1/\tilde{M}_2\right)^{1/2}}{p\sigma_{12}^2 \Omega} \tag{9.35}$$

in which D is the diffusion coefficient, measured in cm^2/s, T is the absolute temperature in K, p is the pressure in atmospheres and the $\tilde{M}_i$ are molecular weights in g/mol.
The quantities σ_{12} and Ω are molecular properties characteristic of the detailed theory. The collision diameter σ_{12}, given in angstroms, is the arithmetic average of the two species present:

$$\sigma_{12} = \frac{1}{2}\left(\sigma_1 + \sigma_2\right) \tag{9.36}$$

Values of σ_1 and σ_2 are listed in Table C.2. The dimensionless quantity Ω is more complex, but usually of order 1. Its detailed calculation depends on an integration of the interaction between the two species. This interaction is most frequently described by the Lennard-Jones 12-6 potential. The resulting integral varies with the temperature and the energy of interaction. This energy ε_{12} is a geometric average of contributions from the two species:

$$\varepsilon_{12} = \sqrt{\varepsilon_1 \varepsilon_2} \tag{9.37}$$

Values of the ε_i are also given in Table C.2. Once ε_{12} is known, Ω can be found as a function of ε_{12}/kT using the values in Table C.3. The calculation of the diffusion coefficients now becomes straightforward.

Table C.2 Lennard-Jones potential parameters found from viscosities
Source: (Cussler, 1997) – Table 5.1-2

Substance		σ(Å)	ε/k_B(°K)
Ar	Argon	3.542	93.3
He	Helium	2.551	10.22
Kr	Krypton	3.655	178.9
Ne	Neon	2.820	32.8
Xe	Xenon	4.047	231.0
Air	Air	3.711	78.6
Br_2	Bromine	4.296	507.9
CCl_4	Carbon tetrachloride	5.947	322.7
CF_4	Carbon tetrafluoride	4.662	134.0
$CHCl_3$	Chloroform	5.389	340.2
CH_2Cl_2	Methylene chloride	4.898	356.3
CH_3Br	Methyl bromide	4.118	449.2
CH_3Cl	Methyl chloride	4.182	350
CH_3OH	Methanol	3.626	481.8
CH_4	Methane	3.758	148.6
CO	Carbon monoxide	3.690	91.7
CO_2	Carbon dioxide	3.941	195.2
CS_2	Carbon disulfide	4.483	467
C_2H_2	Acetylene	4.033	231.8
C_2H_4	Ethylene	4.163	224.7
C_2H_6	Ethane	4.443	215.7
C_2H_5Cl	Ethyl chloride	4.898	300
C_2H_5OH	Ethanol	4.530	362.6
CH_3OCH_3	Methyl ether	4.307	395.0
CH_2CHCH_3	Propylene	4.678	298.9
CH_3CCH	Methylacetylene	4.761	251.8
C_3H_6	Cyclopropane	4.807	248.9
C_3H_8	Propane	5.118	237.1
$n\text{-}C_3H_7OH$	n-Propyl alcohol	4.549	576.7
CH_3COCH_3	Acetone	4.600	560.2
CH_3COOCH_3	Methyl acetate	4.936	469.8
$n\text{-}C_4H_{10}$	n-Butane	4.687	531.4
iso-C_4H_{10}	Isobutane	5.278	330.1
$C_2H_5OC_2H_5$	Ethyl ether	5.678	313.8
$CH_3COOC_2H_5$	Ethyl acetate	5.205	521.3
$n\text{-}C_5H_{12}$	n-Pentane	5.784	341.1
$C(CH_3)_4$	2,2-Dimethylpropane	6.464	193.4
C_6H_6	Benzene	5.349	412.3
C_6H_{12}	Cyclohexane	6.182	297.1
$n\text{-}C_6H_{14}$	n-Hexane	5.949	399.3
Cl_2	Chlorine	4.217	316.0
F_2	Fluorine	3.357	112.6
HBr	Hydrogen bromide	3.353	449
HCN	Hydrogen cyanide	3.630	569.1
HCl	Hydrogen chloride	3.339	344.7
HF	Hydrogen fluoride	3.148	330
HI	Hydrogen iodide	4.211	288.7
H_2	Hydrogen	2.827	59.7
H_2O	Water	2.641	809.1
H_2O_2	Hydrogen peroxide	4.196	289.3
H_2S	Hydrogen sulfide	3.623	301.1

Hg	Mercury		2.969		750
I_2	Iodine		5.160		474.2
NH_3	Ammonia		2.900		558.3
NO	Nitric oxide		3.492		116.7
N_2	Nitrogen		3.798		71.4
N_2O	Nitrous oxide		3.828		232.4
O_2	Oxygen		3.467		106.7
PH_3	Phosphine		3.981		251.5
SO_2	Sulfur dioxide		4.112		335.4
UF_6	Uranium hexafluoride		5.967		236.8

Table C.3 The collision integral Ω
Source: (Cussler, 1997) – Table 5.1-3

k_BT/ε	Ω	k_BT/ε	Ω	k_BT/ε	Ω
0.30	2.662	1.65	1.153	4.0	0.8836
0.35	2.476	1.70	1.140	4.1	0.8788
0.40	2.318	1.75	1.128	4.2	0.8740
0.45	2.184	1.80	1.116	4.3	0.8694
0.50	2.066	1.85	1.105	4.4	0.8652
0.55	1.966	1.90	1.094	4.5	0.8610
0.60	1.877	1.95	1.084	4.6	0.8568
0.65	1.798	2.00	1.075	4.7	0.8530
0.70	1.729	2.1	1.057	4.8	0.8492
0.75	1.667	2.2	1.041	4.9	0.8456
0.80	1.612	2.3	1.026	5.0	0.8422
0.85	1.562	2.4	1.012	6	0.8124
0.90	1.517	2.5	0.9996	7	0.7896
0.95	1.476	2.6	0.9878	8	0.7712
1.00	1.439	2.7	0.9770	9	0.7556
1.05	1.406	2.8	0.9672	10	0.7424
1.10	1.375	2.9	0.9576	20	0.6640
1.15	1.346	3.0	0.9490	30	0.6232
1.20	1.320	3.1	0.9406	40	0.5960
1.25	1.296	3.2	0.9328	50	0.5756
1.30	1.273	3.3	0.9256	60	0.5596
1.35	1.253	3.4	0.9186	70	0.5464
1.40	1.233	3.5	0.9120	80	0.5352
1.45	1.215	3.6	0.9058	90	0.5256
1.50	1.198	3.7	0.8998	100	0.5130
1.55	1.182	3.8	0.8942	200	0.4644
1.60	1.167	3.9	0.8888	300	0.4360

C.1.3.5　　Calculating Enhancement Factor E

The absorption of CO_2 in alkanolamine under industrial operating conditions (strength of amine and temperature) exhibits first order behavior with respect to both CO_2 and alkanolamine, thus making it an overall second order reaction.

There are several cases to be defined based on properties of the reaction. The first equation that is introduced here is the Hatta number. (Hatta, 1932), in the form used by (Roizard and Wild, 2002).

$$Ha = \frac{\left\{ \frac{2}{m+1} D_{CO_2,L} k_{mn} \left(y_{CO_2,i} \right)^{m-1} \left(y_{freeMEA,L} \right)^{n} \right\}^{0,5}}{k_L} \tag{9.38}$$

With

- **m & n** representing the reaction order with respect to CO_2 and MEA, respectively.
- **$D_{CO2,L}$** is the diffusivity of CO_2 in the MEA solution
- $y_{CO_2,i}$ is the concentration of CO_2 at the gas-liquid interface in equilibrium with the liquid, [kmol/m^3]
- $y_{freeMEA,L}$ is the free amine concentration [kmol/m^3]
- **k_L** is the liquid side mass transfer coefficient [m/s]

When m and n are both taken to be 1, thus overall second order, one can simplify equation (9.38) to equation (9.39), revealing the Hatta number for this particular case, shown in equation (9.39)

$$Ha = \frac{\left\{ D_{CO_2,L} k_2 \left(y_{freeMEA,L} \right)^{n} \right\}^{0,5}}{k_L} \tag{9.39}$$

The Hatta number, Ha, compares the maximum chemical conversion in the mass transfer film to the maximum diffusion flux through this liquid film. This dimensionless number is of prime importance since it indicates where the chemical reaction occurs.
When $Ha^2 \ll 1$ (or Ha < 0,3) the conversion rate in the liquid film is negligible and the chemical reaction occurs in the liquid bulk. This case is called the 'slow regime'. Liquid flow behavior in the reactor then has to be taken into account.
On the other hand, when $Ha^2 \gg 1$ (or Ha > 3), chemical reaction occurs totally in the boundary layer. This case is called the 'fast regime' and the liquid hydrodynamics is of less importance per se, although the interfacial area of course also depends on hydrodynamics.

The q criterion is the ratio of maximum diffusion fluxes of MEA and CO_2 species

$$q = \frac{\left(y_{freeMEA,L} \right)}{w \left(y_{CO_2,i} \right)} \frac{D_{MEA,L}}{D_{CO_2,L}} \tag{9.40}$$

With **w** the stoichiometric coefficient of reaction.
The maximum enhancement factor is noted as E_i and thus denotes then enhancement factor when the reaction between CO_2 and MEA is instantaneous.

$$E_i = 1 + q \tag{9.41}$$

Finally an average enhancement factor can be calculated for most 'fast regime' cases, denoted by E_{avg}

$$E_{avg} = \left\{ \frac{Ha^4}{4(E_i-1)^2} + \frac{Ha^2 E_i}{(E_i-1)} + 1 \right\}^{0,5} - \frac{Ha^2}{2(E_i-1)} \tag{9.42}$$

The enhancement factors used under various regimes of operation are listed in Table C.4.

Table C.4 Enhancement factor 'E' under various conditions of operation
Source: (DeCoursey, 1974)

Regime	Criteria	Value Enhancement factor
Slow	$Ha < 3$ AND $Ha \ll q$	$\sqrt{Ha^2 + 1}$
Intermediate	$3 < Ha \ll q$	Ha
Fast	$Ha > 3$ AND $Ha \approx q$	E_{avg}
Very Fast	$Ha > 5$ AND $Ha \gg q$	E_i

Note that $Ha = \sqrt{M}$ in (Vaidya and Mahajani, 2006) & (DeCoursey, 1974)

C.1.3.6   Calculating the mass-transfer coefficients

A theoretical model, created by (Billet and Schultes, 1993), is used here that allows mass transfer to be described in terms of packing geometry and physical properties which influence the gas-liquid or vapor-liquid systems in absorption, desorption and rectification columns. The relationships derived from the model can be applied to all countercurrent-flow columns, regardless of whether the packing has been dumped at random or arranged in a geometric pattern

Liquid Phase
The liquid must flow in the form of a thin film and be distributed as uniformly as possible over the entire cross-section of the column in order to ensure large throughputs, effective mass transfer and moderate pressure drops. The surface of the packing should be wetted as much as possible and the countercurrent flow of gas should also be uniformly distributed over the column cross-section. Thus, the factors that govern the fluid dynamics and mass transfer of a column are the physical properties of the system, its capacity range and the shape and structure of the packing.

The efficiency of a packing is influenced by the length of flow path l_T, which has to be traversed before the surface of the liquid in contact with the gas is renewed. Since the liquid is continually remixed at the points of contact with the packing, the mass transfer in the liquid phase occurs by non-steady state diffusion, as seen in equation (9.43). D_L is the diffusion coefficient of the transferring component and τ_L is the time necessary for the renewal of interfacial area is determined by equation (9.44) with liquid hold-up h_L, length of flow path l_T, and liquid load u_L. A list of used symbols in this paragraph is given in Table C.6.

$$k_L = \frac{2}{\pi}\sqrt{D_L \frac{1}{\tau_L}} \qquad (9.43)$$

$$\tau_L = h_L l_\tau \frac{1}{u_L} \qquad (9.44)$$

If the packing is regarded as a large number of Channels through which the liquid of density ρ_L and viscosity μ_L flows as a film with a local velocity $\bar{u}_{L,s}$, countercurrent to a stream of gas, liquid flow can be described by the equilibrium of forces, equation (9.45), provided that the forces of inertia are negligible. This equation applies at any given point $0 \leq s \leq s_0$ in the laminar liquid film.

$$\frac{d\left(\eta_i \dfrac{d\bar{u}_{L,s}}{ds}\right)}{ds} = -\rho_L g \qquad (9.45)$$

Gravity and shear forces in the film are maintained at equilibrium with the frictional forces by the shear stress τ_v in the gas or vapor flow at the surface of the film, equation (9.46). In equation (9.46), ρ_v is the gas density, $\bar{u}_V$ the average effective gas velocity and ψ_L the drag coefficient for the gas-liquid or vapor-liquid countercurrent flow.

$$\tau_V = -0,5\psi_L \rho_V \bar{u}_V^2 \qquad (9.46)$$

Integration of equation (9.45) and substitution of the frictional force of the gas, acting at the surface of the liquid, by equation (9.46), lead theoretically to equation (9.47), valid for the liquid hold-up h_L at and below the loading point. In equation (9.47), u_L is the liquid load based on the column cross-section and a the total surface area of the packing.

$$h_L = \left(12\frac{1}{g}\frac{\eta_L}{\rho_L}u_L a^2\right)^{1/3} \qquad (9.47)$$

Combining equations (9.43), (9.44) and (9.47) gives rise to equation (9.48) for the mass transfer coefficient k_L and equation (9.50) for the height of a transfer unit HTU_L on the liquid-side.

$$k_L = C_L\left(\frac{D_L}{l_\tau}\right)^{1/2}\left(\frac{g}{\nu_L}\right)^{1/6}\left(\frac{u_L}{a}\right)^{1/3} \qquad (9.48)$$

Or

$$k_L a_i = C_L\left(\frac{D_L}{l_\tau}\right)^{1/2}\left(\frac{g}{\nu_L}\right)^{1/6}a^{2/3}u_L^{1/3}\left(\frac{a_i}{a}\right) \qquad (9.49)$$

$$HTU_L = \frac{1}{C_L}\left(\frac{\nu_L}{g}\right)^{1/6}\left(\frac{l_\tau}{D_L}\right)^{1/2}\left(\frac{u_L}{a}\right)^{2/3}\left(\frac{a}{a_i}\right) \qquad (9.50)$$

In these equations, a_i is the effective interfacial area for mass transfer and C_L is a constant, characteristic of the shape and structure of packing. From the combination of the equations (9.43), (9.44) and (9.47), C_L obtains the value

$$C_L = \frac{2}{\sqrt{\pi}}\left(\frac{1}{12}\right)^{1/6} = 0,74575 \qquad (9.51)$$

But usually values for C_L are listed per packing type by the manufacturer.

Gas Phase
The theoretical model is based on the assumption that the gas flows through the packing in different directions, passing mixing zones as well as those where mass transfer occurs. The theoretical time interval τ_v required for the renewal of the contact area between the phases is defined by the length of the flow path l_T, the superficial gas velocity u_v, the void fraction ε and the liquid hold-up h_L, as seen in equation (9.52)

$$\tau_V = (\varepsilon - h_L)l_\tau \frac{1}{u_V} \tag{9.52}$$

The time of contact τ_v corresponding to the flow path l_T, is comparatively short in conventional packed beds, and mass transfer takes place in a very thin sublayer. Therefore, it can be assumed that for mass transfer in the gas phase, the law of nonsteady state diffusion described by equation (9.53) also follows. This equation contains the coefficient of diffusion D_V for the solute in the gas phase.

$$k_G = \frac{2}{\sqrt{\pi}}\sqrt{D_v \frac{1}{\tau_V}} \tag{9.53}$$

Together with equations (9.47) and (9.52), equation (9.53) gives rise to equation (9.54) for the mass transfer coefficient k_G and to equation (9.56) for the height of a transfer unit HTU_V on the gas side, in which the exponents $m = 3/4$ and $n = 1/3$ on the gas Reynolds number and the Schmidt number, respectively, allow the best correlation of obtained test results. (Billet and Schultes, 1993)

$$k_G = C_V \frac{1}{(\varepsilon - h_L)^{1/2}}\left(\frac{a}{l_\tau}\right)^{1/2} D_V \left(\frac{u_V}{av_V}\right)^m \left(\frac{v_V}{D_V}\right)^n \tag{9.54}$$

$$k_G a_i = C_V \frac{1}{(\varepsilon - h_L)^{1/2}}\frac{a^{3/2}}{l_\tau^{1/2}} D_V \left(\frac{u_V}{av_V}\right)^m \left(\frac{v_V}{D_V}\right)^n \left(\frac{a_i}{a}\right) \tag{9.55}$$

$$HTU_V = \frac{1}{C_V}(\varepsilon - h_L)^{1/2}\frac{l_\tau^{1/2}}{a^{3/2}}\frac{u_V}{D_V}\left(\frac{av_V}{u_V}\right)^m \left(\frac{D_V}{v_V}\right)^n \left(\frac{a}{a_i}\right) \tag{9.56}$$

Again, in these equations, a_i is the effective interfacial area for mass transfer and C_V a constant, characteristic of the shape and structure of the packing, which has to be determined experimentally and is supplied by the manufacturer.

In accordance with (Vaidya and Mahajani, 2006), this work uses $1^{1/2}$ inch Rachsig Rings, with a void fraction of 0,68 and a value $C_L = 1,563$ and $Cv = 0,23$, as found in the packing characteristics tables in (Billet and Schultes, 1993)

C.1.3.7   *Calculating the Effective interfacial area*
(Billet and Schultes, 1993) also reported the results of an extensive analysis of experimental data and a dimensional analysis of the influencing parameters showed that the volumetric mass transfer coefficients could be determined most accurately if the characteristic length of the flow path l_T, was described in terms of the hydraulic diameter

d_h, as seen in equation (9.57). The ratio between effective gas-liquid interfacial area, $\underline{a}$, and the surface area of the packing, a, was best represented by equation (9.58).

$$l_\tau = d_h = 4\frac{\varepsilon}{a} \tag{9.57}$$

$$\frac{\underline{a}}{a} = 1{,}5\left(ad_h\right)^{-0{,}5}\left(\frac{u_L d_h}{\nu_L}\right)^{-0{,}2}\left(\frac{u_L \rho_L d_h}{\sigma_L}\right)^{0{,}75}\left(\frac{u_L^2}{gd_h}\right)^{-0{,}45} \tag{9.58}$$

$$\frac{\underline{a}}{a} = 1{,}5\left(ad_h\right)^{-0{,}5}\left(\text{Re}_L\right)^{-0{,}2}\left(We_L\right)^{0{,}75}\left(Fr_L\right)^{-0{,}45} \tag{9.59}$$

Thus, the factors governing the ratio of the interfacial to the geometric surface area are the density ρ_L, the kinematic viscosity ν_L and surface tension σ_L of the liquid, area of the unwetted packing a, hydraulic diameter d_h and liquid load u_L.

The surface tension of the liquid can be found in literature, for instance the research by (Fu et al., 2012), shows the following graph for the surface tension of a MEA-solution loaded with CO_2, shown in Figure C.5.
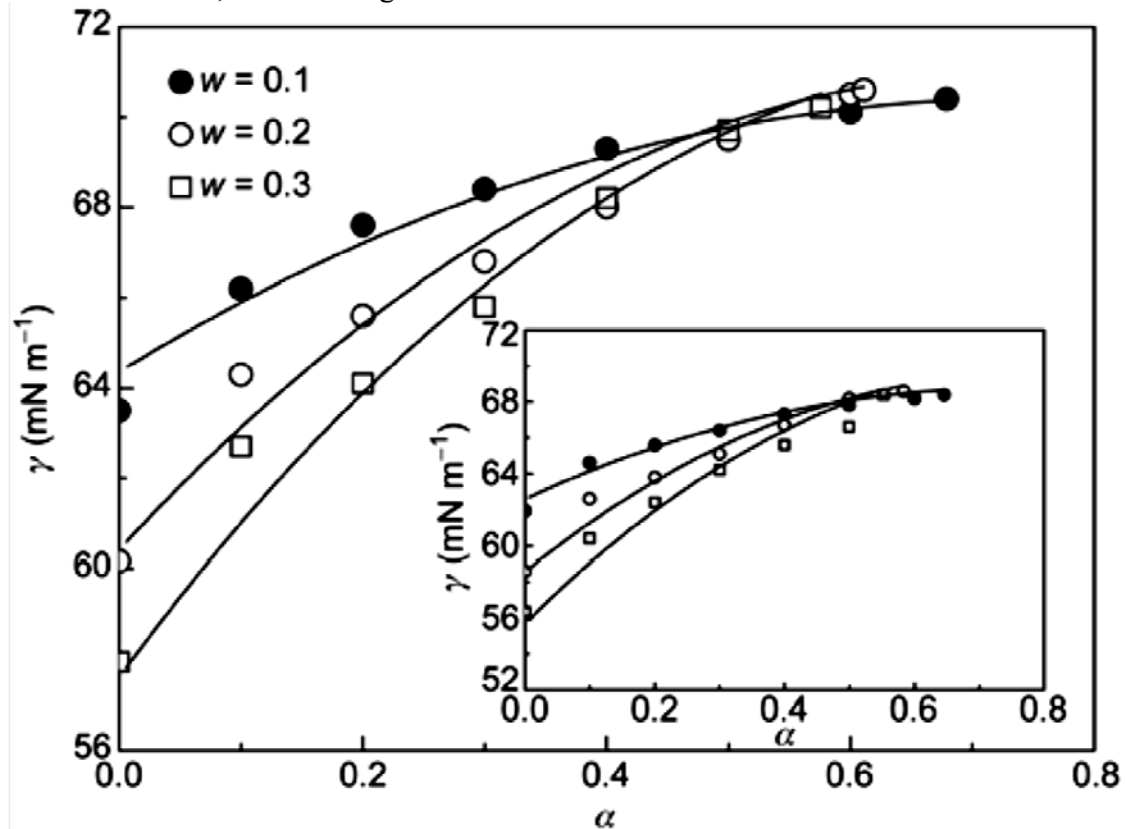
Figure C.5 Effects of mass fraction and CO2 loading on the surface tension of carbonated MEA aqueous solutions. T = 313.15 and 323.15 K (insert). Symbols: experimental data; lines: calculated results. Source: (Fu et al., 2012)

Equation (9.58) can be verified by the reader by calculating the interfacial area for some widely used types of packing and comparing these values with literature, such as the research of (Kolev et al., 2006).

However, because the surface tension changes with loading and Temperature, thus changes over the height of the tower, it is slightly beyond the scope of this work to incorporate this surface tension gradient and the corresponding correction on the a_{ph}. The reader is referred to the work of (Billet and Schultes, 1993) for more information on this subject.

This work assumes an effective interfacial area of 140 m^2/m^3, as suggested by (Vaidya and Mahajani, 2006)

C.1.3.8 Total Height of Packing

The method works as indicated in the logic-block diagram in Figure C.6. One chooses a new concentration y_2 for the top of the control volume. This new concentration corresponds to a new β. If the value of the new beta is less than 10% different from the value of the old β the choice of y_2 is acceptable. One calculates an average β and solves equation (9.27) or (9.28) for the height, Z of the volume, depending on if the backpressure has to be taken into account. All the parameters valid for the top of the control volume become the parameters for the bottom of the next volume and the process repeats itself, until the desired concentration is reached.
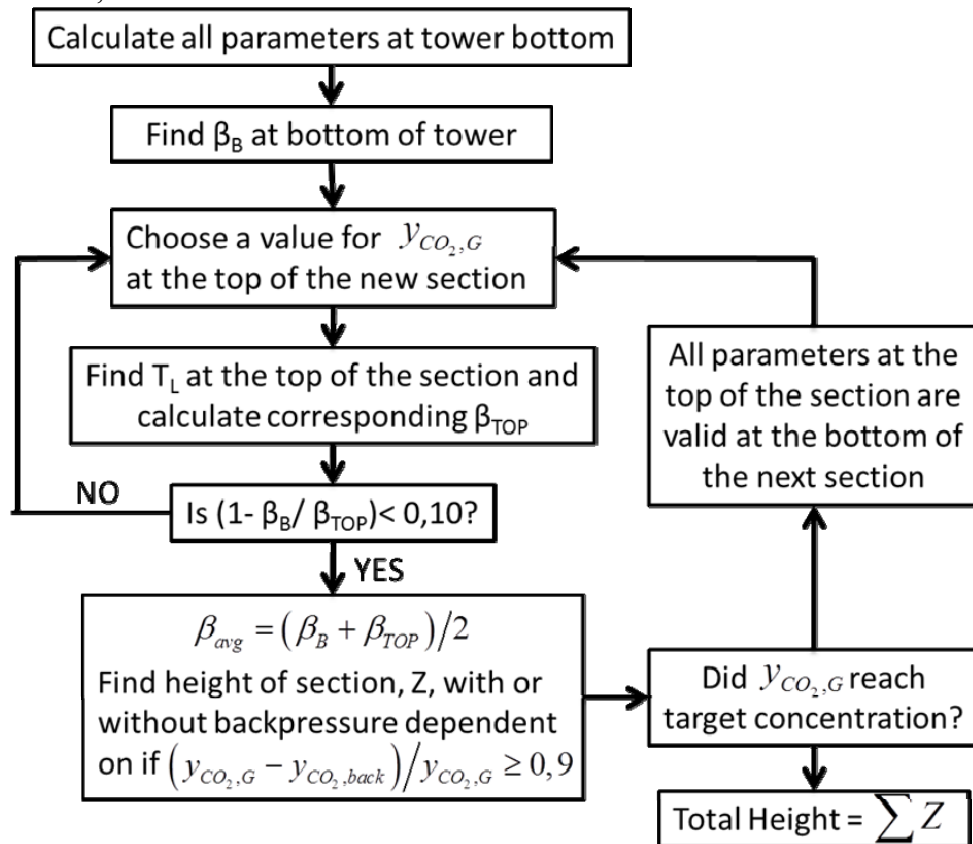
Figure C.6 Logic Block Diagram for packing height calculation

87

C.1.3.9   Total Tower Height

With paragraphs equation (9.27) & (9.28) one can calculate the required height of packing in the absorber tower. There are several other devices in an absorber tower that increase the height.

Height of Liquid distribution

Liquid redistributors are used to funnel the liquid back over the entire surface of packing, because the liquid tends to flow towards the column wall, following the path of least resistance. Liquid redistributors are placed after every 10 feet (3,1 meters) of packing height (or 5 tower diameters, whichever is smaller) to ensure equal spreading of liquid over the packing. (APTI, 1999)

Another reason to limit the continuous height of packing is the deformability of the packing under its own weight. (Kohl and Nielsen, 1997) state that for every form of random packing the maximum height of packing is 20-25 feet (6-7,5 meters) for metal packing and 10-15 feet (3-4,5 meters) for plastics.

Between 2 layers of packing, there's usually: (Schultes and Halbirt, 2010) & Figure A.2
- A support plate for the top layer of packing (250 mm)
- A manhole in the column wall for maintenance and inspection (480mm)
- A liquid inlet + liquid distributor (200 + 250 mm)
- A hold down plate for the next layer of packing (150 mm)
- Room to maneuver for maintenance crew

Therefore the height of a liquid distribution section is assumed to be 1,5 meters.

Top of tower; Carryover reduction

Entrained amine in the gas stream on top of the last layer packing can potentially cost a lot of amine and thus money. Therefore most modern designs include either a water wash at the top of 4 to 6 trays or a system of mist eliminators. (Sheilan et al., 2009). Alternatively mist eliminators can be used, as explained in section B.8.5.

This height is estimated to be 2 meters from the top of the liquid inlet.

Bottom of tower

At the tower bottom, there are systems to accumulate the downcoming solution before it enters the rich amine piping and spread the upwards flowing gas stream over the tower cross-sectional area. This takes up approximately 4 m of the total height and this includes the tower base and support. (Kohl and Nielsen, 1997)

Table C.5 Subscripts used in paragraph C.1.3

Subscript	Description
D	Top product
L	Liquid
o	Surface
i	Interface
s	Film thickness
V,G	Vapor, Gas
W	Bottom product

Table C.6 Symbols used in paragraph C.1.3

Symbol	Unit	Description
a	m^2/m^3	Total surface area per unit packed volume
$\underline{a}$	m^2/m^3	Effective interfacial area per unit packed volume
C	[-]	Constant
d_h	m	Hydraulic diameter
D	m^2/s	Diffusion coefficient of transferring component
g	m/s^2	Gravitational acceleration
H	m	Height
h_L	m^3/m^3	Liquid hold-up
HTU	m	Height of a mass transfer unit
HTU_O	m	Overall height of a mass transfer unit
L	$kmol/h$	Molar flow rate of liquid
l_T	m	Length of flow path
M	$kg/kmol$	Molar mass
m_{yx}	$kmol/kmol$	Slope of the equilibrium line
n,m	[-]	Exponents
n_{th}	[-]	Number of theoretical stages
N	$1/m^3$	Packing density
r	[-]	Reflux ratio
s	m	Film thickness
T	K	Temperature
u_L	$m^3/(m^2 s)$	Liquid load
$\bar{u}_{L,s}$	m/s	Local liquid velocity
u_V	m/s	Superficial gas or vapor velocity
$\bar{u}_V$	m/s	Average effective gas or vapor velocity
V	$kmol/h$	Molar flow rate of gas or vapor
k	m/s	Mass transfer coefficient
x	$kmol/kmol$	Mole fraction in liquid phase
y	$kmol/kmol$	Mole fraction in gas or vapor phase
α	[-]	Relative volatility
δ	%	Relative error
ε	m^3/m^3	Void fraction
η	$kg/(m\ s)$	Viscosity
λ	[-]	Stripping factor
v	m^2/s	Kinematic viscosity
ρ	kg/m^3	Density
σ	kg/s^2	Surface tension
τ	s	Duration of contact
τ	$kg/(ms^2)$	Shear stress
ψ	[-]	Drag coefficient

C.2   Stripper

Like the absorber, the stripper is either a tray type or packed column with approximately 20 trays or the equivalent height in packing, see Figure B.5. To minimize amine vaporization loss, there may be a water wash section at the top of the column with an additional four to six trays. (Kohl and Nielsen, 1997)

C.2.1   Diameter

The diameter of the stripper tower can be estimated in the same way as the diameter for absorber towers. As a side note, when one would like to use a tray column tower one can use the downcomer area instead of the void fraction of packing in the calculation using the superficial gas velocity, to find an approximate value for the diameter.

C.2.2   Height

The height of a stripper tower is somewhat more difficult to calculate than the height of the absorber tower, not easily found in literature. However there are quite a lot of sources stating that the height of a stripper tower is usually fairly constant, between certain margins.

This can be understood when one realizes that the stripper tower is basically a heat exchanger, exchanging heat between the upward flowing steam + sour gas mixture coming from the reboiler and the downward flowing rich amine stream.

The rise in temperature of the rich amine stream required is given by the temperature at which the bond between amine and sour gas molecules breaks and the temperature at which the rich amine stream enters the tower. Reboiler temperatures are usually between 116 and 127 °C and entering rich amine streams between 93 and 99 °C. (Sheilan et al., 2009).

As an increase in flow of amine results in a direct increase of diameter, not in height, one can assume that the height of the tower only scales with the temperature difference between rich amine inlet and reboiler inlet. Strippers in practice also have between 16 and 26 trays or an equivalent height of packing (Kohl and Nielsen, 1997)

As this work keeps both inlet and outlet temperature values constant, the height is also assumed constant. Therefore this height is assumed to be 19,3 meters, based on operating data found in (Kohl and Nielsen, 1997).

C.3   Reboiler

The Kettle Reboiler is used to heat the tower bottoms (lean amine) stream to vaporize the last of the captured CO_2 and H_2S from the liquid. The vapor returns to the stripper, while the lean amine is pumped from the bottom of the Reboiler. A schematic of a typical Kettle Reboiler is given in Figure B.14.
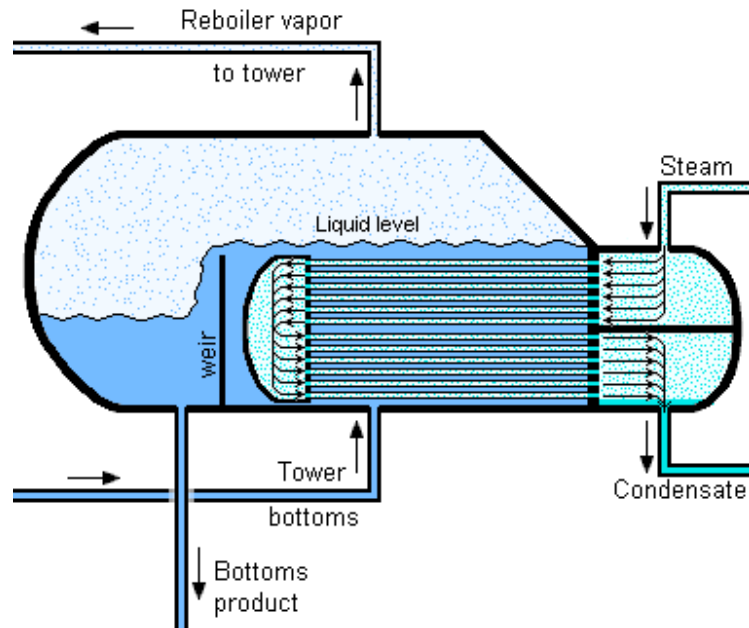
Figure C.7 Schematic of a Kettle Reboiler

The reboiler heat duty includes

- The sensible heat required to raise the temperatures of the rich amine feed, the reflux, and the makeup water to the temperature of the reboiler
- The heat of reaction to break chemical bonds between the acid gas molecules and the amine
- The heat of vaporization of water to produce a stripping vapor of steam.

This required heat is supplied by the condensing of steam from the steam furnace. Equation (9.60) shows the heat balance.

$$
\begin{aligned}
&\underbrace{\dot{m}_{steam} \cdot \dot{Q}_{cond}\left(T_{steam}, P_{steam}\right)}_{\text{Steam Condensation}} = \\
&\underbrace{\dot{m}_{vapor} \cdot \dot{Q}_{vaporisation}\left(T_{liquid}, P_{liquid}\right)}_{\text{Water Vaporization}} \\
&+ \underbrace{\dot{Q}_{reaction} \cdot \dot{m}_{CO_2}}_{CO_2 \text{ stripping}} + \underbrace{\dot{Q}_{reaction} \cdot \dot{m}_{H_2S}}_{H_2S \text{ stripping}} \\
&+ \underbrace{\dot{m}_{rich} \cdot c_p \cdot \Delta T}_{\text{Heating Rich Stream}} + \underbrace{\dot{m}_{reflux} \cdot c_p \cdot \Delta T}_{\text{Heating reflux}} \\
&- \text{Reclaimer Duty}
\end{aligned}
\tag{9.60}
$$

Note that when one uses a reclaimer one has to subtract the heat duty done be the reclaimer, equation (9.61), from the right-hand-side of equation (9.60).
This valid when one assumes that 100% of the flow to the reclaimer is evaporated and returned to the stripper. There it will give its excess heat to the down coming liquid, cooling itself toward reclaimer operating temperature, returning all duty performed by the reclaimer into the stripper. As the concentration of heat stable salts and other

contaminants removed by the reclaimer is usually a very small percentage of the lean amine flow per second, this is a valid assumption.

In order to strip the Rich Amine stream from its CO_2 and/or H_2S this stream has to be heated to a certain temperature in the tower and reboiler. This temperature is the temperature at which the bond between the amine and the CO_2 and/or H_2S breaks. The value of this temperature depends on the type of amine used.

The temperatures and pressures in the reboiler are cited from 2 different sources below.
- "For a MEA absorption system, a consensus exists that the reboiler temperature should be approximately 120 to 125 °C in order to prevent solvent degradation and corrosion. Assuming a 124 °C temperature in the reboiler and ten degree pinch, the reboiler should use saturated steam at 134 °C and approximately 3 bar." (Bashadi and Herzog, 2011)
- "To prevent thermal degradation of the amine solvent, steam or hot oil temperatures providing heat to the reboiler should not exceed 350 °F (177 °C). Superheated steam should be avoided. 50 psig (350 kPa) saturated steam is recommended. The maximum bulk solution temperature in the reboiler should be limited to 260 °F (127 °C) to avoid excessive degradation." (Sheilan et al., 2009)

This provides a target temperature for the rich amine stream and the reflux stream. The rich amine stream enters the stripper tower at between 93 and 99 °C. The reflux drum operates at a temperature of 40 °C. The vapor mass flow is given by the 2:1 molar ratio of steam to CO_2 in the stripper tower and is assumed to be equal to the reflux mass flow. The heat of reaction ($Q_{reaction}$) is listed in Table A.4. Heat of condensation and vaporization of water can be found in literature.
Using equation (9.60), one can obtain the required mass flow of steam from the steam furnace.
The installed volume of the reboiler is not easily found in literature, but is assumed to be approximately equal to the reclaimer installed volume.

C.4   Reclaimer
To determine the reclaimer capacity, a side stream of 1 to 3% of the total amine circulation rate is normally used. It is sometimes desirable to design the capacity on the basis of the time required to "turn over" an amount of solution equivalent to the plant charge. A plant circulating 200 gallons of solution per minute might have a total solution charge of 9000 gallons. Using the 1 percent basis, the reclaimer circulation rate will be 2 gpm and an equivalent of the total plant charge would be distilled in three days. A 3 percent reclaimer rate will theoretically turn the solution over in one day. The reclaimer vessel normally has a liquid capacity in volume of approximately 100 times the feed rate of the reclaimer in the same volume per minute. (Sheilan et al., 2009). One can assume that the liquid capacity is 2/3[rds] of the total volume of the reclaimer.

The heat duty of the reclaimer, when in the steady state boiling step, is based on
- Heating the incoming lean amine solution to the operating temperature.

- Vaporizing an equal amount of mass per second as comes into the reclaimer, both water and MEA, which have a different Heat of Vaporization. The latent Heat of Vaporization of MEA is 837 J/g (NOAA, 1999)

This is shown in equation (9.61)

$$\text{Reclaimer Duty} = \dot{m}_{lean,rec} \cdot \begin{bmatrix} cp_{lean} \cdot \left(T_{reclaimer} - T_{reboiler} \right) \\ + wt\%MEA \cdot \dot{Q}_{vap,MEA} \\ + \left(1 - wt\%MEA \right) \cdot \dot{Q}_{vap,water} \end{bmatrix} \qquad (9.61)$$

The inlet temperature is equal to the reboiler operating temperature. During the reclaimer steady-state boiling step the boiling temperature of the solution gradually rises from 285 to 300 °F, due to the build-up of impurities in the reclaimer. Heating is done using steam from a steam furnace with a pressure of 1035-1205 kPa, corresponding to 181,3-188,0 °C. (Sheilan et al., 2009)

C.5 Steam Furnace

The steam furnaces provide the steam for the reboiler and reclaimer, by evaporating the condensate from the reboiler and reclaimer respectively.

The required heat is supplied by burning natural gas in the furnace. Each furnace has a two efficiencies, Combustion efficiency and Boiler efficiency

Combustion efficiency is defined as the percentage of energy in the fuel that is released after combustion within the boiler. Some of the energy contained in the fuel is lost due to incomplete combustion.

Combustion efficiency (%)
=(Actual energy released during combustion x 100)/Total energy content of the fuel.
= 100 – % heat lost due to incomplete combustion of fuel.

Boiler efficiency is defined as the percentage of useful energy output compared with energy input. Energy output being the energy put into heating the condensate to superheated steam, energy input being actual energy released during combustion. It takes account of heat losses to the flue gases, losses due to incomplete combustion of the fuel, radiation losses (for example, from the exposed boiler surfaces), convection losses, conduction losses and other ancillary losses.

Combustion efficiency for gas and liquid fuels is usually quite high, at around 99%. **Boiler efficiencies** of around 80% are normal for all modern boilers (based on the gross calorific value of the fuel). Higher efficiencies (of up to 85%) are possible for condensing gas boilers and for plant fitted with economizers. However, note that the efficiencies that can be achieved by steam boilers are different from those available to hot water boilers. The type of economizer will have significant impact on the efficiency improvement achieved. (Carbontrust, 2012)

As well as the energy losses associated with boilers, there will also be losses associated with the distribution of the steam and hot water. These losses will be due to heat loss from pipework, malfunctioning steam traps, and leaks and unnecessary use of the steam and hot water at the point of use.

At the reboiler entrance the steam has to be 134 °C at 3 bar.
One can assume a temperature loss in the piping to and from the steam furnace and the reboiler of about 10 degrees, therefore the steam furnace has to heat condensate 10 degrees, evaporate the condensate and superheat the steam another 10 degrees.
The same assumptions are valid for the reclaimer, where the entrance pressure has to be 1035-1205kPa, corresponding to 181,3 – 188,0 °C.

The incoming energy content of natural gas per second, $Q_{required}$, is given in equation (9.62)

$$\dot{Q}_{required} = \dot{m} \cdot \left(\underbrace{c_p \cdot \Delta T}_{\text{Heating Condensate}} + \underbrace{\dot{Q}_{vaporisation}(T_{liquid}, P_{liquid})}_{\text{Condensate Vaporization}} + \underbrace{c_p \cdot \Delta T}_{\text{Heating Steam}} \right) \Big/ \left(\eta_{boiler} \cdot \eta_{combustion} \right) (9.62)$$

C.6 Lean/Rich Heat Exchanger

A shell and tube configuration (rich amine on the tube side and lean amine on the shell side) has been used commonly, but plate/frame exchangers have come into use more frequently in recent years.

Generally speaking, the temperature of the lean amine from the reboiler is 240 to 260 °F (116 to 127°C). The rich amine outlet from the lean/rich cross exchanger is typically designed for a temperature of 200-210°F (93 to 99°C), although some amine systems designs based on MDEA and formulated MDEA solvents have been designed around a rich amine feed temperature to the stripper of 220 °F (104 °C).
The rich amine inlet to the heat exchanger follows from the temperature at the outlet of the absorber/3phase flash tank. Finally, the lean amine outlet temperature of the exchanger can be calculated based on the other 3 temperatures.
For a rich amine inlet temperature of 130 to 160 °F (54 to 71°C), the lean amine outlet temperature from the exchanger is about 180 °F (82 °C). (Sheilan et al., 2009)
A recommended maximum velocity to minimize corrosion in the tubes is 3 or 3.5 feet/sec. (Kohl and Nielsen, 1997)

Transferred energy follows from $Q = mc_p\Delta T$, also for the lean amine cooler and the condenser.

In terms of volume the Lean/Rich Heat Exchanger is relatively small as it's a liquid-liquid contactor, therefore it's not taken into account in this work. The same assumption is made for the other cooling systems, the lean amine cooler and the condenser. A calculation method to assess the volume of a heat exchanger is given in section D.3.

C.7   Three Phase Flash Tank

The total flow through the Three Phase Flash Tank is given by the rich amine stream coming from the absorber bottom. The operating pressure is between 35 and 525 kPa depending upon the disposition of the flash tank vent stream. (Sheilan et al., 2009) & (RefiningOnline, 2007). When the flash tank operates at low pressure, 0 to 350 kPa, a rich amine pump is usually required, because of the pressure drop over the lean/rich cross exchanger the height of the stripper inlet and the operating pressure of the stripper column.

A minimum residence time for a three phase flash tank of 20 minutes is recommended, based on the flash tank operating half full. (Sheilan et al., 2009) Amine systems treating very dry natural gas (<2% C_2^+) or syngas streams with very little hydrocarbon content can utilize a lower flash tank residence time of 5 minutes if a flash tank is incorporated into the amine unit design.

Using the density of the rich amine solution, a total volume flow per minute can be calculated. Multiplying this value with the residence time yields a liquid capacity.

Using a value for the liquid level as percentage of total flash tank capacity, obtained from Table C.7, one can calculate the total capacity of the flash tank. When one assumes a ratio between the length and diameter of the vessel, one can also obtain these values from the total volume.

Table C.7 Liquid level as percentage of total flash tank capacity
Source: (RefiningOnline, 2007)

Liquid	Percentage of total capacity
Amine Solution	40 to 75%
Hydrocarbons	0 to 5%

Note: This work assumes 50% amine level and 1% hydrocarbons level, in accordance with (Sheilan et al., 2009) and an operating pressure of 4 bar in order to have no need for a rich amine pump.

C.8   Condenser & Reflux Drum

The condenser cools the tower top flow to the temperature of the reflux drum, which usually is between 90 and 130 °F (32,2 to 54,4°C). (RefiningOnline, 2007) & (Kohl and Nielsen, 1997)

This work uses a reflux drum temperature of 40 °C and a pressure of 1 atm. When a sulfur recovery unit (SRU) is used downstream of the reflux drum its standard practice to use the operating pressure and temperature of the SRU. However, this report only focuses on CO_2 separation. When considering the energy output, one has to keep in mind that the mass flow of CO_2 and H_2S does not condense at 40 °C.

The size of the reflux drum can be assessed by a 20 minute liquid hold up inside the drum. This capacity is taken to enable a steady flow of reflux water during the first 20 minutes of start-up of the stripper column, after a turn-around or shut-down. One can assume the liquid capacity is 50% of the total installed volume of the reflux drum.

C.9   Pumps

Pumps increase the pressure for a liquid flow, either to match the pressure of the next destination of the liquid, compensate for the static pressure due to height difference and/or overcome pressure loss due to friction in the piping/equipment. A schematic is shown in Figure C.8. Source for this section is (EngineeringToolbox, 2012)
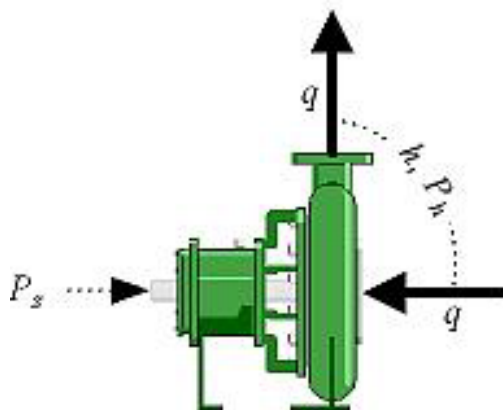
Figure C.8 Pump Schematic

In order to calculate pump shaft power one can convert its pressure requirement into a differential height, as shown in equation (9.63).

$$h = p \cdot 10,197 / SG + \Delta h \qquad (9.63)$$

with

- h = differential height [m]
- p = pressure in bar the pump has to generate, to offset pressure loss and pressure differences.
- SG = specific gravity of the substance, also known as the Relative density of a substance, is the ratio of the substance to the density of water at 4 °C.
- Δh = height difference between the pump and the vessel the liquid travels to.

One can then use this value to calculate the ideal hydraulic power that needs to be delivered by the pump, which depends on the mass flow rate, the liquid density and the differential height, as shown in equation (9.64).

$$P_h = q\rho g h \qquad (9.64)$$

Where
- P_h = Hydraulic Pump Power [W]
- q = flow capacity [m^3/sec]
- ρ = density of the liquid being pumped [kg/m^3]
- g = gravitational constant [9,81 m/s^2]
- h = differential height [m]

The shaft power, the power required transferred from the motor to the shaft of the pump, depends on the efficiency of the pump in converting shaft power into hydraulic power. This pump efficiency can be estimated of this pump efficiency is between 80 and 90%. (Conlon et al., 1999). This work uses 85% efficiency.

The electrical power deliver to the electromotor is calculated from the shaft power using the motor efficiency. This efficiency is a subject international legislation, which in America is responsibility of the National Electrical Manufacturers Association (NEMA, 2012), shown in Figure C.9. This means that the total electrical power supplied to the pump motor can be calculated as shown in equation (9.65).

$$P_e = P_h \big/ \left(\eta_{pump} \cdot \eta_{motor} \right) \qquad (9.65)$$
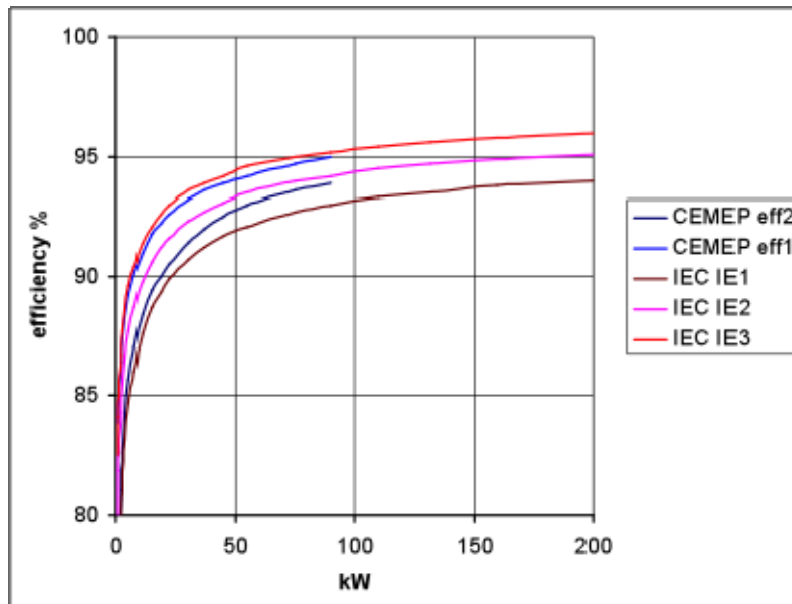

Figure C.9 Required efficiencies per kW of power for several different classes of electromotor
Source (NEMA, 2012)

This work therefore assumes an electro motor efficiency of 96% .
Just like the compressor for the CRS process, the pump volume is not considered in this work, as there are many types of pumps on the market and usually the required power in kW is enough to obtain an idea of the size of the machine.

C.10 Converting Electrical Power Consumption to Natural Gas Consumption

When one knows the sum the kilowatts of electrical energy used by all machines one can calculate the number of kWh per second by dividing the sum of kilowatts by 3600.

The Energy Content of burned product required to create 1 kWh of Electrical Energy can be found in Table A.6, given in kJ/kWh. This work assumes that the electricity is generated in a power plant using carbon sequestration.

This results in a kJ/s requirement of gross heating value of natural gas for the electrical consumption.

C.11 Equating Energy Cost to Natural Gas Consumption

The gross heating value used in this paper is 37800 kJ/m^3, based on the average value for natural gas in the United states.. This value is chosen as this paper also uses the composition of natural gas as is sold in the United States, see (NAESB, 2010), Table A.1. This makes it possible to convert this value to 50615 kJ/kg, using the molar mass of the gas according to its composition and the molar volume at standard pressure and temperature. For calorific values of other countries, see (IEA, 2012), Table A.2

The total mass flow of natural gas to the steam boilers (and power plants for electrical energy) is given by taking the total energy content of natural gas required (adding steam and electric) and dividing this by the gross heating value.

The molar flow of gas to the steam boilers can be calculated using the molar weight. One can divide this "burned" molar flow by the molar flow of gas out of the top of the absorber to find the % of the heating value of the gas coming from the top of the absorber that has to be burned in order to keep the processes running.

Appendix D   Condensed Rotational Separation – Process Description and Components

Condensed Rotational Separation, abbreviated by CRS, is a novel separation method for mixtures of gases, which uses elements of cryogenic distillation (Brouwers et al., 2006), (van Wissen et al., 2007). Cryogenic distillation enables the separation of 2 gases by cooling the gases to semi-cryogenic temperatures, whereby the contaminant condenses partially and after which the condensate is separated.

Several other processes have been developed on this principle, for example
- The Total Sprex process to remove H_2S from natural gas (Mougin et al., 2008), (Lallemand et al., 2006)
- Cryocell by CoolEnergy to remove CO2 from natural gas (Hart and Gnanendran, 2009)
- Controlled Freeze Zone by Exxon for sour gas fields (Valencia and Mentzer, 2008), (Mart et al., 2010)
- The Alstom Anti-Sublimation process (Clodic et al., 2005).

In comparison with amine absorption the energy consumption involved with these processes is limited at high contaminant levels. However, these processes use fractional distillation, employing temperature differences, which still requires large installations and there are thus large capital costs involved.

Instead of fractional distillation employing temperature differences, one can separate by flash evaporation or pressure distillation. CRS uses expansion through a valve or turbine to achieve this goal. This development is enabled by the availability of efficient cryogenic expanders that are able to work in the condensing area (e.g. GE, Atlas-Copco, Cryostar, Petrogas).

The advantage is simplicity and short residence time, i.e. small equipment and limited investment costs, while keeping the low energy cost, as cryogenic separation to certain specifications by the route of distillation or flash evaporation requires the same amount of work. (van Kemenade et al., 2011). Furthermore natural gas fields are usually pressurized and thus deliver a high pressure gas stream to the treatment facility. In amine absorption and fractional distillation this is mainly useful because it keeps the volume flow of natural gas down, somewhat decreasing the size of the treatment installations. However for expansion cooling it is particularly useful as the pressure can be used directly to cool the gas to condensing temperature, saving energy. Next to applications in standard sour gas cleaning, CRS is particularly applicable to systems where reduction in size and weight is advantageous, like floating LNG production. (van Wissen, 2006), (Willems, 2009).

There is however a downside to cooling gases to condensing temperature using fast expansion. Rapid cooling of binary or multi component mixtures of gases to temperatures where one, or some of the components preferentially condenses, leads to a mist of very small droplets with diameters of 1 to 10 micron (Schaber et al., 2002). The phenomenon is known to occur by:
aerosol formation in flue gases of biomass combustion installations (De Best et al., 2007), condensate droplets resulting from cooling of wet natural gas (Austrheim, 2006)

and has also been measured in experiments with CH4/CO2 mixtures (Willems et al., 2010a). As the micron sized droplets are difficult to separate from the gas stream (Hinds, 1982), the size advantage of pressure distillation is often lost in the required separator.

For a process which relies on fast phase change as a means of separation to be economical and practical, it is necessary to have a device capable of capturing micron-sized droplets with high collection efficiency at low pressure drop and a small footprint. Cyclones are standard for liquid/gas separation in hydrocarbon processing plants (Strauss, 1975), (Campbell et al., 1984). These cyclones are used for water and condensate removal but have not been applied for removing condensed contaminants, such as CO2 or H2S. This is because cyclones can only handle condensing droplet sizes above 15 μm (Purchas, 1981), (Clift, 1997), (Svarovsky, 1984). To achieve such droplet sizes requires unrealistically large, highly cooled droplet growth pipes. It is well known in laboratory chemical applications that microcyclones can separate micron-sized droplets having diameters as small as one micron, but then the flow is very small and orders of magnitude less than the flow in gas well applications. Alternatively one can improve separation efficiency by increasing swirl velocity to supersonic velocity but at the costs of large pressure drops (Schinkelshoek and Epsom, 2008).

The solution to this problem is provided by the Rotational Particle Separator, abbreviated by RPS (Brouwers, 1994), (Brouwers and Hoijtink, 2007), which is able to separate the micron sized droplets from the gas stream. This device is relatively small and thus keeps the size advantage of pressure distillation over fractional distillation intact. The device is shown in Figure D.3 and explained in detail in section D.2.

D.1   Process Thermodynamics

The process of condensing a gas by expansion is governed by thermodynamical correlations. The composition of the vapor and liquid phases depend on the pressure and temperature, which can be visualized in a phase diagram. In Figure D.1 the phase diagram of the CH_4-CO_2 system is shown. The solid-phase boundaries are shown by the dash-dotted lines. These lines represents the limit of CRS in the binary system, as below and to the right of these lines only vapor and pure solid CO_2 are present, or even liquid and pure solid CO_2.

The overall flow scheme of the process and its components are shown in Figure A.5, but is also depicted in Figure D.1. The process uses a 2 stage system where the liquid stream out of the first RPS is flashed again and fed into a second RPS. Due to the second flash, the liquid is purified, while most of the gas which was dissolved in the liquid/solid slurry evaporates. This gas is re-fed into the gas stream in the first part of the process.
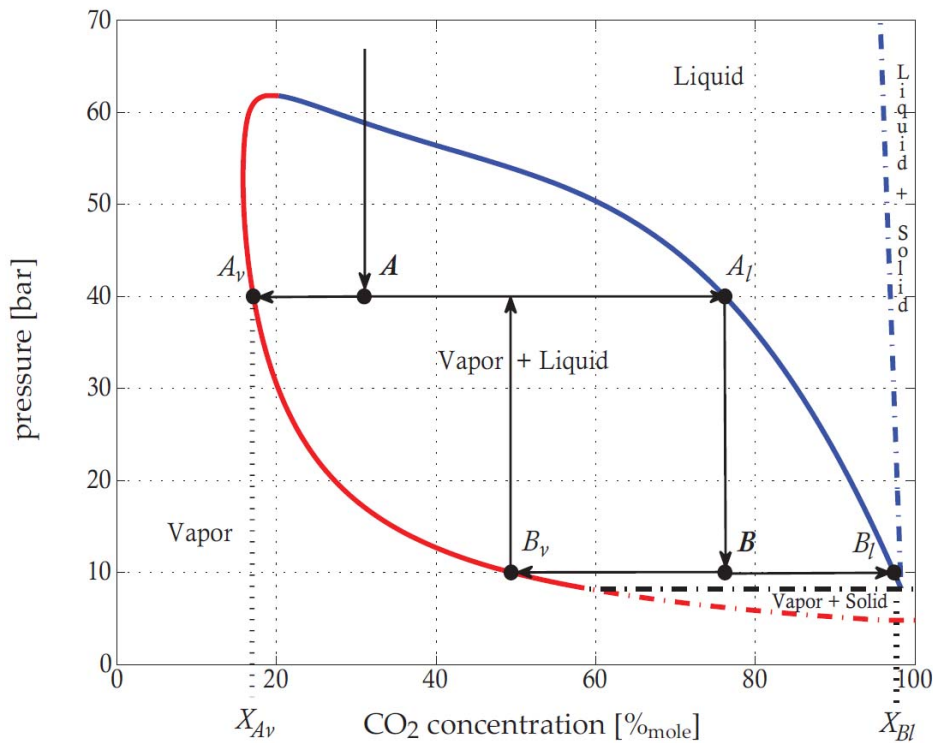
Figure D.1 P-X diagram for the CH₄-CO₂ system.
The incoming gas mixture is cooled and expanded to point A in the phase diagram where it is separated in a gas stream with composition X_{Av} and a liquid stream with composition X_{Al}. In the second flash the liquid is separated into a liquid with compostion X_{Bl} and a gas X_{Bv}. This gas is mixed with the incoming gas on line $A_v - A_l$. Source: (van Kemenade et al., 2011)
Note: In this work X_{Av} is 13,60%, this figure serves as an example.

In the first stage of the process, the incoming mixture, with methane concentration X_{in}, is chilled by a combination of cooling and expansion to a point close to the solid boundary of the vapor-liquid phase (within 5 °C), where the recovery of methane is maximal. (van Wissen, 2006). This point is indicated by A in Figure D.1. Because of binary condensation a mist of small droplets is formed within a vapor. The vapor phase has a composition X_{Av}, the droplets have a composition X_{Al}. The liquid phase is separated from the vapor by the first Rotational Particle Separator, to obtain a liquid stream.

In the second stage of the process this liquid stream is heated and expanded to obtain liquid droplets with composition X_{Bl} and a gas with composition X_{Bv}, at a point *(p, T)* even closer to the solids boundary. These are separated from each other by a second RPS. The resulting gas has a composition that is not far from the original untreated feed gas and is re-fed to the original gas entering the installation, to enter the first RPS again.

In case of the CH₄-CO₂ system, CRS has the potential to reach a purity of about 87% on the methane side and 98% on the CO₂ side. This compares to fractional distillation at 40 bar between the temperatures T_1 and T_2 as is shown in Figure D.2.

At the liquid outlet of the CRS process, shown in Figure A.5, 1,7 volume percentage of the flow is CH₄. This methane is considered 'lost', as there is no easy way of recovering it from the flow. This amounts to a certain % of the original CH₄ flow that is considered lost, shown in Table D.1.

Table D.1 Percentage of CH₄ lost in the solute stream of CRS

Original CO2 Content	13,6%	15%	30%	50%	70%	mol%
CRS Methane Loss	0,0%	0,03%	0,5%	1,5%	3,8%	mol%

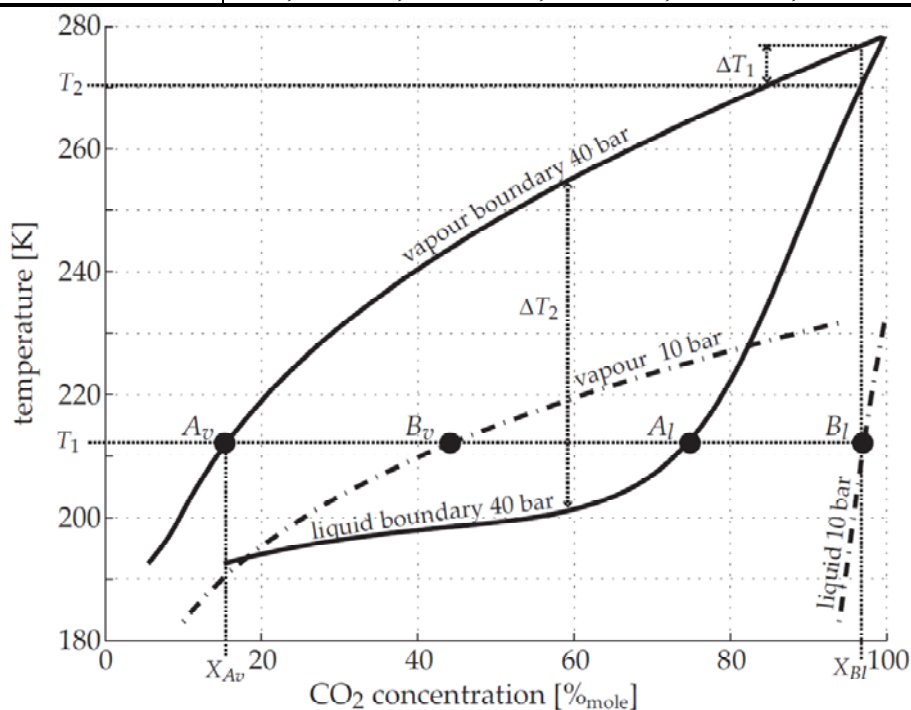**Figure D.2 T-X diagram for the CH₄-CO₂ system**

In reality raw natural gas is not a binary mixture, but contains traces of N_2, C_2H_6 and H_2. The presence of H_2S in a CO_2-CH_4 system lowers the temperature at which solids are formed. In that case significantly higher purities of methane in the gas phase can be reached while operating in the vapor-liquid regime. There is however a more important benefit of ternary or multi-component mixtures, like the system CH_4-CO_2-H_2S. At temperatures below the solid boundary, multi-component mixtures have a vapor-liquid-solid region instead of a vapor-solid region. This makes operation of CRS possible in this region, as long as the solid fraction does not become dominant. By operating CRS in the VLS-region, much higher purities of methane on the gas phase can be achieved, compared to operation of CRS in the vapor-liquid region. (van Kemenade et al., 2011). Figure D.2 also shows an interesting difference between fractional distillation and CRS. The design goal for a distillation column is maximum selectivity, or local thermodynamic equilibrium between the gas and liquid phase. The consequence is that the maximum temperature difference that can be used for heat transfer is ΔT_1 in Figure D.2. As the heat exchangers in the CRS process are not used for separation, the full temperature difference ΔT_2 between the bubble and dew point line can be used for heat transfer. For an equal design, the size of the heat exchangers in CRS are at least $\Delta T_1/\Delta T_2$ smaller than a distillation column. In practical circumstances of methane production this amounts to a factor 0.1 or less. This is also the factor by which CRS as a whole is smaller when compared to a complete distillation process with the same separation performance.

D.2 Rotating Particle Separator

A key feature of the described setup is the rotational particle separator (RPS), designed to separate large amounts of liquid CO2/H2S droplets, down to 1 μm from a gas stream. The RPS is basically an axial flow cyclone containing a rotating element, as can be seen in Figure D.3 (Left). The rotating element is a simple rotating body consisting of a very large number of axial channels of a few millimeters in diameter. In such channel the micron-sized droplets are centrifuged to form a liquid film at the channel-wall, which breaks up at the exit of the channel in the form of droplets; typically 20 μm or larger. These droplets are separated according the working principles of ordinary axial cyclones. The rotating element can receive its momentum for rotation by pre-rotation of the gas entering the rotating element, called natural drive, and/or by external drive through an electrical motor which is indirectly connected through a magnetic field.

The device can be divided into 3 in-line sections, the pre-separator, the filter element and the post-separator, which are placed in a vertical pipe, in which the downward flow direction prevents plugging and other undesirable effects.

Pre-separator

The pre-separator is constructed with a tangential inlet to provide the rotating flow and designed such that the diameter of the particles to be separated is well above the diameter of the channels in the filter element to prevent blocking. According to (Willems, 2009), the size of the droplets collected in the pre-separator can then be described by:

$$d_{p,50\%pre} = \sqrt{\frac{9\mu_g v_{ax,pre}\left(r_{pre}^2 - r_{shaft}^2\right)}{2\left(\rho_l - \rho_g\right)v_{in}^2 L_{pre}}} \tag{10.1}$$

where $d_{p,50\%pre}$ is the diameter of the droplets collected with a 50% probability, μ_g is the dynamic viscosity of the gas, $v_{ax,pre}$ is the axial gas velocity in the pre-separator, r_{pre} is the radius of the pre-separator, r_{shaft} is the radius of the shaft, ρ_l and ρ_g are the liquid and gas density respectively, v_{in} is the velocity of the fluid as it enters the pre-separator and L_{pre} is the length of the pre-separator. The pre-separator separates droplets of 20 μm and upwards diameter.

Filter element

In Figure D.3 (Right), a single channel is depicted rotating around a central axis at a radius r. A droplet that enters the channel on the left side is forced to the outer wall of the channel with a velocity equal to the Stokes velocity. In that case we can derive for the droplet diameter that can be captured with 50% efficiency (Brouwers, 2002):

$$d_{p,50\%} = \sqrt{\frac{27 d_c \mu \varphi}{2\pi\left(\rho_l - \rho_g\right)L_{element}\left(1-\varepsilon\right)\left(r_o^3 - r_i^3\right)\Omega^2}} \tag{10.2}$$

d_c denotes the channel diameter, μ the dynamic viscosity, φ the volume flow, ρ_l and ρ_g the liquid and gas density respectively, $L_{element}$ the length of the filter element, r_o and r_i the outer and the inner radius respectively and finally Ω the rotational speed. The correction factor *(1-ε)* is used to correct for the axial flow, cross-sectional area that is occupied by the channel walls, thus resulting in a higher gas velocity inside the channels. Experiments under both laminar and turbulent flow conditions have shown that equation

(10.2) predicts the separation efficiency sufficiently well for design purposes: (Mondt et al., 2006) & (Brouwers et al., 2012). The $d_{p,50\%}$ varies between 0,5 and 1 µm depending on the rotational speed of the separator.
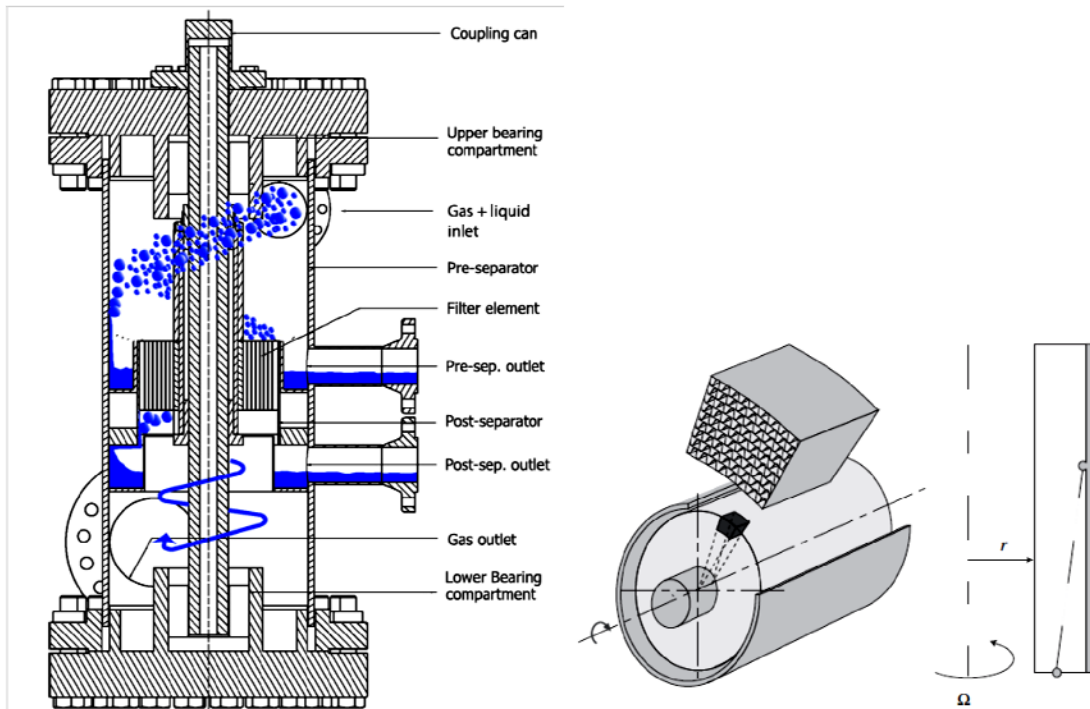

Figure D.3 Left: Rotating Particle Separator (RPS) built into a droplet catcher.
Right: Rotating Filter Element.
Source: (van Benthum et al., 2011)

The rotational speed, Ω, can be established with an external drive, or without. As a result of the torque imposed by the tangentially entering flow, the filter element will rotate without the help of an external drive, i.e. the element is naturally driven. The resulting rotational speed can be determined by balancing the momentum of the incoming flow with the loss terms, like bearing friction. However, for design purposes it is sufficient to assume that the angular speed of the filter element at its outer radius will eventually match the velocity of the incoming flow: $\Omega = v_{in}/r_{pre}$. This assumption is valid as long as the momentum of the incoming flow is large enough compared to the friction losses.

Post-separator
At the exit of the channels the liquid films break up into large droplets which are removed from the gas flow in a similar way as in the pre-separator. The diameter of the droplets that are formed at the end of the channels is determined by a balance between three forces. A shear force and centrifugal body force try to rip off the droplet, while the surface tension force pulls the droplet towards the channel wall. This balance is a cubic function, which can be solved to find an expression for the droplet diameter:

$$d_{p,post} = \frac{3}{\rho_l \Omega^2 r_o} \left(\sqrt{\frac{\rho_l \Omega^2 r_o \sigma}{3} + \frac{\rho_g^2 C_D^2 v_{ax,ch}^4}{256}} - \frac{\rho_g C_D v_{ax,ch}^2}{16} \right) \qquad (10.3)$$

Where $d_{p,post}$ is the droplet break-off diameter, σ is the surface tension and C_D the drag coefficient, which is approximately equal to 0,44 for a particle Reynolds number larger than 10^3 (Hinds, 1982). Once the droplet diameter is known, the residence time of the droplet in the post-separator, τ_{post}, can be determined. The radial speed at which a droplet travels is given by (Willems, 2009).

$$\frac{dr}{dt} = v_{p,r}(r) = \sqrt{\frac{4(\rho_l - \rho_g)d_{p,post}\Omega^2 r}{3C_D \rho_g}} \qquad (10.4)$$

With the radial velocity of the CO2 droplet known, the required residence time, τ_{post}, within the post-separator collector can be determined. This is the time it takes for a particle to travel from the inner radius, r_i, to the outer radius, r_o, of the post-separator. Because this is the largest distance to travel this will determine the length of the post-separator. Integrating equation (10.4) and writing $r_i = \delta r_o$, the residence time of the particle in the post-separator can be calculated as.

$$\tau_{post} = \sqrt{\frac{3C_D \rho_g r_o \left(1 - \sqrt{\delta}\right)^2}{(\rho_l - \rho_g)d_{p,post}\Omega^2}} \qquad (10.5)$$

The length of the post-separator then follows from

$$L_{post} = \tau_{post} \cdot v_{ax,post} \qquad (10.6)$$

For a detailed derivation of the droplet residence time and break-off diameter, the reader is referred to (Willems, 2009)

Summarizing, the pre-separator collects droplets from 20 μm upward and the coagulation element collects droplets as small as 0.5–1 μm. The droplets that can reach a channel wall in the filter element form a liquid film. At the exit of the channels, the film breaks up due to the fluid shear force and centrifugal force acting on the surface of the droplet. The smallest droplet size is calculated assuming that both forces act in the same direction counteracting the surface tension. The length of the separator is based on this minimum droplet size. Theoretically the droplets can still break up while migrating to the collection wall due to centrifugal and/or turbulent forces. In all cases considered so far, the minimum droplet diameter predicted for this mechanism is well above the minimum diameter as a result of film break-up. This is even true when taking into account the reduction in surface tension at elevated mixture pressure and low temperature. Many RPS devices have been designed and tested over the past 15 years for other areas of application: e.g. ash removal from flue gas of combustion installations, air cleaning in domestic appliances, product recovery in pharmaceutical and food industry and oil/water separation. Illustrations of designs applied in these areas, as well as CRS, are shown in Figure D.4.

Figure D.4 Applications of the Rotating Particle Separator
Source: (van Benthum et al., 2011)

D.2.1   Past Prototypes of CRS

In the last few years some significant milestones in the development of the CRS process were reached by experimental measurements on prototypes. The proof of principle was given by measurements on an experimental setup at a flow of 0,016 Nm^3/s (van Wissen, 2006). As flow rates from natural gas wells are in the order of 100 Nm3/s, more experiments were performed with a large scale atmospheric prototype, 24 Nm3/s (80 MMscf/d), which proved that the RPS is capable of handling large liquid loading under large flow rates (Willems, 2009), (Willems et al., 2010b). As the actual operating pressures are not at atmospheric pressure, a pressurized prototype of the separation process was constructed and tested by (Buruma et al., 2012). This prototype separated fine water droplets from a 230 m3/hr air flow at a pressure of 4 bar and a temperature of 23°C. A section view of the prototype RPS is depicted in Figure D.5 and Table D.2 lists the main geometric values of the device. The engine was mainly mounted to be able to change the radial velocity of the filter element at will. It should be noted that the particular engine used on this prototype was quite a bit larger and more powerful than was necessary for the setup.

The setup with 4 bar air flow modeled a 3.1 Nm^3/s (9.5 MMscf/d) equivalent installation on a natural gas well, assuming process conditions as presented in (Brouwers and van Kemenade, 2010): a pressure of 32 bar, a temperature of -80°C and a gas composed of 61%mole CH4, 23%mole H2S and 17%mole CO2. The flow properties of set-up, model and equivalent flow in standard volume are listed in Table D.3.
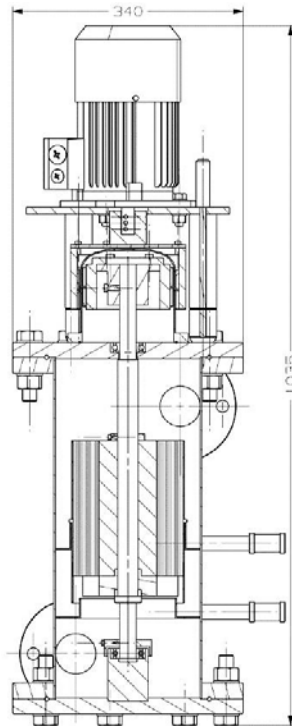
Figure D.5 Section view of the prototype used by (Buruma et al., 2012)
Dimensions are: Height 1035 mm, Width 340 mm.

Table D.2 Geometry of the prototype used by (Buruma et al., 2012)

Total Height	*1,035*	*m*
Engine Height	0,530	*m*
Shell Height	0,505	*m*
Pre-separator Height	0,121	*m*
Filter element Height	0,200	*m*
Post-separator Height	0,184	*m*
Shell Inner Diameter	0,214	*m*
Core Inner Diameter	0,085	*m*
Core Outer Diameter	0,162	*m*
Channel Diameter	0,002	*m*
Free Area Core, ε	50,00%	*m2/m2*

Table D.3 Used flow properties by (Buruma et al., 2012)

Property	*Experiment*	*Gas Field*	*Standard*	*Unit*
Pressure	4	32	1	*[bar]*
Temperature	20	-80	20	*[°C]*
Mass flow	300	3200	3200	*[g/s]*
Density	4,75	50,02	1,03	*[kg/m3]*
Volume flow	0,06	0,06	3,11	*[m3/s]*
Volume flow	227,21	230,29	11184,71	*[m3/hr]*

Note: The column 'Experiment' denotes the actual flow,
the column 'Gas Field' denotes the flow the experimental set-up was simulating.

D.2.2 Sizing the Rotational Separation element

In order to size the process with mainly the volume flow, but also the pressure and density, while still keeping the same $d_{p,50\%}$ at every stage it is important to make some assumptions. A good way to ensure the flow behavior remains the same is to keep the velocities constant.

Pre-separator

Considering Equation (10.1), when one assumes velocities constant and $r_{shaft} \propto r_{pre}$

$$v_{ax,pre} = \text{constant} = \frac{\varphi}{\pi\left(r_{pre}^2 - r_{shaft}^2\right)} \Rightarrow r_{pre} \propto r_{shaft} \propto \sqrt{\varphi} \tag{10.7}$$

$$v_{in} = \text{constant} = \frac{\varphi}{\pi r_{in}^2} \Rightarrow r_{in} \propto \sqrt{\varphi} \tag{10.8}$$

$$L_{pre} = \frac{\overbrace{9 v_{ax,pre}}^{\text{constant}}}{2 d_{p,50\% pre}^2 v_{in}^2 L_{pre}} \frac{\mu_g}{\left(\rho_l - \rho_g\right)}\left(r_{pre}^2 - r_{shaft}^2\right) \tag{10.9}$$

$$\Rightarrow L_{pre} \propto r_{pre}^2 \propto \varphi \text{ and } L_{pre} \propto \frac{\mu_g}{\left(\rho_l - \rho_g\right)}$$

Filter element

Considering equation (10.2), when one assumes velocities constant and $r_i \propto r_o$

$$v_{ax,channel} = \text{constant} = \frac{\varphi}{\pi\left(r_o^2 - r_i^2\right)(1-\varepsilon)} \Rightarrow r_o \propto r_i \propto \sqrt{\varphi} \tag{10.10}$$

When the filter element is naturally driven, the angular velocity over time approaches $\Omega = v_{in}/r_{pre}$, otherwise, the angular velocity is driven by the engine and can be assumed constant. Thus, for natural drive system equation (10.2) can be rewritten to

$$L_{element} = \frac{\overbrace{27 d_c}^{\text{constant}}}{2\pi d_{p,50\%}^2 (1-\varepsilon) v_{in}^2} \frac{\mu}{\left(\rho_l - \rho_g\right)} \frac{\varphi}{\left(r_o^3 - r_i^3\right)r_{pre}^{-2}} \tag{10.11}$$

$$\Rightarrow L_{element} \propto \frac{\varphi}{\left(\varphi^{1,5}\right)\varphi^{-1}} \propto \varphi^{0,5} \text{ and } L_{element} \propto \frac{\mu}{\left(\rho_l - \rho_g\right)} \tag{10.12}$$

for a fixed drive system it depends on the choice of Ω.

Post-separator

Considering equation (10.5)&(10.6), for a natural drive system

$$\tau_{post} = \sqrt{\frac{\overbrace{3 C_D\left(1-\sqrt{\delta}\right)^2}^{\text{constant}}}{d_{p,post} v_{in}^2}} \sqrt{\frac{\rho_g}{\left(\rho_l - \rho_g\right)}} \sqrt{r_o r_{pre}^2} \tag{10.13}$$

$$\Rightarrow L_{post} \propto \sqrt{\varphi^{0,5} \cdot \varphi} \propto \varphi^{\frac{3}{4}} \text{ and } L_{post} \propto \sqrt{\frac{\rho_g}{(\rho_l - \rho_g)}} \tag{10.14}$$

for a fixed drive system it depends on the choice of Ω again.

To find the total outer volume one can use for the radius R and the height Z

$$R = r_{pre} + R_{constant} \tag{10.15}$$

$$Z = L_{pre} + L_{element} + L_{post} + Z_{constant} \tag{10.16}$$

Where $R_{constant}$ is a value for the wall thickness and flanges etc. and $Z_{constant}$ takes the height of the shell above the pre separator entrance, engine height and height below the post separator exit and vessel mount into account.

These sizing correlations make it possible to adjust the geometry of the prototype used by (Buruma et al., 2012) for other flows and thus obtain an estimate for the size of the separation element. In order to keep the size within realistic boundaries, as it contains rotating elements, the decision was made to limit the height of the RPS (without engine) to about 2,5 meters and the diameter to about 1 meters. When 1 of these values was crossed the flow was split up over multiple parallel devices.

D.3 Heat Exchangers

Estimation of the dimensions of the heat exchangers used in the CRS process is based on a multi-stream, spiral-wound-type (Linde, 2012b) as commonly applied in LNG plants. In Figure D.6 a principal sketch of a multi-stream spiral-wound heat exchanger can be seen. The different tubes are coiled in layers around the central core. The coiling direction alternates from one layer to the next. Radial and longitudinal distances between the tubes are held constant by use of space bars. The tubes are connected to tube sheets at both ends of the heat exchanger.

These type of heat exchangers are used instead of plate-fin heat exchangers because of their robustness. Coil- and spiral-wound heat exchangers can handle large temperature gradients and large temperature differences, whereas plate-fin types are more vulnerable. Plate-fin heat exchangers are made out of aluminum, while coil-wound heat exchangers can be made out of a number of materials including aluminum, carbon steel and stainless steel. Therefore these types of heat exchangers can handle corrosive streams better as well.

The downside to this choice is that they are relatively expensive (about 3 to 4 times as expensive as plate-fin) and have a lower heat exchanging surface per m^3 (50 to 300 m^2/m^3, whereas plate-fin can reach 300 to 1000 m^2/m^3), resulting in a larger installation. (Linde, 2012a) An example of a coil wound heat exchanger is shown in Figure D.7.
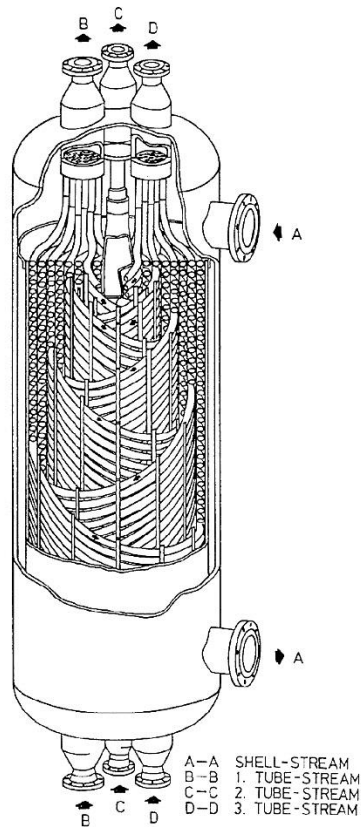
Figure D.6 Principal sketch of a multi-stream spiral-wound heat exchanger
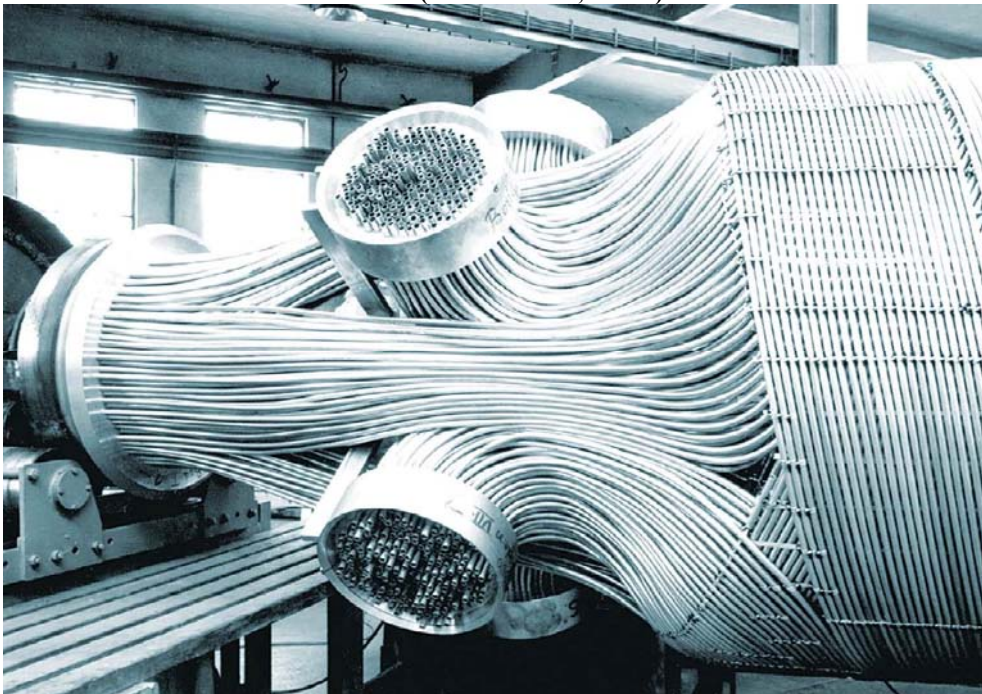**Source: (Neeraas et al., 2004a)**

Figure D.7 Coil Wound Heat Exchanger
Source: (Linde, 2012a)

To estimate the size of the heat exchangers a transfer unit approach is used. The number of (heat) transfer units is defined as

$$NTU_H = \alpha A / C_{min} \tag{10.17}$$

where α is the overall heat transfer coefficient, A the heat transferring surface, and C_{min} the smallest capacity flow. The capacity flow is defined as

$$C = \dot{m}(h_{in} - h_{out})/(T_{in} - T_{out}) \tag{10.18}$$

For a single phase flow C is equal to $\dot{m}c_p$. With the definition of the capacity flow, the effectivity can be written as:

$$\varepsilon = \frac{C_h(T_{h,in} - T_{h,out})}{C_{min}(T_{h,in} - T_{c,in})} = \frac{C_h(T_{c,out} - T_{c,in})}{C_{min}(T_{h,in} - T_{c,in})} \tag{10.19}$$

where the denominator, or maximum possible rate of heat transfer, is based on the stream with the smallest capacity flow. The effectivity is a function of the ratio $C_r = C_{min}/C_{max}$ and the number of transfer units $NTU = UA_w/C_{min}$. For a counter flow heat exchanger we can obtain the following relation (Bejan, 1997)

$$\varepsilon = \frac{1 - \exp\left[(C_r - 1)NTU\right]}{1 - C_r \exp\left[(C_r - 1)NTU\right]} \tag{10.20}$$

Introducing an entropy generation number as the entropy generation per unit heat transferred $N_s = \left[S_{gen}(T_{h,in} - T_{c,in})\right]/\dot{Q}$, the entropy production due to the unbalance C_r can be derived as

$$N_{s,C_r} = \left\{\frac{1}{C_r}\ln\left[1 - \varepsilon C_r(1-R)\right] - \ln\left[1 - \varepsilon(1-R)\right]\right\}/\varepsilon \tag{10.21}$$

Where $R = T_{h,in}/T_{c,in}$. The derivative of relation (10.21), dimensionalized with the maximum entropy production to the number of transfer units is depicted in Figure D.8. For all values of C_r the decrease in entropy production becomes small for NTU numbers larger than 2. We therefore fix the size of the heat exchangers to be used in the first stage at $NTU = 2$.
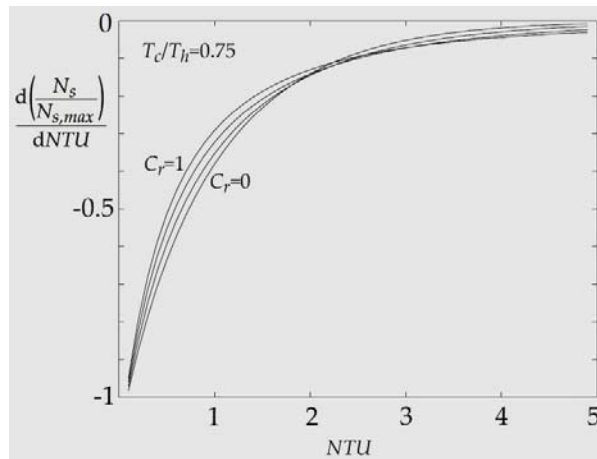

Figure D.8 Derivative of the dimensionless energy production to the number of transfer units

D.3.1   Heat Transfer Coefficients

Heat transfer from one side to the other is limited by three coefficients: the heat transfer coefficients on either side and the conductivity of the wall in between the 2 sides. In this work the wall conductivity is considered negligible.

For the calculation of the **shell-side** heat-transfer coefficient in gas flow a method from (Gnielinski et al., 1983) for tube banks is applied, as suggested by (Neeraas et al., 2004b)

$$Nu = \frac{\alpha \cdot L}{\lambda} = f_A \cdot \left(0,3 + \sqrt{Nu_{lam}^2 + Nu_{turb}^2} \right) \tag{10.22}$$

$$Nu_{lam} = 0,664 \cdot \sqrt{Re} \cdot Pr^{1/3} \tag{10.23}$$

$$Nu_{turb} = \frac{0,037 \cdot Re^{0,8} \cdot Pr}{1 + 2,443 \cdot Re^{-0,1} \cdot \left(Pr^{2/3} - 1 \right)} \tag{10.24}$$

$$f_A = 1 + \frac{0,7 + \left(P_l / P_r - 0,3 \right)}{\gamma^{1,5} \cdot \left(P_l / P_r + 0,7 \right)^2} \tag{10.25}$$

$$Re = \frac{u \cdot L \cdot \rho}{\gamma \cdot \mu}, Pr = \frac{\mu \cdot c_p}{\lambda}, \gamma = 1 - \frac{\pi \cdot D_{tube}}{4 \cdot P_r}, L = \frac{\pi \cdot OD_{tube}}{2} \tag{10.26}$$

f_A is the geometry arrangement factor for in-line tube banks, with P_l and P_r the longitudinal- and radial pitch between tubes. (EngineeringPage, 2012) lists the common tube diameters and wall thicknesses used in industrial heat exchangers. (Neeraas et al., 2004b) used a heat exchanger with a radial pitch, $P_r = 1,25 \cdot OD_{tube}$ and a longitudinal pitch, $P_l = 1,10 \cdot OD_{tube}$, in correspondence with the recommended pitch layout listed by (EngineeringPage, 2012). This report uses tubes with an outer diameter of 3/4" and a wall thickness of 1,651 mm corresponding to BWG-16, as is common industrial heat exchangers.

γ is the void fraction used to calculate the average velocity between the tubes for an in-line tube bank. L is the characteristic length on the shell side which is the stream length of a single tube, or half the (outer) circumference.

Finally u is the flow velocity in the empty cross section, which is assumed to be in the order of 1 m/s

For the calculation of the **tube-side** heat transfer coefficient a method from (Janna, 1999) is used

$$Nu_{lam} = 1,86 \cdot \left(\frac{ID_{tube} \cdot Re \cdot Pr}{L} \right)^{\frac{1}{3}} \tag{10.27}$$

$$Nu_{turb} = 0,023 \cdot Re^{0,8} \cdot Pr^x \tag{10.28}$$

x = 0,4 when T_{out}-T_{in}>0 and otherwise 0,3

$$Re = \frac{u \cdot L \cdot \rho}{\mu}, Pr = \frac{\mu \cdot c_p}{\lambda} \tag{10.29}$$

The characteristic length L on the tube side equals 0,5 times the inner diameter of the tube. u is again assumed to be in the order of 1 m/s.

$$Nu = Nu_{lam} \text{ when}$$
- the Reynolds number is smaller than 2200
- The Prandtl number is between 0,48 & 16700

$$Nu = Nu_{turb} \text{ when}$$
- The Reynolds number is larger than 10000
- The Prandtl number is between 0,7 & 160

The heat transfer coefficients for the **shell-side** and the **tube-side** are given by equation (10.30) based on their respective values for Nu, λ and L.

$$\alpha_S = \frac{Nu_S \cdot \lambda_S}{L_S}, \alpha_T = \frac{Nu_T \cdot \lambda_T}{L_T} \qquad (10.30)$$

The overall heat transfer coefficient is then given by

$$\alpha = \left(\frac{1}{\alpha_S} + \frac{1}{\alpha_T} \right)^{-1} \qquad (10.31)$$

From equation (10.17) it follows that the required surface area for heat transfer is given by

$$A = NTU_H \cdot C_{min} / \alpha \qquad (10.32)$$

The surface area to volume ratio of a coil wound heat exchanger is given by (Linde, 2012b) to be between 20 and 300 m^2/m^3 for spiral wound heat exchangers and between 50 and 150 m^2/m^3 for coil wound heat exchangers. This work therefore uses a value of 150 m^2/m^3. This enables one to calculate the volume requirement of the heat exchanger from the calculated heat transfer coefficient.

D.3.2   Dealing with 2 phase flow and phase changes

When considering the choice of heat transfer coefficient for the tube and shell side, the volume% of gas and liquid flow is of great importance. A gas flow has a lower thermal conductivity and therefore a lower heat transfer coefficient, not to mention the difference in Reynolds and Prandtl numbers.

Therefore it is a good idea to make parallel calculations, one assuming 100% gas flow, one assuming 100% liquid flow, with all their respective properties considered and one interpolating between these calculations based on the volume %.

A further complication is given by the fact that evaporation or condensation may occur inside the heat exchanger, on either side. The heat of evaporation and condensation needs to be considered. A possible solution is assuming this heat of evaporation is incorporated in the specific heat capacity, simulating a linear temperature profile.
A second calculation option is to calculate the heat transfer coefficient between the shell and tube side separately for the inlet and the outlet and performing a (weighted) average between these 2 for the overall heat transfer coefficient.

D.3.3   Coupling streams into heat exchangers

In Figure A.5 HEX1 and 3 are streams that need to be cooled, while HE2,4 and 5 can supply the required cooling power.

Stream 4 leads to the amine absorption process and thus is eventually required to be at 20 °C. When possible, it is preferable to keep Stream 5 at low temperature, as CO_2 is easier to handle when liquefied.

The figure is a somewhat simplified version of the total process, as it's a good idea to first cool stream 3 with a conventional cooling water supply to a lower temperature. Also in the current figure there is a pinch point present at -64,2 °C, therefore it can be suggested that the compressor should create a slightly higher pressure than suggested in the figure, which can be used after HEX3 to expand and cool the gas towards -64,2 °C.

With these changes, for all 4 cases the hot streams didn't require additional cooling, as the cooling power available was more than adequate. The compressor pressure ratio can be increased by 3 bar to account for the approximated extra energy required in the energy calculation.

D.4 Compressor

In this work the compressor has a pressure ratio of [41bar/9bar]=4,56, independent of the process feed composition. The specific work in [J/kg] for an isentropic compressor process can be expressed by (EngineeringToolbox, 2012)

$$W_{\text{specific}} = \frac{\gamma}{\gamma - 1} R_{\text{specific}} T_1 \left[\left(P_2 / P_1 \right)^{\frac{\gamma-1}{\gamma}} - 1 \right] \tag{10.33}$$

With $\gamma = c_p / c_v$, $R_{\text{specific}} = R_{\text{universal}} / M$, *M* is the average molar mass of the gas, *T_1*&*P_1* are the temperature and pressure at inlet and *P_2* is the pressure at outlet.
Multiplying this specific work with the total mass flow through the compressor gives the work done on the mass flow in *[J/s]*, *P_{flow}*.

The efficiency of the engine power delivered to the flow, *η_{drive}*, is assumed to be 85% and the efficiency of the electro motor, *η_{motor}*, is taken to be 96%, as in section C.9, (NEMA, 2012). This means that the total electrical power supplied to the compressor engine can be calculated as shown in equation (10.34)

$$P_e = P_{flow} / \left(\eta_{\text{drive}} \cdot \eta_{\text{motor}} \right) \tag{10.34}$$

As explained in section C.10, this required electrical energy can be converted to gross heating value of natural gas using the value found in Table A.6

Just like the pumps for the amine process, the compressor volume is not considered in this work, as there are many compressor types and usually the required power in kW is enough to obtain an idea of the size of the compressor.

D.5 CRS as bulk separator in combination with an Amine Absorption plant.

As shown in the main text, the energy demand of the classic amine absorption process increases rapidly with the contamination level. Therefore it is interesting to use a bulk separation process prior to the amine absorption process to reduce the size and energy consumption of the latter. CRS is an excellent candidate, as it is able to separate CO_2 from a binary CO_2-CH_4 mixtures of up to 70% CO_2 concentration to achieve a remaining 13,60% CO_2 content in the gas stream towards the amine absorber.

Separating CO_2 from the gas stream to bring the CO_2 content down removes a significant portion of the total flow. From the remaining mass flow shown at the gas outlet in Figure A.5 and the composition of 13,6% CO_2 one can calculate the corresponding MMscf/day that are fed to the Amine absorption plant. These values are shown in Table D.4.

Table D.4 Volume flow to Amine at 13,6% CO_2 content after the CRS bulk separation step.
Note: at 13,6% CO_2 content no CRS is used and the full flow is delivered to the amine process.

Original CO2 Content	13,6%	15%	30%	50%	70%	mol%
Volume Flow Rate	125	122	100	71	42	MMscf/day

This smaller flow has a significant impact on the volume and energy cost of the amine plant, as is shown in section 5, "Comparison Results".

Another potential advantage of including CRS into the separation process is the fact that it cleans the gas stream from the well from more than just the liquid CO_2. The same advantages apply using to CRS as apply to using the inlet gas knockout drum.

A general rule for amine treating is that the cleaner the inlet feed gas into the absorber tower is, the better the system operates. Many of the contaminants that cause poor performance enter the amine system via the inlet feed gas. Liquid hydrocarbons and well-treating chemicals can cause foaming, brine can lead to corrosion and iron sulfide can contribute to foaming and plugging.

Entrained droplets or slugs of liquid are removed from the gas stream by CRS and there is no need for extra mist eliminators, as CRS separates smaller particles than that. Even if aerosols are determined to be present, there's no need for high technology coalescing filtration systems unless the aerosols are in the sub-micron range.

Appendix E   Bibliography

ALAMI, I. Wasit gas plant: New Sour Gas Developments in Saudi Arabia. 6th Sour Oil and Gas Advanced Technology, 2010 Abu Dhabi.

AMISTCO. 2004. *Mist Eliminators* [Online]. Available: http://www.amistco.com/products/eliminators/index.html [Accessed 21 november 2012].

APTI. 1999. *Control of Gaseous Emissions - Course 415 - Student Manual* [Online]. United States Environmental Protection Agency, department: Air Pollution Training Institute (APTI). Available: http://www.epa.gov/apti/catalog/cc415.html [Accessed November 10 2012].

AUSTRHEIM, T. 2006. *Experimental characterization of high-pressure natural gas scrubbers.* PhD thesis, University of Bergen.

BASHADI, S. O. & HERZOG, H. J. 2011. Using auxiliary gas power for CCS energy needs in retrofitted coal power plants. *Energy Procedia,* 4**,** 1828-1834.

BEJAN, A. 1997. *Advanced engineering thermodynamics*, Wiley New York.

BELLMAN, D., BLANKENSHIP, B., IMHOFF, C., DIPIETRO, J., REDERSTORFF, B. & ZHENG, X. 2007. *Electric Generation Efficiency* [Online]. NATIONAL PETROLEUM COUNCIL. Available: http://www.npc.org/study_topic_papers/4-dtg-electricefficiency.pdf [Accessed November 10 2012].

BILLET, R. & SCHULTES, M. 1993. Predicting mass transfer in packed columns. *Chemical engineering & technology,* 16**,** 1-9.

BROUWERS, J. 2002. Phase separation in centrifugal fields with emphasis on the rotational particle separator. *Experimental thermal and fluid science,* 26**,** 325-334.

BROUWERS, J., KEMENADE, H. P. & KROES, J. 2012. Rotational particle separator: an efficient method to separate micron-sized droplets and particles from fluids. *FILTRATION,* 12**,** 57.

BROUWERS, J., VAN WISSEN, R. & GOLOMBOK, M. 2006. Novel centrifugal process removes gas contaminants. *Oil and Gas Journal,* 104**,** 37.

BROUWERS, J. J. H. 1994. *ROTATING PARTICLE SEPARATOR WITH NON-PARALLEL SEPARATING DUCTS, AND A SEPARATING UNIT*. WO/1994/023823 patent.

BROUWERS, J. J. H. & HOIJTINK, R. 2007. *DEVICE AND METHOD FOR SEPARATING A FLOWING MEDIUM MIXTURE INTO FRACTIONS*. WO/2007/097621 patent.

BROUWERS, J. J. H. & VAN KEMENADE, H. P. Condensed Rotational Separation To Upgrade Sour Gas. SOGAT, 2010 Abu Dhabi.

BURUMA, R., BROUWERS, B. & VAN KEMENADE, E. 2012. Rotational Particle Separator as a Compact Gas Scrubber. *Chemical engineering & technology*.

CAMPBELL, J. M., LILLY, L. L. & MADDOX, R. N. 1984. *Gas Conditioning and Processing: Volume 2: The Equipment Modules*, Campbell Petroleum Series.

CARBONTRUST. 2012. Steam and high temperature hot water boilers. Available: http://www.carbontrust.com/media/13332/ctv052_steam_and_high_temperature_hot_water_boilers.pdf [Accessed November 21, 2012].

CHAPMAN, S. & COWLING, T. G. 1991. *The mathematical theory of non-uniform gases: an account of the kinetic theory of viscosity, thermal conduction and diffusion in gases*, Cambridge university press.

CLIFT, R. 1997. *Inertial separators: basic principles in gas cleaning in demanding applications.,* ed. Seville JPK; London, Blackie.

CLODIC, D., EL HITTI, R., YOUNES, M., BILL, A. & CASIER, F. CO2 capture by anti-sublimation Thermo-economic process evaluation. Fourth Annual Conference on Carbon Capture & Sequestration, 2005 Alexandria, USA. 2-5.

COHEN, P. 1989. The ASME handbook on water technology for thermal power systems. American Society of Mechanical Engineers, New York, NY (USA).

CONLON, T., WEISBROD, G. & SAMIULLAH, S. We've Been Testing Water Pumps For Years - Has Their Efficiency Changed? ACEEE Summer Study of Energy Efficiency In Industry, 1999.

CONNERS, J. 1958. Aqueous-Amine Acid-Removal Process Needn't be Corrosive. *Oil and Gas J,* 56**,** 100-120.

CUSSLER, E. L. 1997. *Diffusion: Mass transfer in fluid systems*, Cambridge university press.

DE BEST, C., VAN KEMENADE, H., BRUNNER, T. & OBERNBERGER, I. 2007. Particulate emission reduction in small-scale biomass combustion plants by a condensing heat exchanger. *Energy & Fuels,* 22**,** 587-597.

DECOURSEY, W. 1974. Absorption with chemical reaction: development of a new relation for the Danckwerts model. *Chemical engineering science,* 29**,** 1867-1872.

DOW. 1998. *Gas Sweetening* [Online]. Midland, Michigan 48674 U.S.A.: The Dow Chemical Company. Available: http://msdssearch.dow.com/PublishedLiteratureDOWCOM/dh_0039/0901b80380 0391f8.pdf?filepath=gastreating/pdfs/noreg/170-01395.pdf&fromPage=GetDoc [Accessed November 9, 2012.

DUPART, M., BACON, T. & EDWARDS, D. 1993. Understanding corrosion in alkanolamine gas treating plants. *Hydrocarbon Processing,* 72**,** 89-94.

ENGINEERINGPAGE. 2012. *Standards for heat exchangers in the industry* [Online]. Available: http://www.engineeringpage.com/engineering/thermal.html [Accessed November 25th 2012].

ENGINEERINGTOOLBOX. 2012. *Pump Power Calculator* [Online]. Available: http://www.engineeringtoolbox.com/pumps-power-d_505.html [Accessed 21 november 2012].

FEAGAN, K., LAWLER, H. & RAHMES, M. 1954. Experience with Amine Units. *Petroleum Refiner,* 33**,** 167.

FU, D., XU, Y. F., WANG, L. F. & CHEN, L. H. 2012. Experiments and model for the surface tension of carbonated monoethanolamine aqueous solutions. *SCIENCE CHINA Chemistry***,** 1-7.

GNIELINSKI, V., ZUKAUKAS, A. & SKRINSKA, A. 1983. Heat exchanger design handbook. *Sec,* 2.

GOLDSTEIN, A., BROWN, E., HEINZELMANN, F. & SAY, G. 1986. New FLEXSORB gas treating technology for acid gas removal. *Energy progress,* 6**,** 67-70.

GPSA 1987. *Engineering Data Book,* Tulsa, Oklahoma, Gas Processing Suppliers Association.

HART, A. & GNANENDRAN, N. 2009. Cryogenic CO2 capture in natural gas. *Energy Procedia,* 1**,** 697-706.

HATTA, S. 1932. On the absorption velocity of gases by liquids. *J. Soc. Chem. Ind.(Jpn.),* 35**,** 559.

HINDS, W. C. 1982. Aerosol technology: properties, behavior, and measurement of airborne particles.

IEA 2012. Key World Energy Statistics 2012. France.

JANNA, W. S. 1999. *Engineering heat transfer*, CRC.

JOU, F. Y., OTTO, F. D. & MATHER, A. E. 1994. Vapor-liquid equilibrium of carbon dioxide in aqueous mixtures of monoethanolamine and methyldiethanolamine. *Industrial & engineering chemistry research,* 33**,** 2002-2005.

KO, C. C., CHANG, W. H. & LI, M. H. 2008. Ternary diffusion coefficients of monoethanolamine and< i> N</i>-methyldiethanolamine in aqueous solutions. *Journal of the Chinese Institute of Chemical Engineers,* 39**,** 645-651.

KOHL, A. L. & NIELSEN, R. B. 1997. *Gas purification,* Houston, Texas, Gulf Professional Publishing.

KOHL, A. L. & RIESENFELD, F. 1985. Gas Purification, Gulf Publishing Company. *Houston, Texas*.

KOLEV, N., NAKOV, S., LJUTZKANOV, L. & KOLEV, D. Comparison of the Effective Surface Area of Some Highly Effective Random Packings Third and Forth Generation. INSTITUTION OF CHEMICAL ENGINEERS SYMPOSIUM SERIES, 2006. Institution of Chemical Engineers; 1999, 754.

LALLEMAND, F., LECOMTE, F. & STREICHER, C. H2S Bulk Removal with the SPREX Process - First Operational Results. GPA Annual Convention, 2006 Grapevine, Texas, USA.

LINDE 2012a. Looking Inside... Plate-Fin versus Coil-Wound Heat Exchangers.

LINDE, A. 2012b. Catalogue entitled Rohrbündel-Wärmeaustaucher. *Linde AG, Werksgruppe, TVT, Munich, Germany*.

MART, C., VALENCIA, J. & NORTHROP, P. Developing Sour Gas Resources: Controlled Freeze Zone Technology with Integrated Acid Gas Management. Sour Oil & Gas Advanced Technology, 2010 Abu Dhabi.

MONDT, E., VAN KEMENADE, E. & SCHOOK, R. 2006. Operating performance of a naturally driven rotational particle separator. *Chemical engineering & technology,* 29**,** 375-383.

MOUGIN, P., RENAUD, X. & ELBAZ, G. 2008. Operational validation of the Sprex process for bulk H2S and mercaptans removal. *The gas industry: current & future (6)***,** 17-19.

NAESB. 2010. *Natural Gas Specs Sheet* [Online]. The North American Energy Standards Board. Available: http://www.naesb.org/pdf2/wgq_bps100605w2.pdf [Accessed November 11 2012].

NEERAAS, B. O., FREDHEIM, A. O. & AUNAN, B. 2004a. Experimental data and model for heat transfer, in liquid falling film flow on shell-side, for spiral-wound LNG heat exchanger. *International journal of heat and mass transfer,* 47**,** 3565-3572.

NEERAAS, B. O., FREDHEIM, A. O. & AUNAN, B. 2004b. Experimental shell-side heat transfer and pressure drop in gas flow for spiral-wound LNG heat exchanger. *International journal of heat and mass transfer,* 47**,** 353-361.

NEMA. 2012. *Premium Efficiency* [Online]. National Electrical Manufacturers Association. Available: http://www.nema.org/Policy/Energy/Efficiency/Pages/NEMA-Premium-Motors.aspx [Accessed 21 november 2012].

NOAA. 1999. *Monoethanolamine Properties* [Online]. Available: http://cameochemicals.noaa.gov/chris/MEA.pdf [Accessed 21 November 2012].

PURCHAS, D. B. 1981. *Solid/liquid separation technology,* Croydon, Uplands Press.

REFININGONLINE 2007. Amine Basic Practises Guidelines. Compiled by several Major Oil and Gas processing companies and indepent consultants.

ROIZARD, C. & WILD, G. 2002. Mass transfer with chemical reaction: the slow reaction regime revisited. *Chemical engineering science,* 57**,** 3479-3484.

SCHABER, K., KÖRBER, J., OFENLOCH, O., EHRIG, R. & DEUFLHARD, P. 2002. Aerosol formation in gas–liquid contact devices—nucleation, growth and particle dynamics. *Chemical engineering science,* 57**,** 4345-4356.

SCHINKELSHOEK, P. & EPSOM, H. Supersonic Gas Conditioning–Commercialization of Twister Technology. 87th GPA annual convention, 2008 Grapevine, USA.

SCHULTES, M. & HALBIRT, P. 2010. *Column Internals Product Bulletin 1101* [Online]. Rachsig Jaeger Technologies. [Accessed November 14 2012].

SHEILAN, M., SPOONER, B. & VAN HOORN, E. 2009. *Amine Treating and Sour Water Stripping*, Amine Experts Inc.

SOUDERS, M. & BROWN, G. G. 1934. Design of Fractionating Columns I. Entrainment and Capacity. *Industrial & Engineering Chemistry,* 26**,** 98-103.

STRAUSS, W. 1975. *Industrial Gas Cleaning: Principles and Practice of the Control of Gaseous and Particulate Emissions,* Oxford, Pergamon.

STRIGLE, R. F. 1987. Random packings and packed towers: Design and applications.

SVAROVSKY, L. 1984. *Hydrocyclones,* London, Holt.

TREYBAL, R. E. 1980. *Mass Transfer Operations*, McGraw-Hill New York.

VAIDYA, P. & MAHAJANI, V. 2006. Quickly design CO2-amine absorber. *Indian Journal of Chemical Technology,* 13**,** 47-52.

VALENCIA, J. & MENTZER, B. Processing of High CO2 and H2S Gas with Controlled Freeze Zone Technology. GASEX, 2008 Hanoi, Vietnam.

VAN BENTHUM, R., VAN KEMENADE, H., BROUWERS, J. & GOLOMBOK, M. 2011. Condensed Rotational Separation of CO2. *Applied Energy*.

VAN KEMENADE, H., BROUWERS, J. & VAN BENTHUM, R. Condensed Rotational Separation. AFS Annual Conference, 2011 Louisville, USA. Eindhoven University of Technology, Netherlands.

VAN WISSEN, R., BROUWERS, J. & GOLOMBOK, M. 2007. In-line centrifugal separation of dispersed phases. *AIChE journal,* 53**,** 374-380.

VAN WISSEN, R. J. E. 2006. Centrifugal separation for cleaning well gas streams: from concept to prototype.

VERSTEEG, G. & VAN SWAAIJ, W. 1988a. On the kinetics between CO2 and alkanolamines both in aqueous and non-aqueous solutions - 1. Primary and secondary amines. *Chemical engineering science,* 43**,** 573-585.

VERSTEEG, G. & VAN SWAAIJ, W. 1988b. Solubility and diffusivity of acid gases (carbon dioxide, nitrous oxide) in aqueous alkanolamine solutions. *Journal of Chemical and Engineering Data,* 33**,** 29-34.

WILLEMS, G., GOLOMBOK, M., TESSELAAR, G. & BROUWERS, J. 2010a. Condensed rotational separation of CO2 from natural gas. *AIChE journal,* 56**,** 150-159.

WILLEMS, G. P. 2009. *Condensed Rotational Cleaning of Natural Gas.* PhD thesis, Eindhoven University of Technology.

WILLEMS, G. P., KROES, J. P., GOLOMBOK, M., VAN ESCH, B., KEMENADE, H. P. & BROUWERS, J. J. H. 2010b. Performance of a novel rotating gas-liquid separator. *Journal of Fluids Engineering,* 132**,** 031301-1.